AD-A042 378 BENDIX CORP SOUTH BEND IND ENERGY CONTROLS DIV F/G 21/5
AN EVALUATION OF THERMOELECTRIC COOLING AS APPLIED TO ENGINE CO--ETC(U)
MAY 77 C S LONGSTREET, W LORENZ, W J MCPHEE F33615-74-C-2068
UNCLASSIFIED AFAPL-TR-77-24 NL

1 OF 2
ADA042378

AFAPL-TR-77-24

AN EVALUATION OF THERMOELECTRIC COOLING AS APPLIED TO ENGINE CONTROL ELECTRONICS

ENERGY CONTROLS DIVISION
THE BENDIX CORPORATION
717 NORTH BENDIX DRIVE
SOUTH BEND, INDIANA 46620

MAY 1977

TECHNICAL REPORT AFAPL-TR-77-24
FINAL REPORT FOR PERIOD JUNE 1974 - SEPTEMBER 1976

Approved for public release; distribution unlimited

AIR FORCE AERO-PROPULSION LABORATORY
AIR FORCE WRIGHT AERONAUTICAL LABORATORIES
AIR FORCE SYSTEMS COMMAND
WRIGHT-PATTERSON AIR FORCE BASE, OHIO 45433

NOTICE

When Government drawings, specifications, or other data are used for any purpose other than in connection with a definitely related Government procurement operation, the United States Government thereby incurs no responsibility nor any obligation, whatsoever; and the fact that the government may have formulated, furnished, or in any way supplied the said drawings, specifications, or other data, is not to be regarded by implication or otherwise as in any manner licensing the holder or any other person or corporation, or conveying any rights or permission to manufacture, use, or sell any patented invention that may in any way be related thereto.

This report has been reviewed by the Information Office (ASD/OIP) and is releasable to the National Technical Information Service (NTIS). At NTIS it will be available to the general public, including foreign nations.

This technical report has been reviewed and is approved for publication.

C E Ryan
Project Engineer

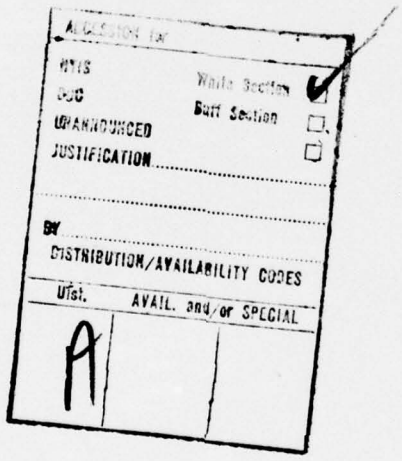

FOR THE COMMANDER

Charles E. Bentz
CHARLES E. BENTZ
Tech Area Manager, Controls

Copies of this report should not be returned unless return is required by security considerations, contractual obligations, or notice on a specific document.

AIR FORCE - 8 JUL 77 - 100

UNCLASSIFIED

SECURITY CLASSIFICATION OF THIS PAGE (When Data Entered)

REPORT DOCUMENTATION PAGE

READ INSTRUCTIONS BEFORE COMPLETING FORM

1. REPORT NUMBER: AFAPL-TR-77-24	2. GOVT ACCESSION NO.
3. RECIPIENT'S CATALOG NUMBER	
4. TITLE (and Subtitle): An Evaluation of Thermoelectric Cooling as Applied to Engine Control Electronics.	5. TYPE OF REPORT & PERIOD COVERED: Technical Report (Final) June 74 - Sept. 76
	6. PERFORMING ORG. REPORT NUMBER
7. AUTHOR(s): C. S. Longstreet, D. C. Thoman, W. Lorenz, W. J. McPhee	8. CONTRACT OR GRANT NUMBER(s): F33615-74-C-2068 Part II
9. PERFORMING ORGANIZATION NAME AND ADDRESS: Energy Controls Division, The Bendix Corporation, 717 N. Bendix Drive, South Bend, IN 46620	10. PROGRAM ELEMENT, PROJECT, TASK AREA & WORK UNIT NUMBERS: 3066/03 67
11. CONTROLLING OFFICE NAME AND ADDRESS: Air Force Aero Propulsion Laboratory (TBC), Wright-Patterson AFB, OH 45433	12. REPORT DATE: May 1977
	13. NUMBER OF PAGES: 114
14. MONITORING AGENCY NAME & ADDRESS(if different from Controlling Office): Final technical rept. Jun 74 - Sep 76,	15. SECURITY CLASS. (of this report): Unclassified
	15a. DECLASSIFICATION/DOWNGRADING SCHEDULE

16. DISTRIBUTION STATEMENT (of this Report)

Approved for public release, distribution unlimited.

17. DISTRIBUTION STATEMENT (of the abstract entered in Block 20, if different from Report)

18. SUPPLEMENTARY NOTES

19. KEY WORDS (Continue on reverse side if necessary and identify by block number)

Electronic engine controls
Thermoelectric cooling
Fuel heat exchanger
Turbine engine environment

20. ABSTRACT (Continue on reverse side if necessary and identify by block number)

Electronic elements of the engine control systems of future military aircraft will require protection against the high ambient temperatures expected at their mounting locations on the engines. The thermally conditioned module built and tested in this program was designed to provide this protection, with substantial margins; ambient temperatures to 750°F and fuel (coolant) temperatures to 300°F were employed. The unit employs thermal shields to minimize heat conducted to the electronics. The

DD FORM 1 JAN 73 1473 EDITION OF 1 NOV 65 IS OBSOLETE

Unclassified

SECURITY CLASSIFICATION OF THIS PAGE (When Data Entered)

electronics themselves were cooled by a thermoelectric cooler. High efficiency heat exchangers were designed for this unit. The unit weighed 1.45 lbs. Under worst case operating conditions, it pumped approximately 1300 BTU/hour to the fuel.

TABLE OF CONTENTS

TABLE OF CONTENTS (Continued)

LIST OF ILLUSTRATIONS

LIST OF ILLUSTRATIONS (Continued)

LIST OF TABLES

SECTION I

INTRODUCTION AND SUMMARY

This final report is submitted to the United States Air Force, Air Force Systems Command, Wright-Patterson Air Force Base, Ohio, in fulfillment of Part II of Contract F33615-74-C-2068. This contract covered the development and evaluation of several Advanced Turbine Engine Controls Components. The Part II effort was directed towards evaluating a means of controlling the temperature environment of signal conditioning electronics for engine control components. The work was performed during the period of June 1974 through September 1976.

Advanced Turbine Engines are expected to have a large number of variable-geometry control functions which will be controlled to provide optimal performance throughout the aircraft mission profile. Engine functions require an integrated control system to ensure their proper scheduling andproper fail-safe interlocking. The number of control parameters to be sensed, the multiple control modes to be established, the large number of control functions to be accomplished, and the requirements to effectively interface with the aircraft control system, all indicate the need for complex engine control systems. In order to satisfy these requirements, electronic computing engine control systems may be necessary, because of their adaptability and flexibility, to satisfy these complex control requirements.

Electronic elements of the engine control systems will require protection against the high ambient temperatures to which they will be exposed at their mounting locations on the engines. Requirements for these assemblies to operate with ambient temperatures up to 500°F are a requirement for advanced transonic/supersonic aircraft. The temperatures in high supersonic (Mach number 3.5) applications reach 750°F. Since electronic components are generally considered to be operable by their manufacturers as long as their temperatures are limited to 257°F or below, some method of environmentally protecting the electronics must be used. The major objective of this project was the design and evaluation of a novel method of maintaining the temperature of an electronic assembly below 257°F when exposed to ambient temperatures up to 750°F. This maximum temperature was selected in order to provide an adequate design margin and to allow for future growth in aircraft/engine performance.

The program was intended to evaluate the ability of thermoelectric cooling elements to provide the necessary cooling in this extreme environment, and to establish the practicality of utilizing this approach for advanced turbine engine controls. A special cooling module was developed as a test vehicle with which the performance and durability of the thermoelectric elements could be evaluated via bench and engine tests. The cooling module design was unique and was based on heat transfer considerations. It employed novel advanced technology heat exchangers and provided an integrated structure to house the thermoelectric elements and the demonstrator package of electronics attached to them for cooling. The secondary cooling source employed JP-4 engine fuel at temperatures up to 330°F.

A signal conditioning circuit for thermocouples was selected to be used for the test program. It was considered to be typical or representative of the types of sensor conditioning circuits that would require thermal protection. The circuit accepted eight thermocouple signal inputs and multiplexed their outputs over a single communication channel.

The electronics consisted of a thermocouple amplifier, an eight channel amplifier, a cold junction reference, and the analog section of a dual-slope analog-to-digital converter on a one inch square thick film hybrid integrated circuit that was packaged into a thermally conditioned module. JP-4 fuel was utilized as a heat sink and thermoelectric cooling elements were used to pump the heat from the hybrid mounting surface to the fuel heat exchanger. The design of the module also shunted the major heat from the environment directly into the fuel heat exchanger.

The concept of thermoelectric cooling utilized in this project is applicable to thermally protecting other engine sensors or signal conditioning electronics. The approach used in this project is intended to point out an alternative to conventional packaging techniques for electronics for advanced high performance aircraft engines.

The unit that was developed and tested weighed 1.45 pounds. It functioned to measure 8 temperatures in range of 0°F to 3000°F and provided nominal accuracies of 0.5% in an environment where the ambient temperature was varied from -65°F to +750°F. The maximum temperature reached by the hybrid electronics was 250°F. Under the worst case operating conditions, 1300 BTU's per hour were pumped to the fuel of which 13 BTU/hr were removed by the thermoelectrics. The thermoelectrics developed under this program were able to maintain a 90°F differential between the hot plate (fuel cooled) and the cold plate (cooling the electronics).

The unit was also operated for 200.5 engine test hours mounted on a PW&A JT9D engine in a test cell. The unit was not used for engine control since the test objectives were to demonstrate the mechanical integrity and durability of the unit under severe engine acoustic and vibration environments. Since the temperature environment in the test cell was very nominal, a full evaluation of the unit under worst case conditions when mounted on the engine could not be demonstrated.

The specific effort performed under the contract included the following tasks which are described in detail in other sections of this report:

a. Preliminary Design
b. Analysis of Alternate Sensor Types
c. Development of the Thermoelectric Cooling Element and Heat Exchanger
d. Fabrication of the Circuit Breadboard
e. Temperature Control of Hybrid Integrated Circuit
f. Read-out Module Design
g. Thick Film Hybrid Circuit Pre-test
h. Component Assembly
i. Component Performance Test
j. Engine Test
k. Preparation of a Final Report

The Thermally Conditioned Module (TCM) demonstrated that electronic devices can be packaged so as to be cooled by thermoelectric cooling elements to survive the environment of high performance aircraft turbine engines. Survivability at ambient temperatures up to 750°F and with cooling fuel temperatures up to 300°F was successfully demonstrated under bench tests.

Detail anlysis and results of the various tests performed are covered in the body of the report. The module designed and tested during the study satisfactorily demonstrated the concept feasibility.

- Correlation between the heat transfer analysis and test data was good.
- Test at 750°F ambient and 300°F fuel temperature showed the signal conditioning circuit temperature to be at 210°F.
- The signal conditioning circuit functioned normally after laboratory vibration tests and after engine testing.
- There was no apparent damage to the module as a result of laboratory vibration testing or engine running. A failure did occur in the heat exchanger. A minor design change would correct this problem.

Using the analysis design techniques and correlation with test data generated during the program, future applications can be specifically designed with a high degree of confidence that results will conform to requirements.

SECTION II

THERMALLY CONDITIONED MODULE DESCRIPTION

2.1. GENERAL DESCRIPTION

The project described in this report included the following major tasks:

- Thermally Conditioned Module (TCM) mechanical design
- Heat transfer analysis
- Signal Conditioning circuit design and manufacture
- Thermoelectric heat pump design and manufacture
- Readout module design and manufacture.
- Test the completed TCM.

Details on each item design and test results are covered in subsequent sections of this report.

A thermally conditioned module was designed to demonstrate a cooling method whereby the electronic control devices installed directly on the engine would be protected from the severe temperature environments associated with Mach 3.5 aircraft. Ambient temperatures up to 500°F in the engine nacelles are expected to be common for future supersonic aircraft. The module was designed to withstand ambient air temperature of 750°F with fuel at temperatures up to 330°F provided as a heat sink. The selected design criteria for the module are:

Air Environment	-65°F to 750°F
Air Velocity	50 ft/sec
Fuel Coolant	Jet fuels conforming to MIL-T-5624 MIL-G-5572 MIL-G-3056 VV-G76

Fuel temperatures	-65°F to 330°F
Fuel flow rates thru module heat exchanger	100 lbs/hr.
Hybrid Circuit Temperature limit	257°F Max.
Circuit Accuracy	0.5% of Full Scale

A thermocouple signal conditioning circuit was selected to be used for demonstrating the performance of a thermally conditioned module. This signal conditioning assembly was considered to be typical of the type of signal conditioning circuits and transducers that would require thermal conditioning. The electronic circuit was designed to accept inputs from eight thermocouples and convert their output signals to digital format. The outputs were multiplexed and transmitted to a remote digital readout module. The thermoelectric cooling technique used in this design could also be applied to pressure sensors, pyrometers, or any other engine mounted sensor and associated electronics that require a thermally conditioned environment.

2.2. MECHANICAL DESIGN

The thermally conditioned module (TCM) is constructed of aluminum to minimize weight and to obtain good heat transfer characteristics. A sectional view showing the major components of the module is shown in Figure 1. A more complete view of the various components of the module is shown in Bendix drawing number FXD-33900, Section III, Figure 10 A photograph of the major subcomponents is shown in Figure 2. Samples of the primary and secondary heat exchanger laminations are shown in Figure 3.

The heat exchanger modules were manufactured at the Bendix Research Laboratories. The heat exchangers are fabricated from 0.010 inch thick sheets of Type 1145 AL alloy. The individual plates were chemically milled, then joined by diffusion bonding. The thermoelectric cooling element was furnished by Ohio Semitronics, Inc. of Columbus, Ohio. Additional discussion of this device can be found in Section V and in the Appendix.

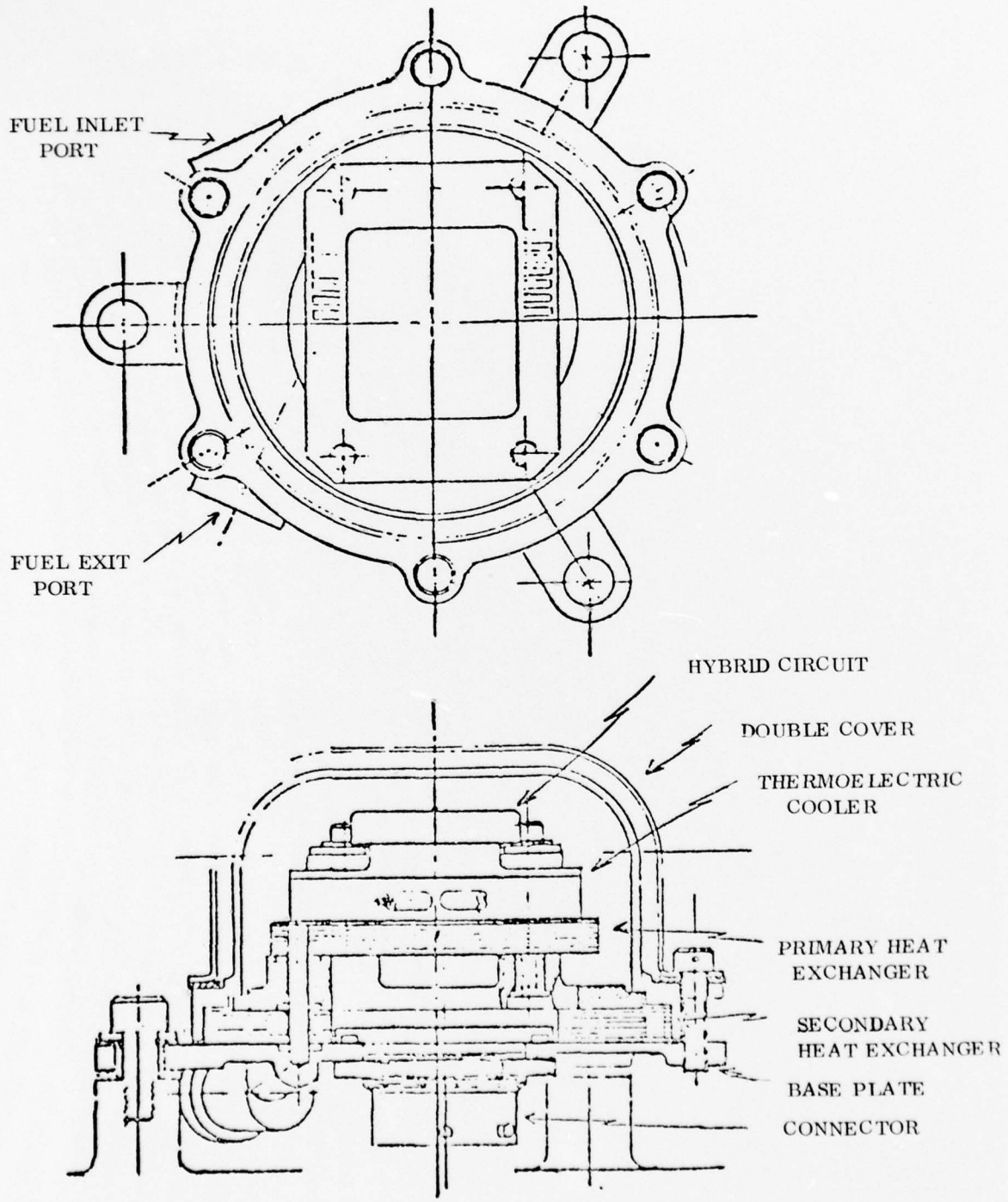

Figure 1 -- Thermally Conditioned Module

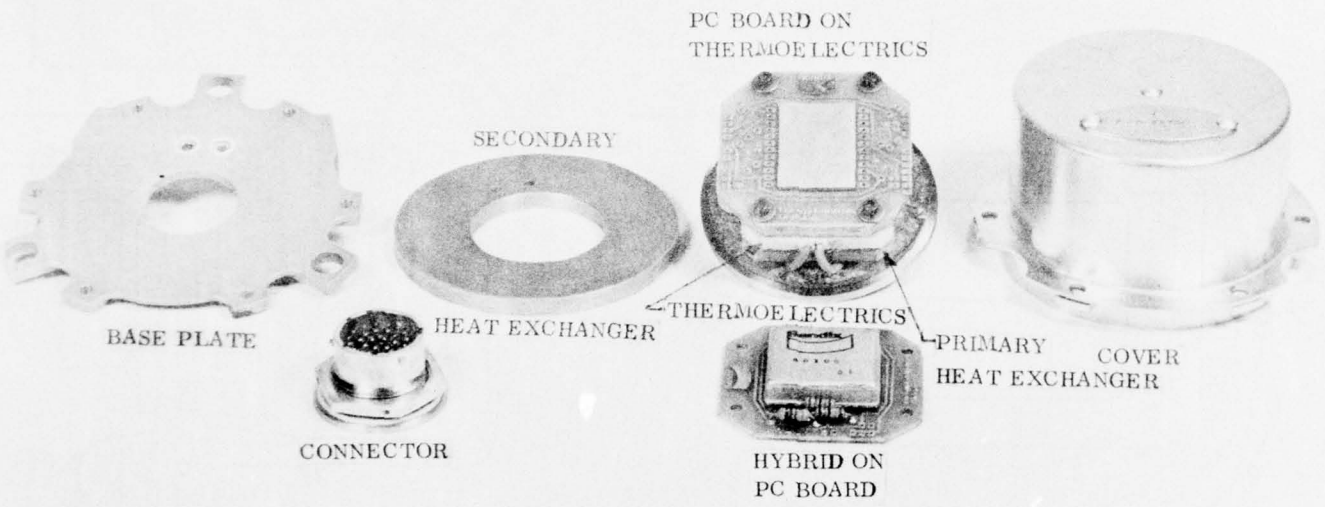

Figure 2 -- Disassembled View of TCM

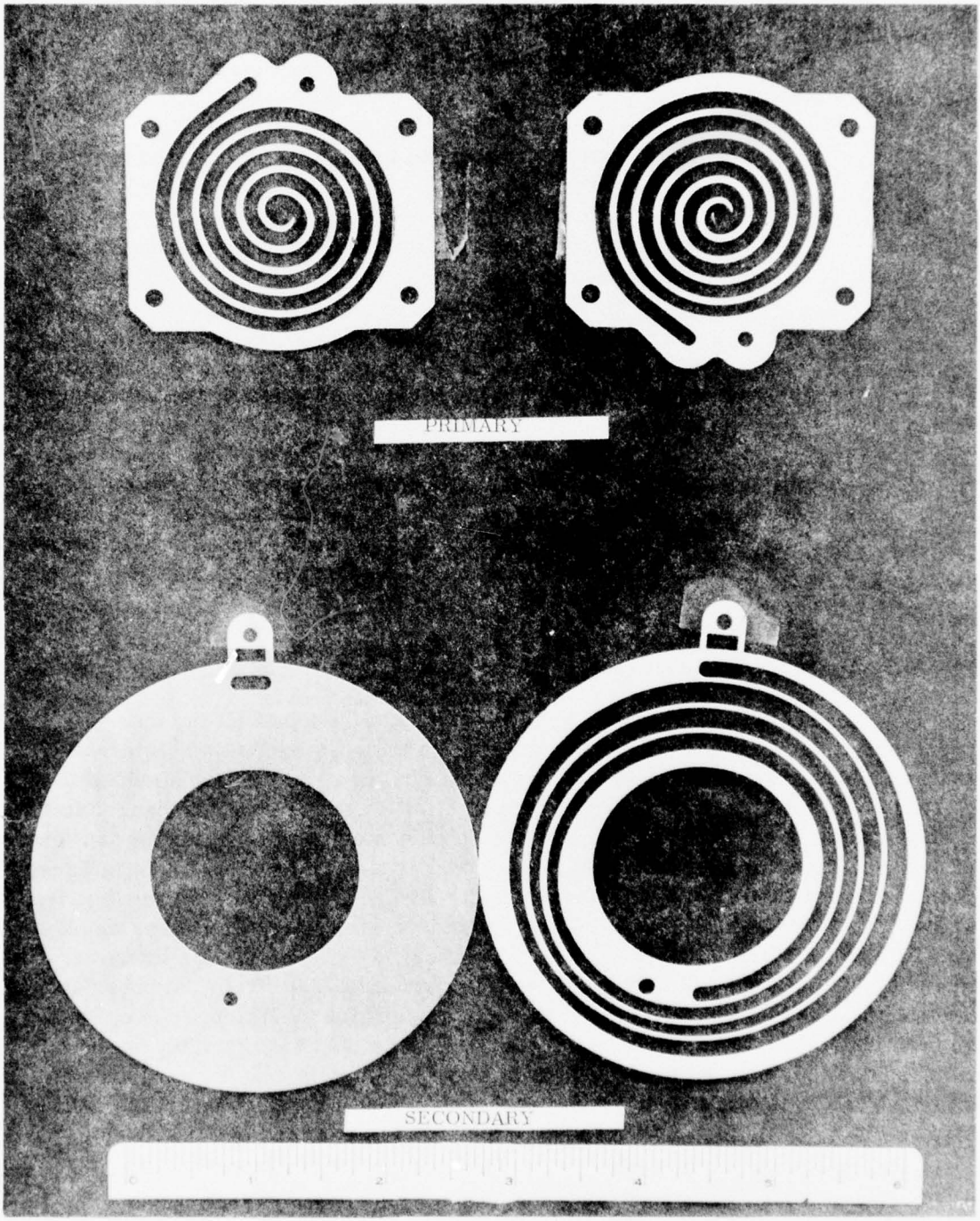

Figure 3 -- Heat Exchanger Lamination Samples

The techniques utilized to meet the design goal can be briefly summarized as:

- A protective outer shield insulated from all other parts of the module.

- An inner cover thermally anchored to a secondary heat exchanger.

  This combination of parts will keep the inner cover at or near fuel temperature. The temperature sensitive elements are further protected by an air gap between the inner cover and electronic circuit.

- Heat is radiated, conducted, and generated by the electronic circuit. The electronic circuit is cooled by the heat pumping action of the thermoelectrics to a temperature ninety (90°) degrees Fahrenheit less than the incoming fuel temperature.

2.3. THERMAL DESIGN

The heat pumped by the heat exchanger includes all the thermal radiation, convection and conduction leaks from the environment and internally generated heat. The internal heat is generated by electrical power dissipation and by frictional losses resulting from the fluid flow through the heat exchanger in addition to the conduction load imposed by the thermoelectrics. Under worst case conditions, the total heat load from these sources amount to 60 watts. The largest component of this load is due primarily to the inefficiency of the thermoelectrics which contributes about 40 watts of heat. The secondary heat exchanger employs the fuel from the primary heat exchanger to serve as a heat sink for the cover and baseplate. The total heat contributed by the conduction path from the cover and the baseplate is 530 watts. Under worse case operating conditions, the operating temperature of the electronics is maintained at less than 250°F. To provide for the capability of pumping about 600 watts, high volumetric heat exchangers were designed. Details of the heat exchanger construction are shown in Figure 10, Sections B-B, H-H, J-J, P-P, F-F and E-E of Bendix Drawing FXD-33900.

2.4. ELECTRONIC DESIGN

A block diagram of the thermally conditioned module system as tested and as envisioned for engine installation is shown in Figure 4. A system block diagram of the electronics within the thermally conditioned module is shown in Figure 27 of Section IV. The module consists of a thermocouple amplifier, an eight channel multiplier, a cold junction reference and the analog section of a dual-slope analog-to-digital converter. The electronics within the module are built on a one-inch square hybrid circuit. The accuracy of each channel is better than 0.2% when operated over a 212°F ambient temperature range. The accuracy is achieved through the use of low-drift integrated circuits and precision thick-film resistors. The unit is a custom hybrid built by the Bendix Aerospace Division. A photograph of the unit is shown in Figure 5. Further details of the electronic design can be found in Section IV.

2.5. ASSOCIATED EQUIPMENT

Two items of support equipment were designed for testing the thermally controlled module which are shown in Figure 6 with the module. A digital readout module was required to monitor the eight (8) thermocouple signals to establish the performance of the signal conditioning electronics located in the thermally conditioned module. The readout module which was remotely located from the module consists of the counter section of the analog-to-digital converter, the numeric displays and the channel select logic. A digital-to-analog converter is also provided to allow analog recording and display of the data channels. The output signal of the thermally conditioned module is in digital form which the readout module translates and displays in decimal form using seven segment light emitting diodes. The readout module would not be required in an engine control application since it would be replaced by an interface circuit in the digital engine controller.

The second piece of equipment was a power supply for the thermoelectric cooling element. The thermoelectric element requires DC current and will provide heating or cooling. The polarity and magnitude of the input current controls the amount of heating or cooling. The temperature of the electronic circuit and in the thermally controlled module was sensed by a thermistor mounted on the hybrid integrated circuit. The thermistor provided a control signal to the remotely located power supply which adjusted the output current to the thermoelectric element as required to maintain the desired temperature environment in the module. This particular module design required approximately 40 watts maximum at eight (8) ampere. Additional data on the power supply design is presented in Section IV.

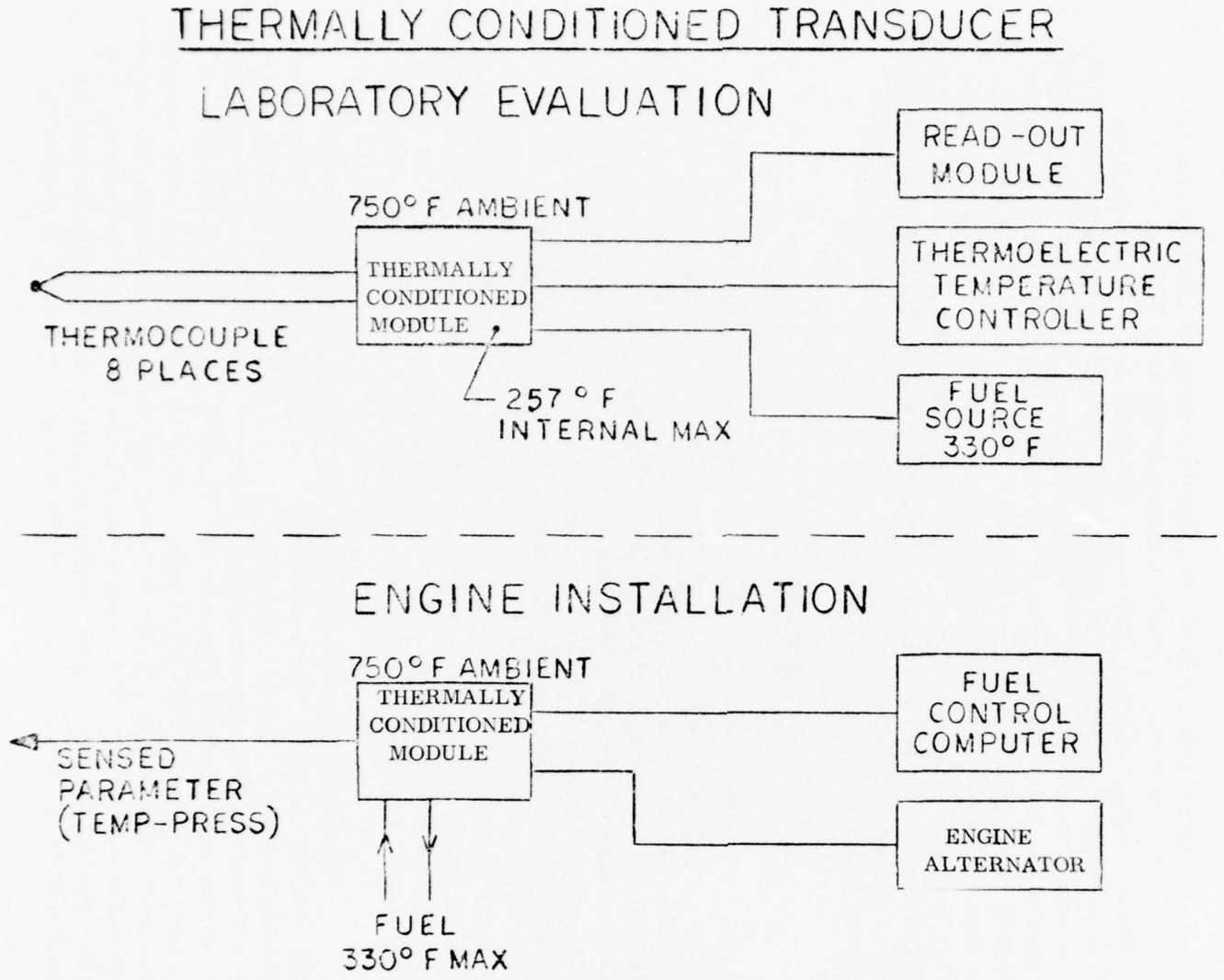

Figure 4 -- Thermally Conditioned Module System

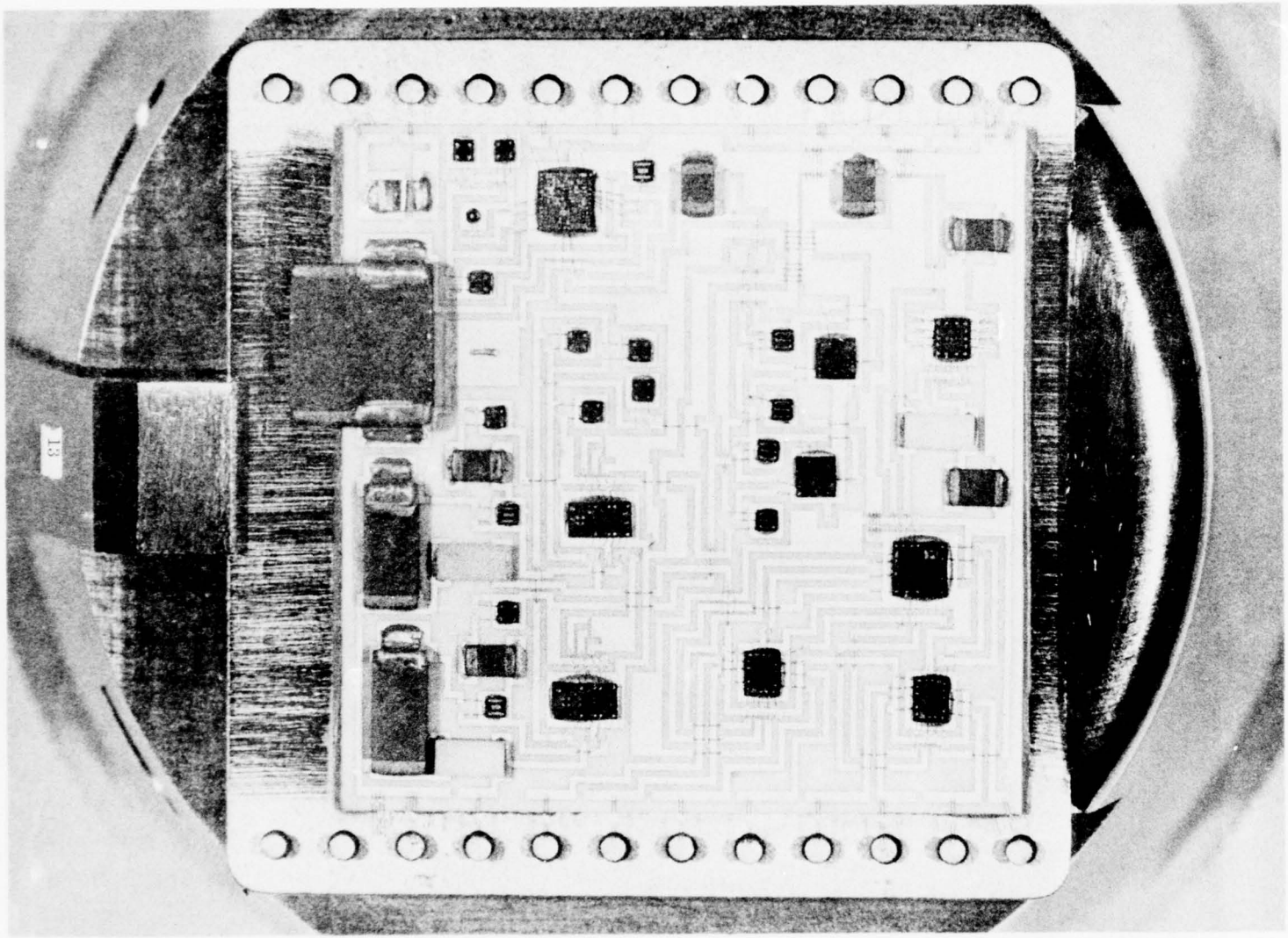

Figure 5 -- Hybrid Circuit

Figure 6 -- Thermally Conditioned Module Elements

It should be noted that an airborne power supply would be required to supply power to the thermoelectrics in an actual engine control application. Such a unit would have to be designed to also survive the aircraft/engine environment. This power supply could be incorporated into the engine electronic controller or in the signal conditioning modules for the engine sensors. It would utilize power directly from an engine furnished alternator. If the engine alternator is a high impedance permanent magnet type, then only a set of rectifiers is required to provide the direct current for the thermoelectric cooler.

SECTION III

THERMAL DESIGN AND DEVELOPMENT

3.1. GENERAL DESCRIPTION

The objective of the thermal design and development phase of this program was to provide for adequate cooling of a hybrid electronic package. Simplified schematics showing the thermally conditioned module construction and associated thermal transfer paths are shown in Figure 7. The baseline for tests and analysis assumed the following conditions:

Variables	Nominal Values
Air velocity	50 ft./sec.
Cooling fuel flow rate	100 lbs/hr
Current through thermoelectrics (T.E.)	8 amps
Voltage through T.E.	2.4 to 8.0 volts
Inlet cooling fuel temperature	-65° F to 330° F
Air temperature	-65° F to 750° F

Figure 8 gives a simplified model of the various thermal transfer mechanisms in operation in the module. Heat enters the module through the cover, the lead wires, the mounting and the fuel lines. Internally heat is generated by the hybrid circuit and the thermoelectric cooler. Heat from the hybrid circuit is conducted to the cold plate and then pumped by the thermoelectric unit to the primary heat exchanger. The cooling fuel flow in the primary heat exchanger carries the heat out of the module. Since the thermoelectric unit can pump heat against large adverse temperature gradients, the cold plate and the hybrid electronics can be maintained at temperatures much cooler than the fuel temperature.

The TCM test unit constructed and tested employed aluminum construction wherever possible to provide low weight while providing good thermal properties at low cost. A cut-away drawing with locations of the thermocouples used to obtain test data is shown in Figure 9. Table 7 lists the corresponding thermocouple location. The unit shown, approximately full size, measures about 3.5 inches in diameter and 2.75 inches high. The layout drawing for the thermally conditioned module, Bendix Drawing FXD-33900, has been reproduced in Figure 10.

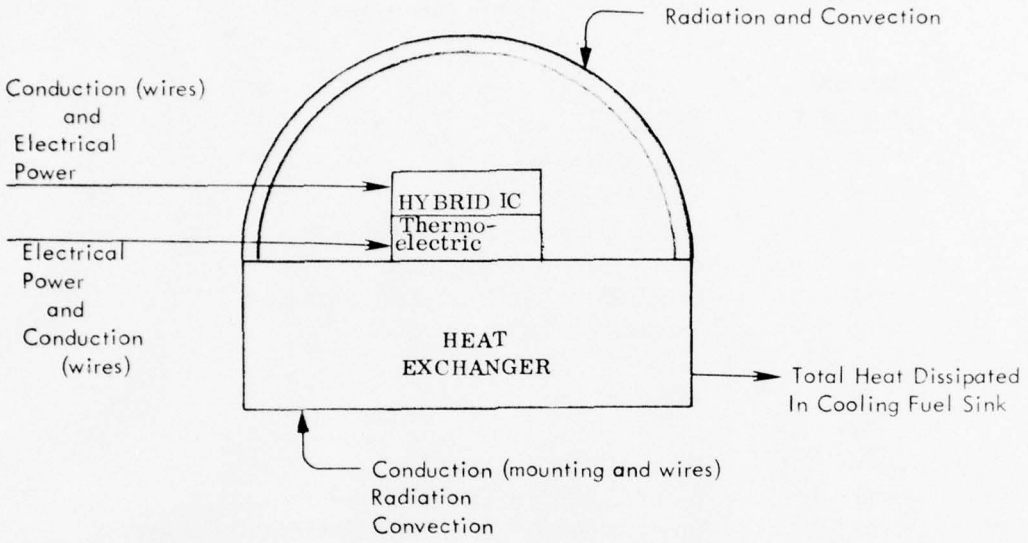

Figure 7 -- Simplified Thermally Conditioned Module Schematic

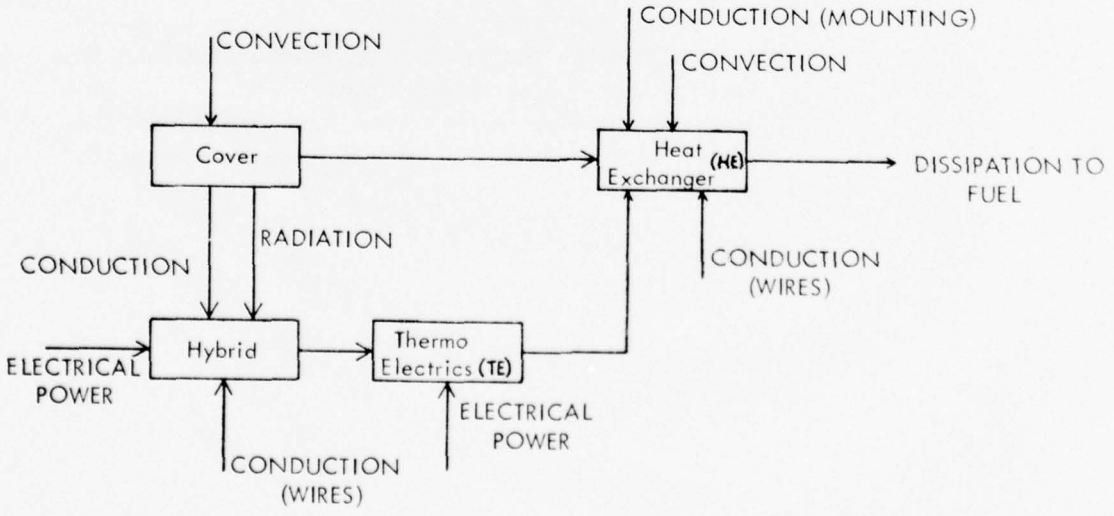

Figure 8 -- Thermally Conditioned Module Thermal Transfer Mechanisms

TABLE 1

Thermocouple Locations

Thermal Couples #	Location
1	Fuel Exit Port
2	Fuel Inlet Port
3	Outer Cover -- Fuel Inlet Side
4	Outer Cover -- Top Side
5	Outer Cover -- Fuel Exit Port Side
6	Electrical Connector Shell
7	Not used
8	
9	
10	Inner Cover - Center
11	Inner Cover -- Fuel Inlet Side
12	Inner Cover -- Fuel Inlet Side Near Flange
13	Hybrid Circuit Cover
14	Hybrid Circuit Mounting Flange
15	Thermoelectric Cooler -- Cold Junction
16	Thermoelectric -- Hot Junction
17	Not used
18	
19	
20	Downstream Ambient Air -- Near Fuel Inlet Port Side
21	Ambient Air -- Near Outer Cover - Top
22	Upstream Ambient Air -- Near Fuel Outlet Port Side
23	Inner Cover -- Fuel Exit Port Side -- On Flange
24	Module Base

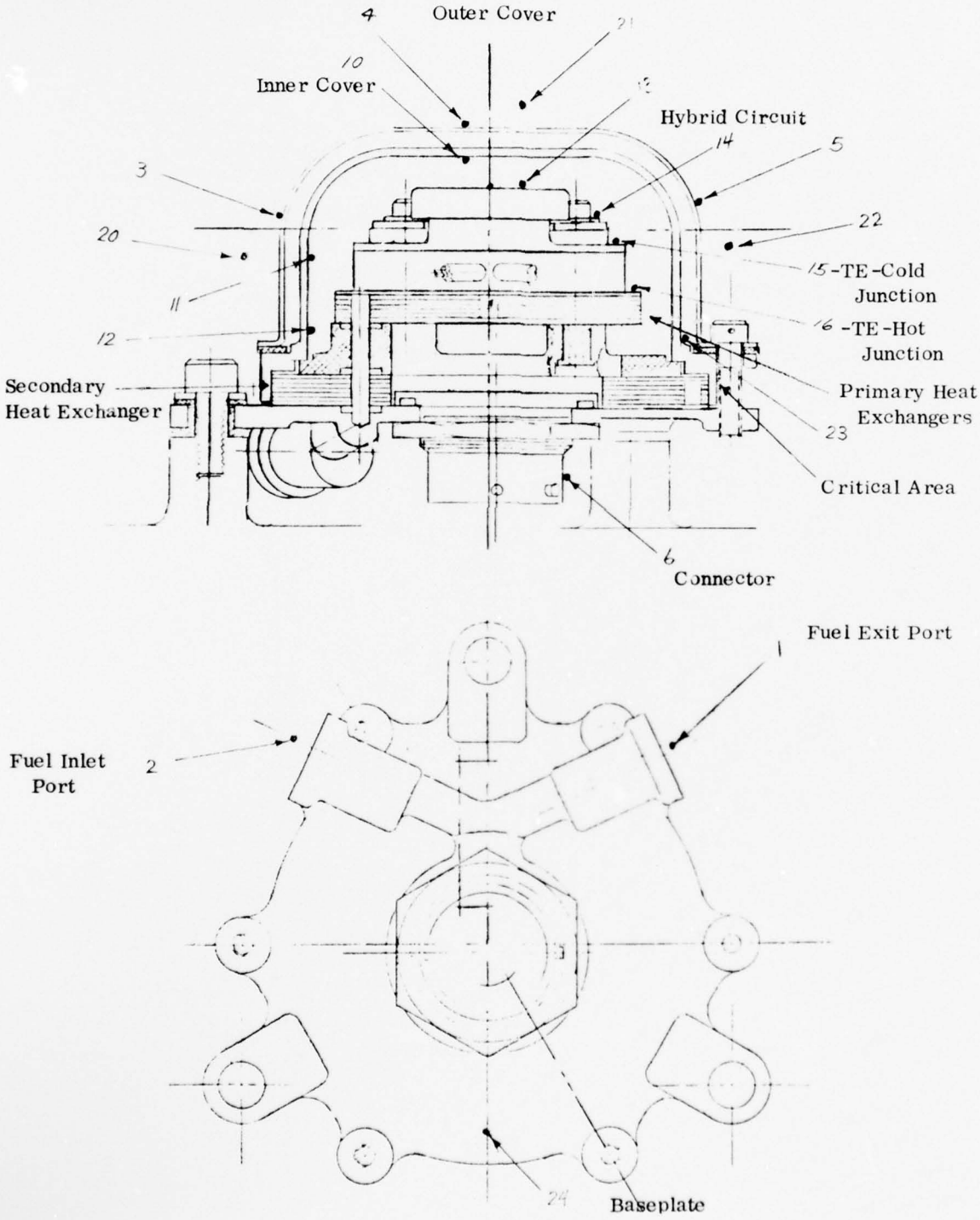

Figure 9 -- Thermocouple Test Locations

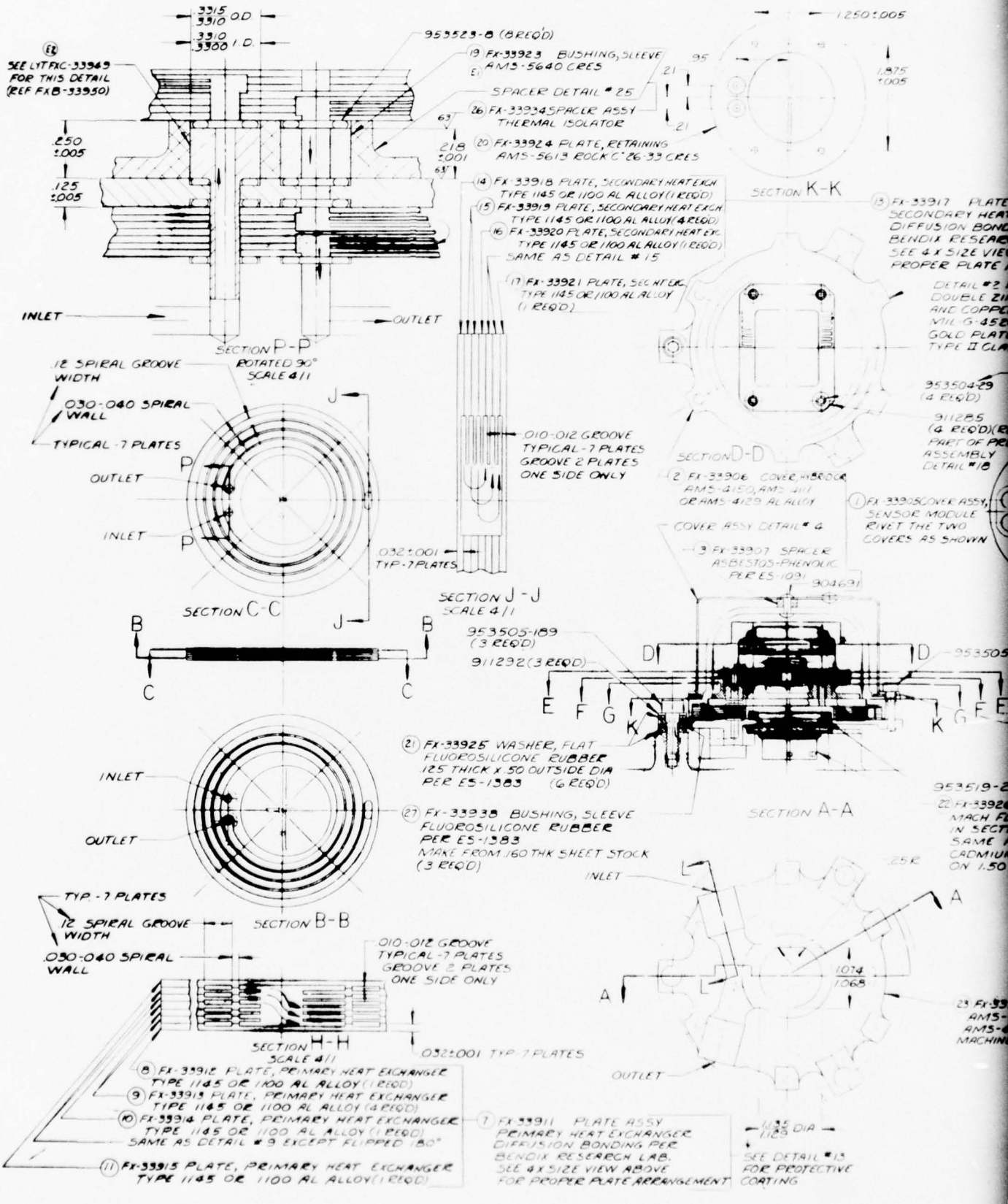
SEE LYTTIC-33949 FOR THIS DETAIL (REF FXB-33950)
.3315 .3310 O.D.
.3310 .3300 I.D.
.250 ±.005
.125 ±.005
955529-8 (8 REQ'D)
(19) FX-33923 BUSHING, SLEEVE AMS-5640 CRES
SPACER DETAIL # 25
(26) FX-33934 SPACER ASSY THERMAL ISOLATOR
(20) FX-33924 PLATE, RETAINING AMS-5613 ROCK C 26-33 CRES
.218 ±.001
(14) FX-33918 PLATE, SECONDARY HEAT EXCH TYPE 1145 OR 1100 AL ALLOY (1 REQ'D)
(15) FX-33919 PLATE, SECONDARY HEAT EXCH TYPE 1145 OR 1100 AL ALLOY (4 REQ'D)
(16) FX-33920 PLATE, SECONDARY HEAT EX. TYPE 1145 OR 1100 AL ALLOY (1 REQ'D)
SAME AS DETAIL # 15
(17) FX-33921 PLATE, SECHTER TYPE 1145 OR 1100 AL ALLOY (1 REQ'D)
INLET
OUTLET
SECTION P-P ROTATED 90° SCALE 4/1
.12 SPIRAL GROOVE WIDTH
.030-.040 SPIRAL WALL
TYPICAL -7 PLATES
OUTLET
INLET
.010-.012 GROOVE TYPICAL -7 PLATES GROOVE 2 PLATES ONE SIDE ONLY
.032±.001 TYP-7 PLATES
SECTION C-C
SECTION J-J SCALE 4/1
953505-189 (3 REQ'D)
911232 (3 REQ'D)
(21) FX-33925 WASHER, FLAT FLUOROSILICONE RUBBER .125 THICK x .50 OUTSIDE DIA PER ES-1383 (6 REQ'D)
(27) FX-33938 BUSHING, SLEEVE FLUOROSILICONE RUBBER PER ES-1383 MAKE FROM .160 THK SHEET STOCK (3 REQ'D)
SECTION A-A
SECTION B-B
TYP. -7 PLATES
.12 SPIRAL GROOVE WIDTH
.030-.040 SPIRAL WALL
.010-.012 GROOVE TYPICAL -7 PLATES GROOVE 2 PLATES ONE SIDE ONLY
SECTION H-H SCALE 4/1
.032±.001 TYP-7 PLATES
(8) FX-33912 PLATE, PRIMARY HEAT EXCHANGER TYPE 1145 OR 1100 AL ALLOY (1 REQ'D)
(9) FX-33913 PLATE, PRIMARY HEAT EXCHANGER TYPE 1145 OR 1100 AL ALLOY (4 REQ'D)
(10) FX-33914 PLATE, PRIMARY HEAT EXCHANGER TYPE 1145 OR 1100 AL ALLOY (1 REQ'D) SAME AS DETAIL # 9 EXCEPT FLIPPED 180°
(11) FX-33915 PLATE, PRIMARY HEAT EXCHANGER TYPE 1145 OR 1100 AL ALLOY (1 REQ'D)
(7) FX-33911 PLATE ASSY PRIMARY HEAT EXCHANGER DIFFUSION BONDING PER BENDIX RESEARCH LAB. SEE 4 X SIZE VIEW ABOVE FOR PROPER PLATE ARRANGEMENT
1.250±.005
.95
.21
1.875 ±.005
SECTION K-K
(13) FX-33917 PLATE SECONDARY HEAT DIFFUSION BOND BENDIX RESEAR SEE 4 X SIZE VIE PROPER PLATE
DETAIL #2 DOUBLE NI AND COPPE MIL-G-45 GOLD PLAT TYPE II CLA
953504-29 (4 REQ'D)
911285 (4 REQ'D)(R PART OF PR ASSEMBLY DETAIL #18
SECTION D-D
(2) FX-33906 COVER, HYBRID AMS-4150, AMS-4111 OR AMS-4129 AL ALLOY
(1) FX-33905 COVER ASSY, SENSOR MODULE RIVET THE TWO COVERS AS SHOWN
COVER ASSY DETAIL # 4
(3) FX-33907 SPACER ASBESTOS-PHENOLIC PER ES-1091
904631
953505
953519-2
(22) FX-3392
MACH F
IN SECT
SAME
CADMIU
ON 1.50
.25R
INLET
OUTLET
1.074
1.068
(23) FX-33
AMS-
AMS-4
MACHIN
1.135 DIA
1.128
SEE DETAIL #13 FOR PROTECTIVE COATING

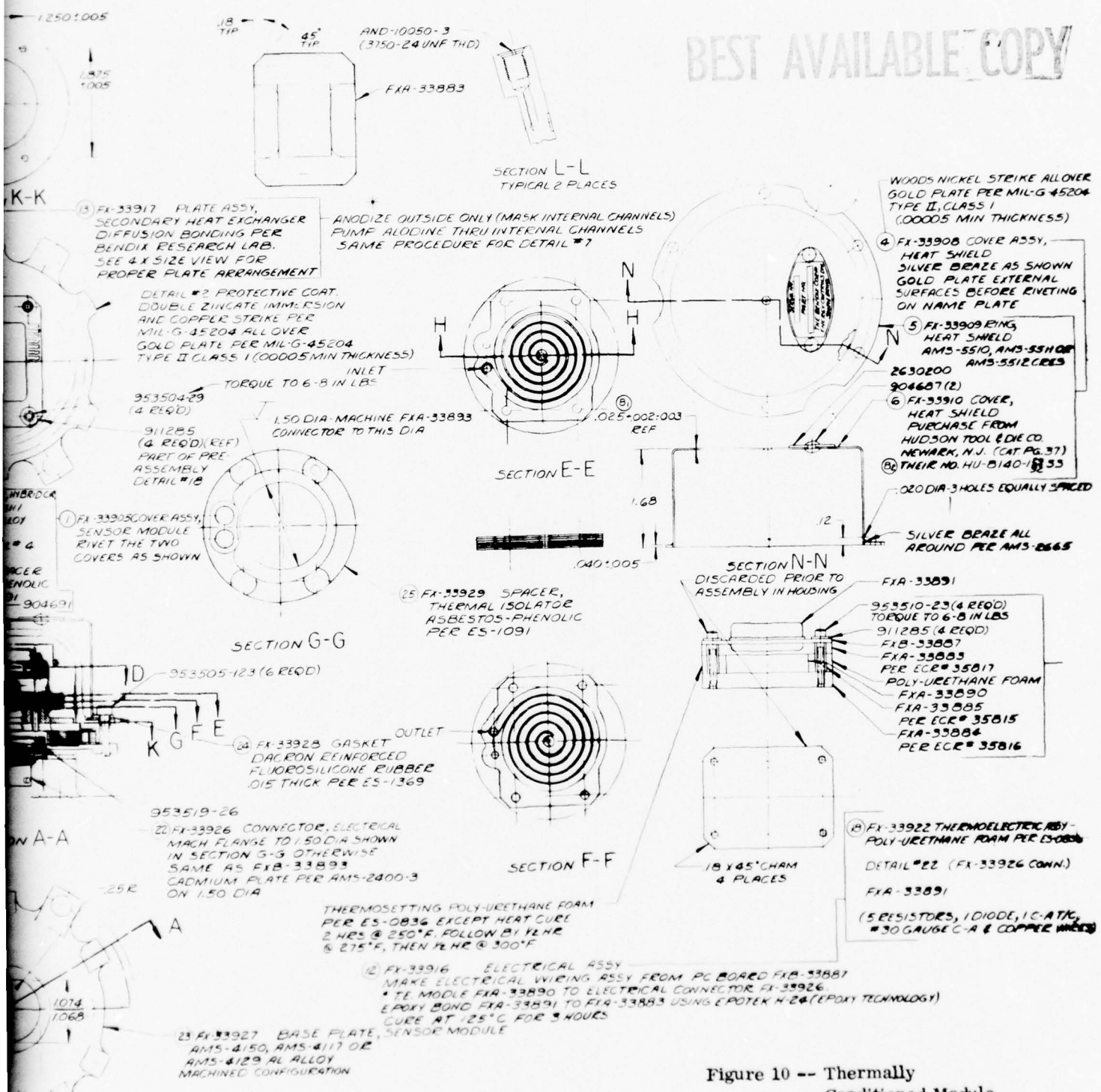

Figure 10 -- Thermally Conditioned Module (FXD-33900)

The hybrid electronics to be cooled are packaged in a 1.25" x 1.25" x 0.25" Kovar package. These circuits, with housing, are mounted on a printed circuit card of 1.75" x 2.25". A cold plate is attached to the printed circuit board and is in direct contact with the electronic package and the cold junction of the thermoelectric cooler. Cooling flow circulation is into the primary heat exchanger (in contact with the T.E. hot junction) and then thru the secondary heat exchanger to the exit port.

The heat exchangers are shown in Figures 11 and 12 . Figure 11 is the primary heat exchanger (also called #1 heat exchanger). The thermoelectric unit is mounted on the primary heat exchanger. The entering cooling flow to the unit is channeled immediately to this primary heat exchanger. The cooling flow after passing through the primary heat exchanger then passes to the secondary heat exchanger (Figure 12) which is mounted to the base plate and is "doughnut" shaped to accommodate the connector in the center of the base plate.

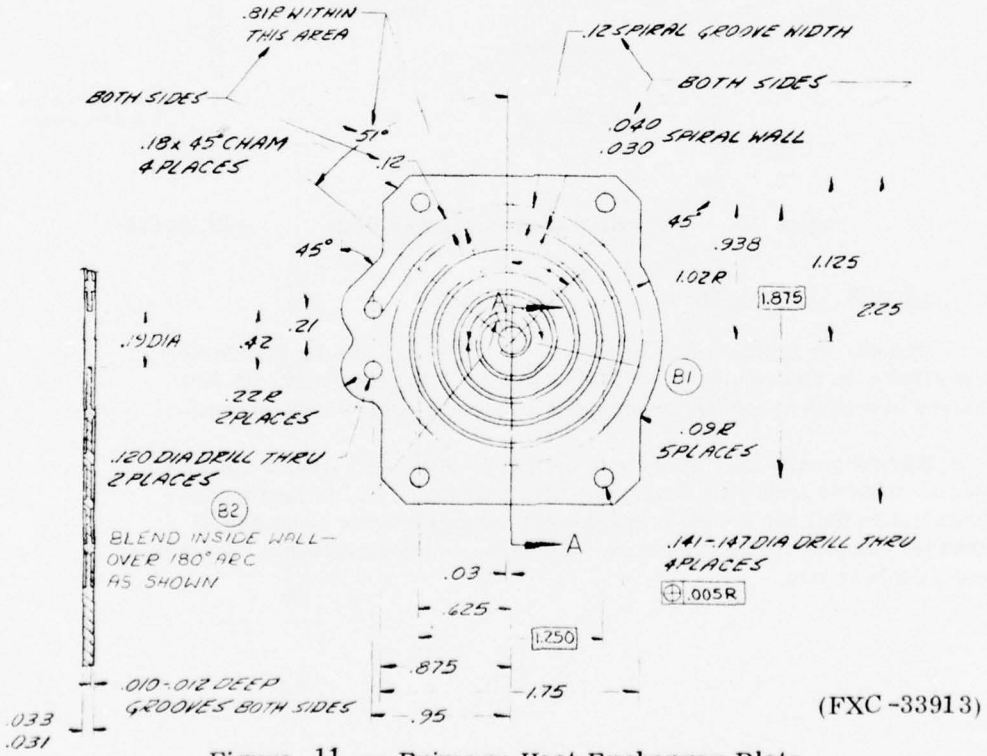

Figure 11 -- Primary Heat Exchanger Plate

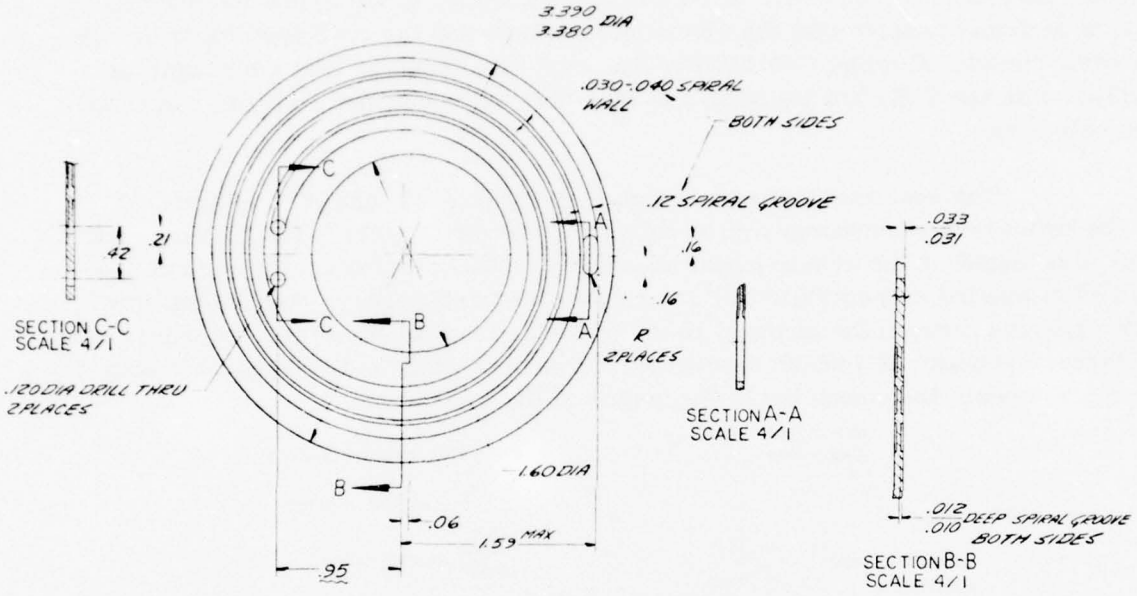

Figure 12 -- Secondary Heat Exchanger Plate (FXC-33919)

3.2. DESIGN APPROACH

The design is illustrated in Figure 9. The use of a thermoelectric heat pump allows the electronics to operate at low temperatures even with fuel temperatures in excess of the maximum rated level for electronic components.

Environmental heat transfer to the region of the electronics must be minimized in order to reduce the thermoelectric heat load. At low heat loads the thermoelectirc unit can maintain the electronic temperatures about 100° F cooler than the entering fuel temperature. This temperature differential decreases with increasing heat load.

Dual heat exchangers and a double wall cover are used to keep the heat load pumped by the thermoelectrics to a minimum. The inner cover is thermally anchored to the secondary heat exchanger and insulated from the outer cover. The objective is to hold the inner cover at or near the cooling fuel temperature. This arrangement shrouds the hybrid circuit and thermoelectric unit in a temperature environment which is essentially equal to that of cooling fuel. The environmental heat is effectively blocked from penetrating this shroud and, therefore, the temperature in this critical space and the heat load that must be pumped by the thermoelectric unit are basically independent of the air temperature surrounding the package. The incoming cooling fuel is routed first to the primary heat exchanger and then to the secondary heat exchanger. This provides a primary heat exchanger temperature very nearly equal to that of incoming fuel. The electronic circuit is mounted directly on the cold plate which is in direct contact with the thermoelectric cooling element.

The design goals of the project were based upon projections of requirements for future high performance aircraft installations. These projections indicate fuel temperatures that are normally below 275° F for the major portions of the aircraft missions but with short term excursions to 330° F at some corner point conditions. The limiting operation temperature of silicon base electronic components is 257° F (125° C). The thermal conditioning must thus maintain temperatures at or below this limit for the most severe conditions. Assuming the maximum temperature rise of 5° F between the cold plate and the electronic components, the limiting cold plate temperature is then 252° F. Under these conditions, the thermoelectric unit must be capable of pumping the heat load from the 252° F cold plate to the 330° F primary heat exchanger, i.e., against a 78° F adverse temperature differential.

For long term reliability of electronic components, it is desirable that component temperature be maintained substantially below the 257° F limit under normal operating conditions. A design goal of the project was to maintain component temperatures below 170° F (cold plate temperature below 165° F) for a fuel temperature of 275° F. This goal requires that the thermoelectric unit be designed to pump the heat load against a 110° F adverse temperature differential. The major heat load source is the heat that is transferred from the inside cover to the electronic circuit and cold plate. This load varies proportionately with the temperature differential between the cold plate and the cover which is essentially equal to the fuel temperature. The design condition thus requires the capability of pumping 40% more heat load against a 40% higher adverse temperature differential than a design based only on maintaining component temperatures below the limiting value. In addition to the reliability consideration, the lower component operating temperatures provide a margin to accommodate heat soak following engine shut down.

Design calculations were made for the following conditions:

Ambient air temperature	750° F
Ambient air velocity	50 ft/sec.
Cooling fuel temperature	275° F
Cooling fuel flow rate	100 lbs/hr.

The analytical heat balance was targeted for:

Thermoelectric cold plate temperature	165° F
Temperature difference cold plate to fuel	110° F

The heat balance analysis based on the above inputs and design targets can be summarized as follows:

1. Heat Load to Thermoelectric Element

· Generated heat -hybrid circuit	2.5 BTU/hr
· Radiated & conducted heat to cold plate	10.3 BTU/hr
TOTAL	12.8 BTU/hr

To meet design targets, this establishes a requirement that the thermoelectric unit meet a requirement of 110° F temperature differential with a 12.8 BTU/hr heat pumping load.

2. Heat Load to Primary Exchanger

· Thermoelectric Pump Load (Item 1 above)	12.8 BTU/hr
· Power to Thermoelectrics	171.0 BTU/hr
TOTAL	183.8 BTU/hr

This sets a requirement for the primary heat exchanger. With a design flow of 100 lbs/hr of fuel, the fuel temperature rise would be 3.7° F.

3. Heat Load to Secondary Heat Exchanger

· Conduction from Inner Cover	81.0 BTU/hr
· Conduction through base	1210.0 BTU/hr
TOTAL	1291.0 BTU/hr

This results in 25.8° F temperature rise in the secondary heat exchanger. Total fuel temperature rise per analysis is then 29.5° F.

Details of the design analysis are presented in a later subheading of Section III.

The test and design analysis are compared in the following table. Test data is taken from the data used to plot Figure 13.

Location in Module	Design Estimate °F	Test Results °F
Ambient	750	750
Outer Cover	713	750/680
Inner Cover	318	330/290
Thermoelectric Unit		
Cold Plate	169	175
Hot Plate	279	*
Hybrid Electronics	174	185
Temperature difference		
Cold plate to primary heat exchanger	110	90
Fuel Inlet Temperature	275	275
Cooling Fuel Flow	100 lbs/hr	100 lbs/hr
Fuel Discharge Temperature	305	*

*Test data temperatures not reliable. Locations were such that radiated and conducted heat resulted in erroneous readings.

In general, the correlation between the theoretical analysis and empirical data is reasonable. The high measured temperature drop of 10° F between the hybrid electronics and the cold plate indicates that the thermal resistance between these elements is twice the estimated value.

3.3. TEST RESULTS

Tests were run with the unit mounted in an air chamber with force flow to obtain the test velocity of 50 ft/sec. A hydrogen burner with exhaust gas mixed with room temperature air was used to obtain the module ambient temperature for testing. The module was instrumented with thermocouples as shown in Figure 9. The thermoelectrics were maintained at 8 amps during the test. A photograph of the test equipment showing the hydrogen burner is given in Figure 13.

Test emphasis was on the high temperature fuel and air conditions. The cooling fuel temperature was set initially to 150° F and the ambient air (air blown past the module) was increased in steps to 750° F. At each test point, data was monitored until thermocouple readings stabilized and then the data was recorded. Stabilization was reached in about three (3) minutes. The recorded temperatures are shown in

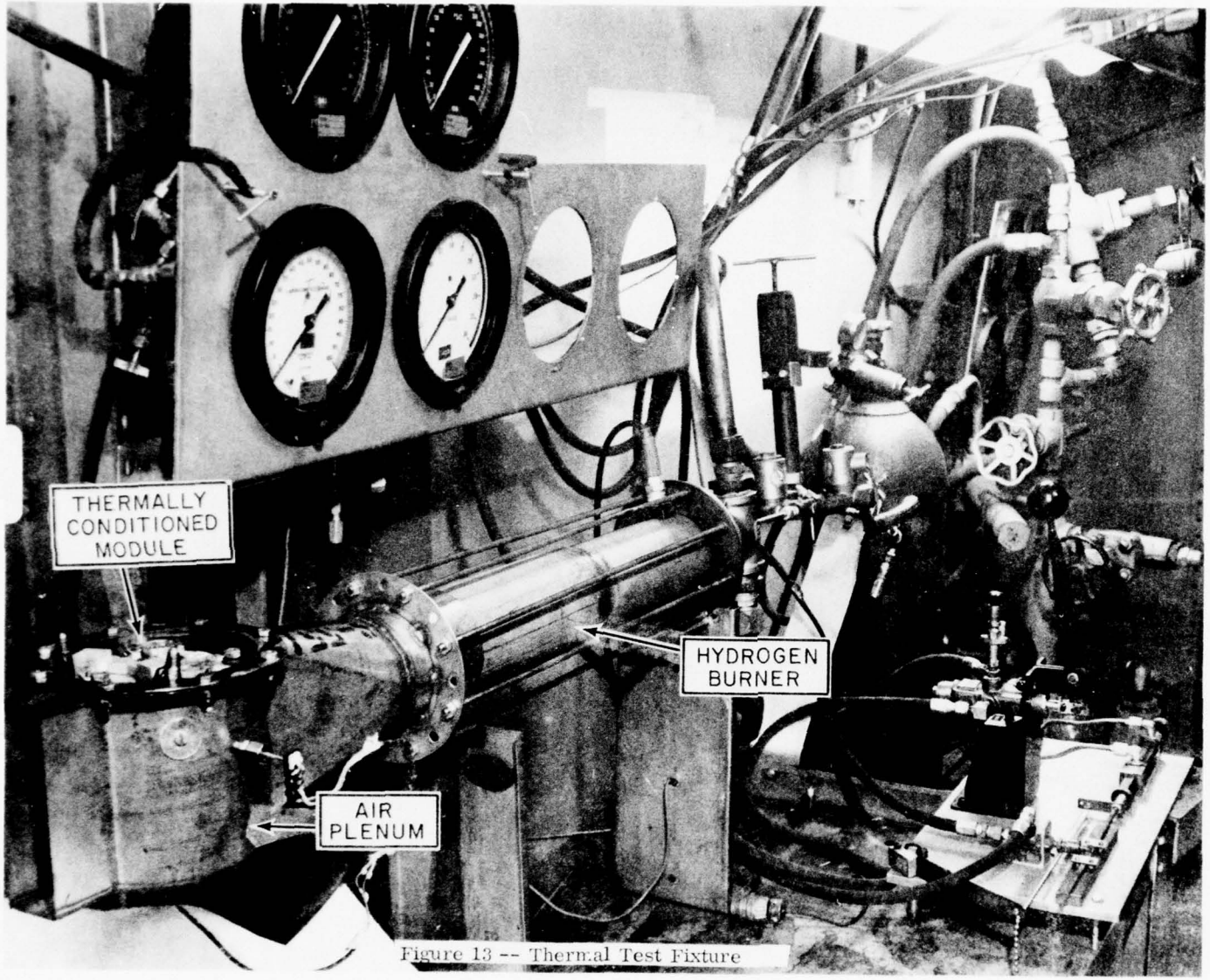

Figure 13 -- Thermal Test Fixture

Figure 14 for these tests. It is seen that the PC board temperature increases only about 35° F for a 700° F increase in the ambient air temperature. This demonstrates the effectiveness of the thermal shield provided by the double cover arrangement.

Tests were also run in which the ambient air temperature was held at 750° F and the fuel temperature varied in steps of 50° F to a maximum of 300° F. The results given in Figure 15 shows that the temperature of the electronics increases in a nearly one-to-one relationship with fuel temperature increase, as would be expected. The electronic circuits ran 80 to 90° F cooler than the entering fuel temperature. The PC board and cold plate temperatures were measured at the edge since it was not possible to locate thermocouples elsewhere. The temperatures shown on the curves for these locations are as much as 50° F higher than at the center of these members.

Note that on Figure 15 the thermocouple locations are marked on the curve. On the inner cover the temperature gradient is such that temperature decreases as the anchor point to the secondary heat exchanger is approached. Orientation of the outer cover thermocouple was such that #5 was on the upstream side of the cover and #3 is on the downstream side of the cover. The thermocouple directly on the top gave the lowest reading.

3.3.1. Initial Testing

The first set of test data is shown on curves of Figures 16 and 17 with some special tests shown on the curve of Figure 18.

The same procedure and sequence was used as described for the second (final) test set already discussed.

Several minor hardware modifications were found to be necessary from these initial test results. These changes were made which provided significant performance improvements.

The difference is clearly indicated by comparing Figures 17 and 15. In the first test set, temperatures are higher at all locations; the T. E. cold plate was within 10° F of the inlet cooling fuel temperature, and the cold plate had reached a temperature of 240° F at the 250° F cooling fuel temperature.

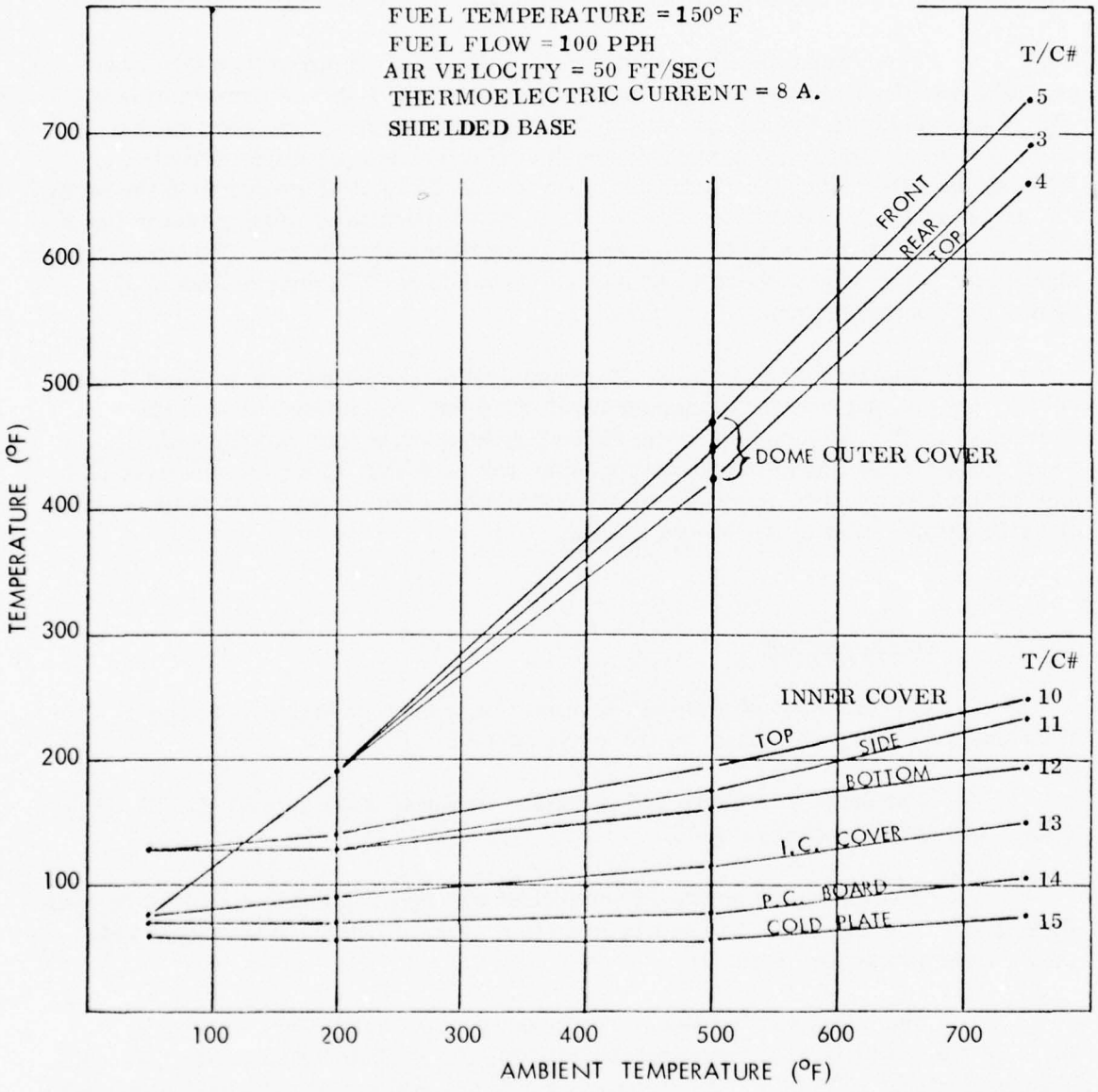

Figure 14 -- Test Results - Temperature Distribution with Constant 150° F Fuel Temperature

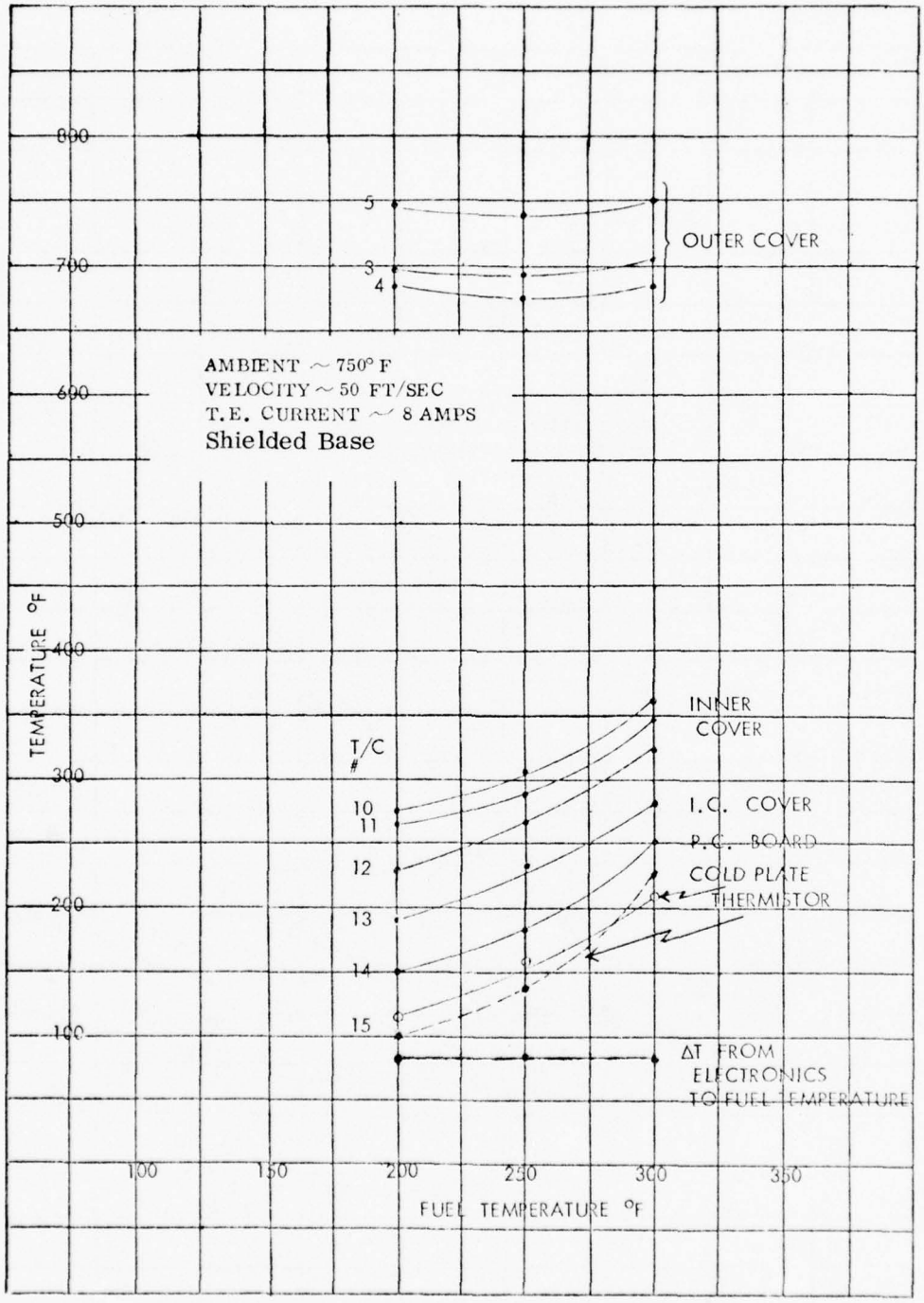

Figure 15 -- Test Results - Temperature Distribution with Constant 750° F Ambient Air Temperature

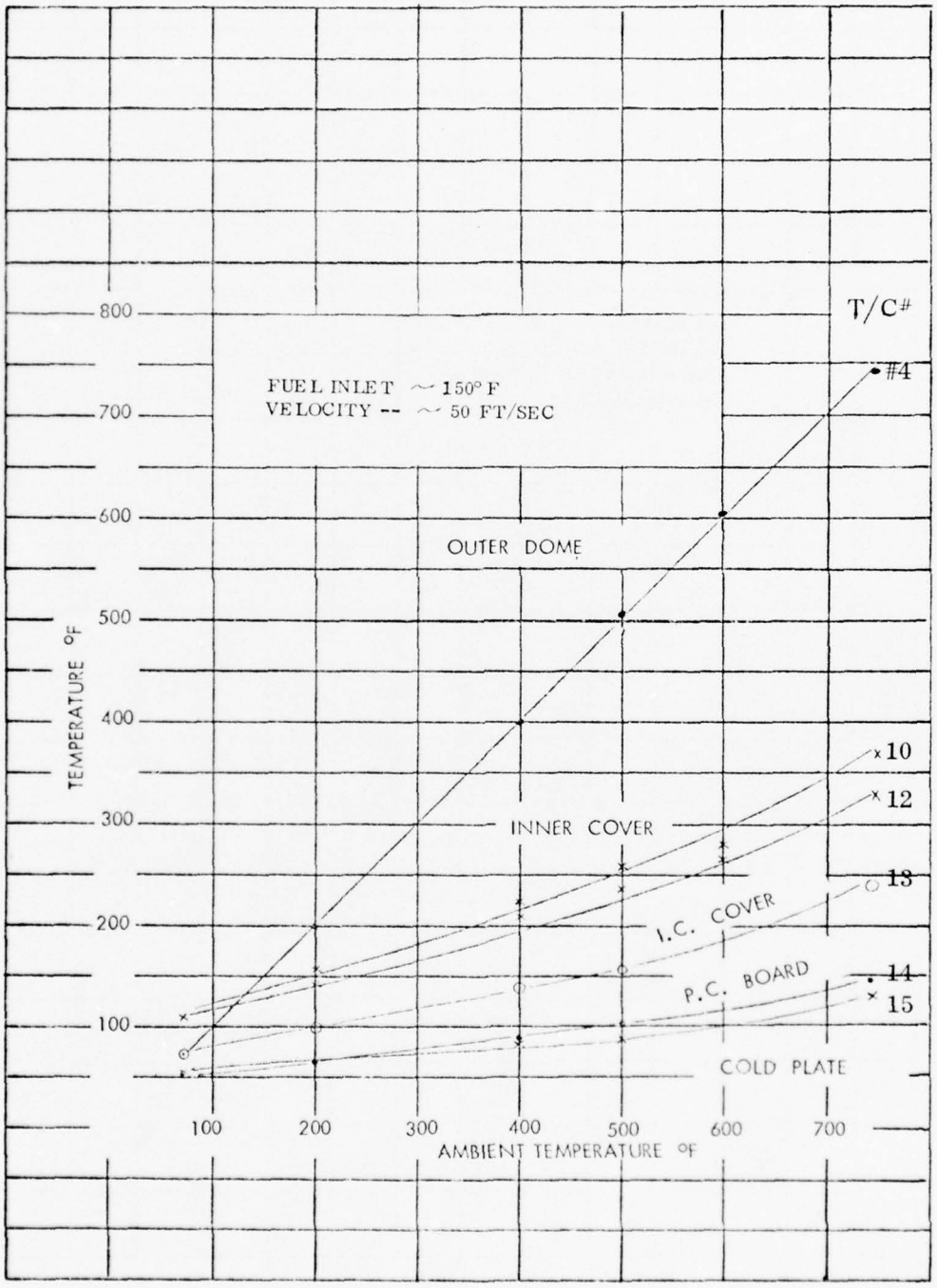

Figure 16 Initial Test Results - Temperature Distribution with 150° F Constant Fuel Temperature

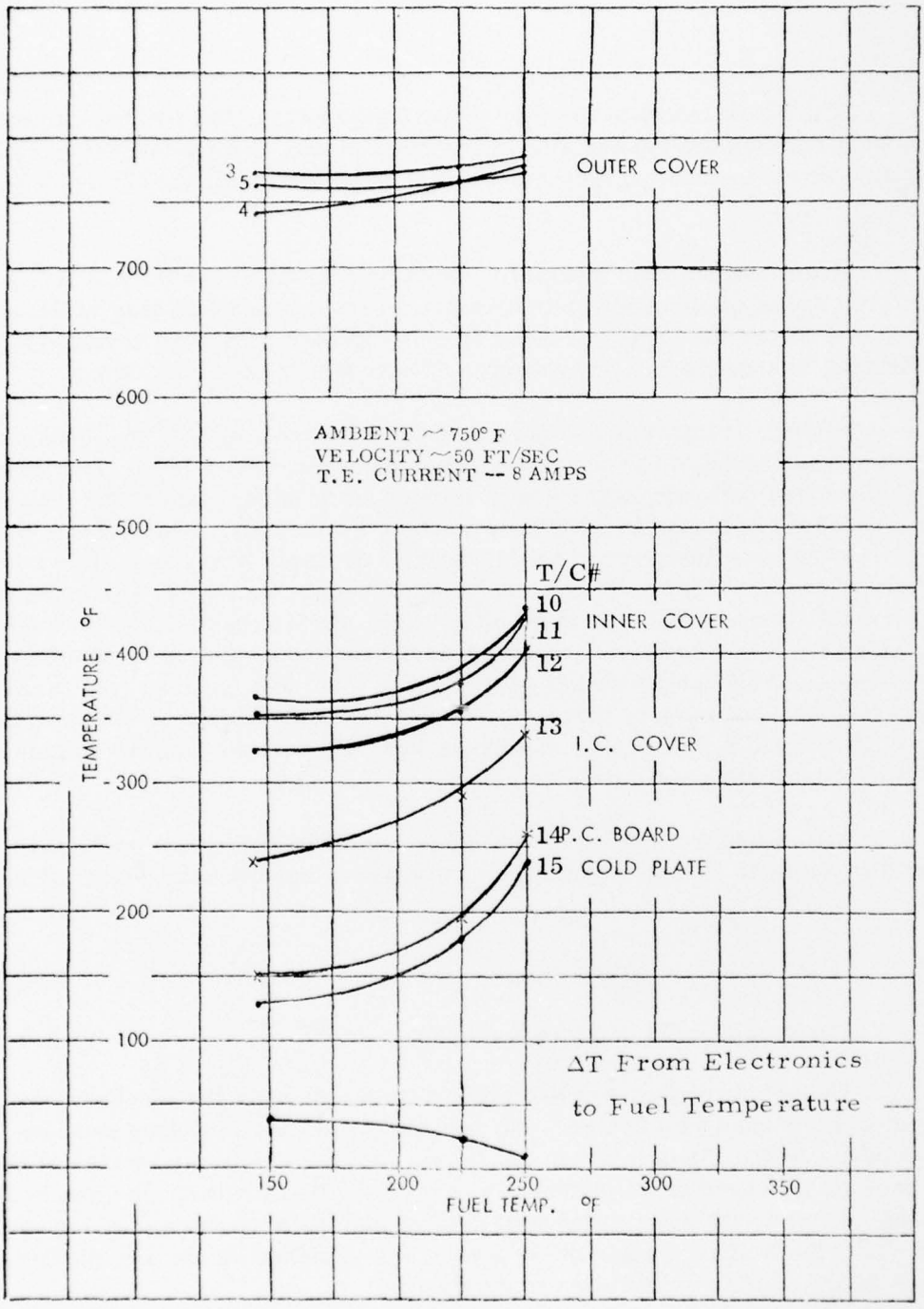

Figure 17 Initial Test Results Temperature Distribution with Constant 750°F Ambient Temperature

The sharp increase in inner cover temperature, the reversal in temperature gradient between the top and side of the inner cover, and the inner cover being significantly above the cooling fuel temperature were inconsistent with the design analysis.

Examination of the thermally conditioned module and the test set up indicated two areas which needed modification. First a rivet was used at the top of the dome to fasten the inner and outer covers together. This was removed as being structually unnecessary and a source of heat flow to the inner cover.

Second, it had been assumed in the design analysis that the inner cover was thermally anchored to the secondary heat exchanger. As designed and tested it was obvious that the inner cover where it extended from the side of the secondary heat exchanger was exposed to the direct ambient air velocity. This area is noted on Figure 3-3 as a critical area. As this area of the inner cover is readily protected (and assumed protected in the design analysis), a simple test baffle was made to provide a dead air space between this critical area and the ambient. This baffle also shielded the lower surface of the secondary heat exchanger. The shielding of the secondary heat exchanger should only effect the fuel temperature rise through the secondary heat exchanger; therefore, there would be little or no effect on the cooling of the hybrid circuit. It is also noted that this surface could be shielded in an actual installation in a similar manner.

The second set of data shown (and previously discussed) on Figures 14 and 15 was then run with results significatnly better and very near the design objectives.

3.3.2. Thermoelectrics Used as Heaters

The hybrid circuit was designed in such a manner that the thermoelectrics could be used as a heater. The circuit is discussed in other sections of this report. Here it is only noted that the thermistor which was located in the hybrid package was used as an indicator to switch the thermoelectrics from cooling to heating. Prior to the start of the first test set as shown on curves of Figures 16 and 17, the heating portion of the circuit was disabled as the test emphasis was to be on the cooling capabilities of the design.

It was not until the second test set that the thermistor was calibrated and read out on the instrumentation. Therefore, no temperatures inside the hybrid package were obtained during the first test set.

Some testing of the unit was done with heating circuit operative and results are shown on the curve of Figure 18. The data points at -60° F and 0° F fuel clearly indicated the effectiveness the thermoelectric elements as a heater.

Probably the most interesting test point is that shown with 330° F fuel and ambient surrounding the module. At this test condition, the thermoelectric elements were in cooling mode. The cold plate temperature is at 245° F.

This test point emphasizes the "reverse" heat transfer characteristics of the device. That is, the inner and outer covers form a barrier to heat transfer regardless of whether the high temperature is fuel inside the heat exchangers or high ambient temperatures outside. It can be seen from this test point, the "cooling" fuel is a heat source and the inner cover is being cooled by heat flow to the outer cover and ambient.

In Figure 18 the curves are not interpolated between the heating mode test data at -60° F and 0° F fuel temperature, and the cooling mode test data at 330° F fuel temperature.

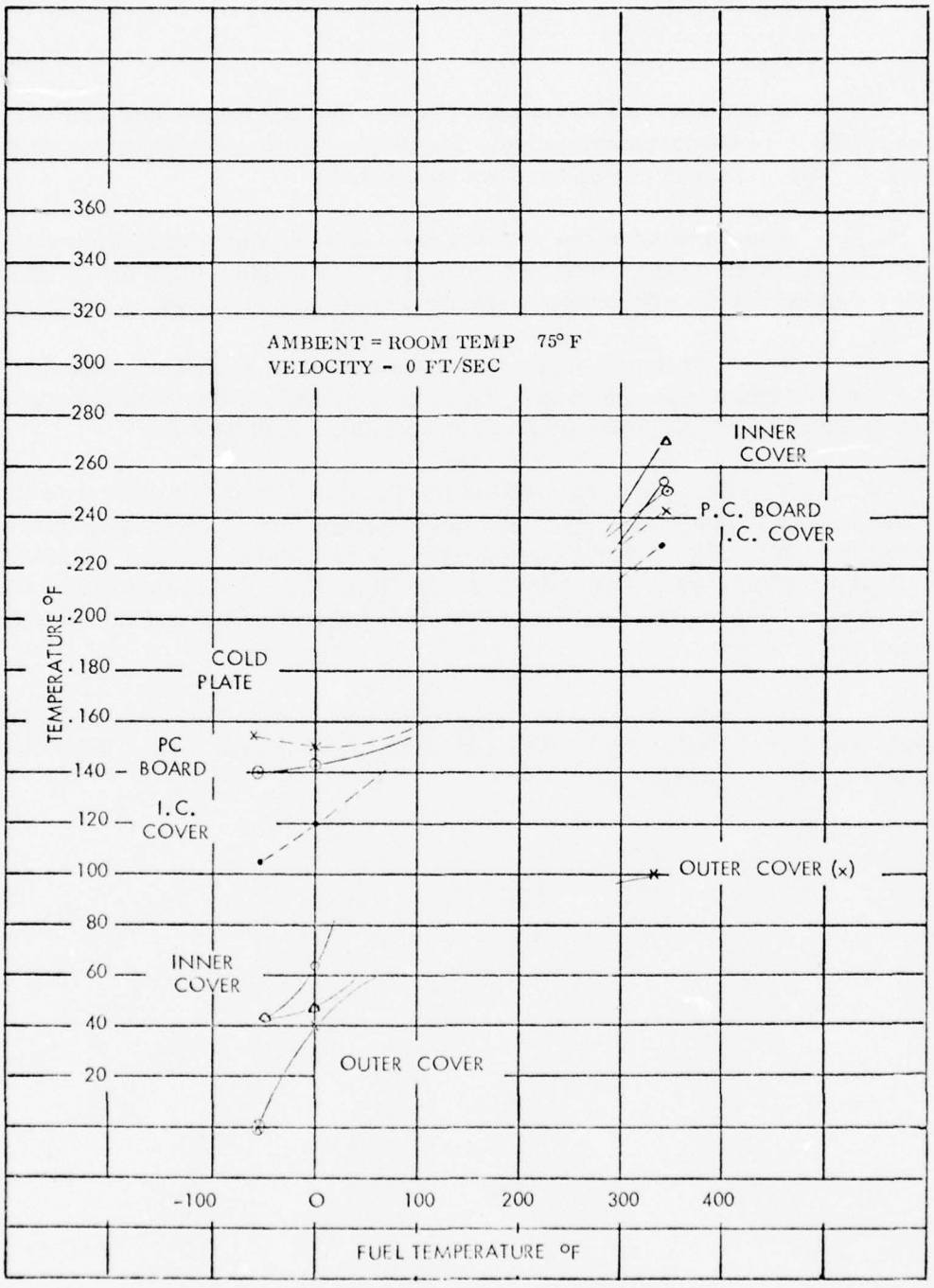

Figure 18 Initial Test Results Fuel Temperature Extremes Hot/Cold Fuel Tests

3.4. THERMAL ANALYSIS

The thermal analysis performed on the module was based upon the thermal model shown in Figure 19. This is a linear analog model in which thermal resistance are represented by electrical resistance and temperatures are represented by voltage levels. The thermal resistances identified in the simplified model of Figure 19 are actually lumped parallel and series restrictors for the various heat transfer mechanisms that occur between the temperature points shown. The thermoelectric heat pump is simulated by a battery with its potential and polarity matched to the expected performance of the thermoelectric unit. The ambient and entering fuel temperature levels are simulated by appropriate voltage sources and the electrical power dissipation in the hybrid circuit and thermoelectrics are simulated by appropriate current generators. The "Super Sceptre" circuit analysis computer program was used to compute temperatures at various locations within the module and the corresponding heat transfer rates between these locations. Input and boundary conditions used for the analysis are as follows:

Ambient Temperature	750° F
Inlet Fuel Temperature	275° F
Ambient Air Velocity	50 ft/sec.
Cooling Fuel Flow Rate	100 lbs/hr.
Thermoelectric Temp. Potential	110° F
Power Dissipation in Hybrid Circuit (Q_4)	2.5 BTU/hr.
Power Dissipation in Thermoelectric Unit (Q_6)	171 BTU/hr
Thermoelectric Current	8 Amps

The temperatures of each member of the module is represented by a discrete point temperature which is intended to represent the average temperature of that member. The calculations for the various thermal resistances between the temperature points are given in the following subsections. The notational convention used is as follows:

1. The heat flow (BTU/hr) between a point "n" at temperature, T_n, and a point "m" at temperature, T_m, is denoted by Q_{n-m}.

2. The thermal resistance (° F/BTU/hr) between these same points is denoted R_{n-m}.

3. The relationship between Q_{n-m}, R_{n-m}, T_m and T_n is then:

$$T_n - T_m = Q_{n-m} \times R_{n-m}$$

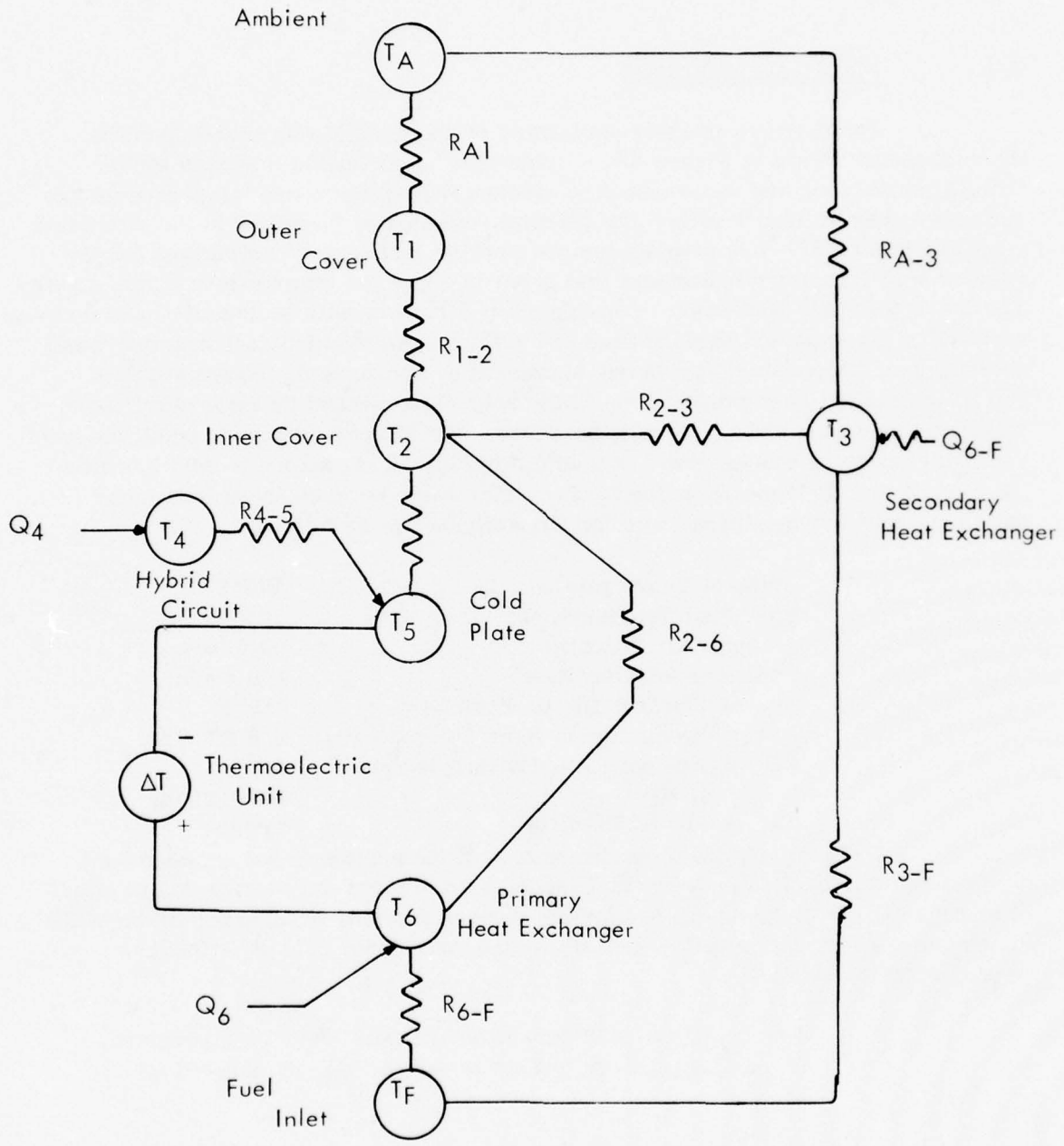

Figure 19 -- Thermal Simulation Model

3.4.1. Ambient Heat Transfer (R_{A-1} and R_{A-3})

The ambient heat transfer to exterior surfaces of the module is primarily due to forced convection. In the Reynold's number range from 25 to 100,000, the equation recommended by the Adams[1] for calculating the heat transfer coefficient, h, for spherical shaped bodies is

$$h_A = .37\ K/D\left(\frac{\rho VC}{\mu}\right)^{.6},$$

where

K = = thermal conductivity of air (.0277 BTU/ft hr° F),

D = effective diameter of module (.3 ft),

ρ = ambient air density (.0328 lbs/ft^3),

V = ambient air velocity (50 ft/sec),

μ = dynamic viscosity of air (2.15×10^{-5} lb/ft sec).

The Reynolds No. ($\rho VP/\mu$) is equal to 22,883 and the heat transfer, h_A, is equal to 14.1 BTU/ft^2 hr ° F.

The outer cover has a surface area, A_1, of .18 ft^2 and the remainder of the module has an exposed surface area, A_3, of .19 ft^2. The thermal resistance R_{A-1} and R_{A-3} are then:

$$R_{A-1} = \frac{1}{h_A A_1} = .394\ ° F/BTU/hr,$$

$$R_{A-3} = \frac{1}{h_A A_3} = .373\ ° F/BTU/hr.$$

3.4.2. Heat Transmission to Inner Cover (R_{1-2})

The heat transmission between the outer and inner cover is due to conduction and radiation across the air gap between them. The thermal resistance, R_{1-2}, is equivalent to parallel conduction and radiation resistances, $(R_{1-2})_c$, and $(R_{1-2})_r$.

[1] McAdams, Heat Transmission, 3rd ed. (New York: McGraw-Hill Book Co., Inc., 1953)

respectively. The conduction resistance is determined from the equation

$$(R_{1-2})_c = L/KA_2,$$

where

K = thermal conductivity of air in the gap (.02 BTU/ft hr ° F),

A_2 = surface area of inner cover (.128 ft^2).

L = air gap thickness (.0125 ft).

The conduction resistance, $(R_{1-2})_c$ is then 4.88° F/BTU/hr. The radiation resistance is established by linearizing the radiation equation about the approximate temperatures of the outer cover, T_1 = 1163° R, and the inner cover, T_2 = 760° R. The radiation equation is:

$$(Q_{1-2})_r = \sigma Fe\, A_2(T_1^4 - T_2^4) = (T_1 - T_2) / (R_{1-2})_r,$$

where

σ = Stefan - Boltzmann constant (.173 x 10^{-8} BTU/ft^2 hr° R^4),

Fe = the emmisivity factor (.04),

A_2 = inner cover surface area (.128 ft^2),

The radiation resistance term is then:

$$(R_{1-2})_r = \frac{(T_1 - T_2)}{\sigma Fe A_2(T_1^4 - T_2^4)} = 30.3° \text{ F/BTU/hr}$$

Therefore

$$R_{1-2} = \frac{1}{1/(R_{1-2})_c + 1/(R_{1-2})_r} = 4.2° \text{ F/BTU/hr}$$

Using approximate values of $T_2 = 760°$ R, and $T_5 = 625°$ R, we have

$(R_{2-5})_c = 15.6\,°$ F/BTU/hr,

and

$(R_{2-5})_r = 167\,°$ F/BTU/hr.

Therefore,

$R_{2-5} = 14.4\,°$ F/BTU/hr

The thermal resistance between the inner cover and region of the primary heat exchanger are calculated in similar manner, using an approximate value for T_6 of 735° R to yield

$(R_{2-6})_c = 15.6°$ F/BTU/hr,

$(R_{2-6})_r = 135°$ F/BTU/hr,

and finally

$R_{2-6} = 14.0.$

For that portion of the inner cover heat flow that conducts through metal down to the secondary heat exchanger, Q_{2-3}, it is necessary to specify an effective conduction length. From the physical arrangement, this length is estimated as 1 inch.

Beside the resistance produced by the metal cover, there is an interface resistance between the inner cover base and the heat exchanger. This resistance is assumed to be equivalent to that of an air gap .0005 inch thick. The resistance R_{2-3} is then the sum:

$R_{2-3} = (R_{2-3})$ metal + (R_{2-3}) interface,

where

$$(R_{2-3})\text{ metal} = \left(\frac{L}{KA}\right)\text{metal} = \frac{.0833}{120 \times .008} = .086°\text{ F/BTU/Hr}$$

3.4.3. Heat Transfer from Inner Cover to the Cold Plate, the Primary Heat Exchanger and the Secondary Heat Exchanger (R_{2-5}, R_{2-6}, and R_{2-3})

Part of the heat that enters the inner cover is transferred by conduction and radiation to the region of the hybrid circuit and cold plate, part by conduction and radiation to the region of the primary heat exchanger and the remainder is conducted through the inner cover metal to the secondary heat exchanger. The heat balance equation for the inner cover is then:

$$Q_{1-2} = Q_{2-5} + Q_{2-6} + Q_{2-3}$$

where

$$Q_{2-5} = (T_2 - T_5)/R_{2-5} = (T_2 - T_5)(1/(R_{2-5})_c + 1/(R_{2-5})_r),$$

$$Q_{2-6} = (T_2 - T_6)/R_{2-6} = (T_2 - T_6)(1/R_{2-6})_c + 1/(R_{2-6})_r),$$

and

$$Q_{2-3} = (T_2 - T_3)/R_{2-3}.$$

Half of the surface of the inner cover transfers heat across the inner air gap, of thickness .24 inches, to the cold plate region. The $(R_{2-5})_c$ and $(R_{2-5})_r$ resistances are then:

$$(R_{2-5})_c = L/.5\ KA_2$$

$$(R_{2-5})_r = \frac{(T2 - T_5)}{.5\ \sigma\ Fe\ A_2(T_2^4 - T_5^4)}$$

where

L = air gap thickness (.02 ft)

K = air gap thermal conductivity (.02 BTU/ft hr ° F)

A_2 = inner cover surface area (.128 ft^2)

σ = Stefan Boltzman constant ($.173 \times 10^{-8}$ BTU/ft^2 hr ° R^4)

Fe = emmisivity factor (.04)

$$(R_{2-3}) \text{ air gap} = \left(\frac{L}{KA}\right) \text{ air gap} = \frac{.0000417}{.02 \times .0276} = .076° \text{ F/BTU/hr}$$

and

$$R_{2-3} = .162° \text{ F/BTU/hr}$$

3.4.4. Heat Transfer from Hybrid Circuit to Cold Plate (R_{4-5})

Heat generated by elements in the hybrid circuit is transferred by conduction to the PC board, through the board and across the interface to the cold plate. The average effective resistance of the path from the elements to the cold plate was calculated at 2.0 °F/BTU/hr.

3.4.5. Fuel Temperature Rise Primary Heat Exchanger (R_{6-F})

The heat balance equation for the primary heat exchanger is:

$$Q_{6-F} = W_f C_p (T_6 - T_F)$$

where

W_f = fuel flow rate (100 lbs/hr)

C_p = fuel specific heat (.5 BTU/lb °F)

It follows that:

$$R_{6-F} = 1/W_f C_p = .02° \text{ F/BTU/hr}$$

3.4.6. Fuel Temperature Rise Secondary Heat Exchanger (R_{3-F})

The heat balance equation for the secondary heat exchanger is:

$$Q_{3-F} = W_f C_p (T_3 - T_F)$$

where

$$Q_{3-F} = Q_{6-F} + Q_{A-3} + Q_{2-3}$$

As before

$$R_{3-F} = 1/W_f C_p = .02° \text{ F/BTU/hr.}$$

3.4.7. Thermal Analysis Results

The "Super Sceptre circuit analysis computer program was used to calculate temperatures and heat flow quantities of the nodal points of the thermal simu-simulation model. The input to the program included:

1. Circuit definition shown in Figure 19.

2. Boundary conditions defined in Subsection 3.4

3. Thermal resistance values calculated in Subsection 3.4.1 through 3.4.6.

The following temperatures and heat flow quantities were calculated:

1. Temperatures

Outer Cover	T_1	--	713° F
Inner Cover	T_2	--	318° F
Hybrid Circuit	T_4	--	174° F
Cold Plate	T_5	--	169° F
Primary H.E.	T_6	--	279° F
Secondary H.E.	T_3	--	305° F

2. Heat Flows

Ambient to outer cover (Q_{A-1})	-- 94 BTU/hr
Ambient to other exterior surfaces (Q_{A-3})	-- 1210 BTU/hr
Outer cover to inner cover (Q_{1-2})	-- 94 BTU/hr
Inner cover to cold plate (Q_{2-5})	-- 10.3 BTU/hr
Inner cover to primary H.E. (Q_{2-6})	-- 2.7 BTU/hr
Inner cover to secondary H.E. (Q_{2-3})	-- 81 BTU/hr
Primary H.E. load (Q_{6-F})	-- 187 BTU/hr
Secondary H.E. load ($Q_{3-F} - Q_{6-F}$)	-- 1291 BTU/hr

The thermoelectric heat load is the sum of the Q_{2-5} and the heat generated by electrical power dissipation in the hybrid circuit.

$$Q_{T.E.} = 10.3 + 2.5 = 12.8 \text{ BTU/hr.}$$

3.5. HEAT EXCHANGER DESIGN

A preliminary model for this application was designed and constructed for the purpose of obtaining test data correlation with the calculated results. Studies showed that a large surface area is required to transfer the heat with a small temperature differential between the wall and the fuel. This requires small channels. To obtain reasonable pressure losses, the small channels are in parallel.

The heat exchanger designs are shown in Figures 11 and 12. In the primary heat exchanger (#1), heat flow enters at the outer diameter of three parallel 0.020 x 0.125 inch paths and flows through the spiral to the center and then back out to the outer diameter through three more parallel spiral paths. In the secondary heat exchanger (#2), the fuel enters at the inner diameter and flows out through a three-path spiral and back through a three-path spiral to the inner diameter. These heat exchangers are constructed by diffusion bonding etched aluminum plates to form the monolithic heat exchanger packages. The respective dimensions of heat exchangers #1 and #2 are 15.3 and 26 inches of channel length and 0.179 and 0.301 square feet of transfer surface area.

3.5.1. Primary Heat Exchanger

The heat load into the primary heat exchanger from Section 3.4.7 is 187 BTU/hr at 100 lbs/hr fuel flow and fuel specific heat of 0.5 BTU/lbs ° F. This would raise the fuel temperature only 3.7° F.

A computation was made to determine if the temperature difference from the wall to fuel temperature was significant. Heat transfer from the wall temperature to fuel temperature can be determined as follows:

$$q = h A \Delta T$$

where

A = channel surface area (.184 ft^2)

q = heat transferred BTU/hr

ΔT = Difference -- wall to fuel temperature ° F

The heat transfer coefficient for turbulent channel flow is given by the equation.

$$h = 0.023\, K(R_e)^{0.8}\,(P_r)^{0.8}/D_H$$

h = heat transfer coefficient BTU/hr ft^2 ° F

K = thermal conductivity = .07 BTU/hr ft ° F

D_H = Hydraulic diameter

D_H = Hydraulic diameter

D_H = 4 (cross section, ft^2)/Perimeter

D_H = 0.034 in or 0.0028 ft.

V = Velocity ft/sec.

This is found to be 12.9 ft/sec. for 100 lbs/hr flowing through three .0024 sq. in. parallel channels, i.e., V = lbs/hr x ft^3/lbs x hr/sec.

R_e = Reynolds Number

$$R_e = \rho V D_H/\mu$$

μ = dynamic viscosity = 1.84×10^{-4} lbs/ft sec.

ρ = density = 43 lbs/ft^2 (275° F fuel)

R_e = 8,600

P_r = Prandtl Number

$$P_r = 3600\, C_p \mu/K$$

C_p = specific heat of fuel = 0.5 BTU/lbs ° F

K = thermal conductivity = .07 BTU/hr ft ° F

μ = dynamic viscosity = 1.84×10^{-4} lb/ft sec

P_r = 4.74

and

$h = 1470$ BTU/ft^2 hr ° F.

Solving $q = h A \Delta T$ for ΔT

$\Delta T = 187/(1470 \times .184 = 0.70°$ F.

This small mean temperature different of .7° F between the fuel and the heat exchanger wall as compared to the 3.7° F temperature rise of fuel through the heat exchanger means that the heat exchanger surface temperature is essentially equal to the temperature of the fuel leaving the unit.

3.5.2. Secondary Heat Exchanger

A similar procedure was used to calculate the secondary heat secondary heat exchanger. The final configuration can be traced with a sample calculation.

The flow from the wall to the fuel is computed in the same manner that the primary heat exchanger was illustrated in Section 3.5.1.

$q_{W-F} = h A \Delta T$

q_{W-F} = Heat flow from wall to fuel. This was found to be 1291 BTU/hr in 3.5.7.

h = heat transfer coefficient = 1470 BTU/ft^2 hr ° F (see 3.5.1)

A = area of channel walls in secondary heat exchanger (.3 ft^2)

$\Delta T = T_W - T_F$

T_W = is again the wall temperature

T_F = Fuel temperature

Solving for ΔT

$\Delta T = q_{W-F}/h_A = 1291/1470 \times .3 = 2.9°$ F

This small ΔT of 2.9° F as compared to the fuel temperature rise of 25.8° F indicates that the heat exchanger wall temperature will be nearly equal to the leaving fuel temperature.

3.5.3. Heat Exchanger Pressure Losses

To determine the pressure loss through the channeling, the formula

$$\Delta P = \rho \frac{V^2}{2g} \left(f \frac{L}{D} + K\right)$$

ΔP = Pressure drop thru the channels lbs/ft^2

ρ = density of fuel in lbs/ft^2 (43 at 275° F)

V = Velocity (12.9 ft/sec previously determined)

L/D = Ratio of channel length to diameter

f = friction factor

K = turning, entrance and exit loss coefficient

The L/D ratio is 888 for the primary heat exchanger and 1520 for the secondary heat exchanger:

$$L/D = 888 + 1520 = 2408$$

The coefficient K is comprised of the following:

K_1 = entrance loss = 1.5

K_2 = exit loss = .5

K_3 = right angle bend losses (8 bends) = 12.2

K_4 = helix turning losses = 48

$K = 1.5 + .5 + 12.2 + 48 = 62.2$

The friction factor per pipe flow curves is .04. The total pressure loss is then:

$$\Delta P = .77 (.04 \times 2408 + 62.2) = 122 \text{ psid.}$$

Measured pressure losses showed 130 psi from inlet to outlet of the two heat exchangers.

3.6. VIBRATION TESTS

Vibration tests were run to find characteristics and any resonant frequencies. Figure 19 shows a photograph of the unit mounted on the vibrator. As shown in the photograph, the adapter to mount the module to the vibrator table was designed so that the module would fit down inside the fixture to simulated proposed mounting on the engine. It can also be mounted as shown in the photo.

The unit is provided with thermal insulating mounting washers which also act as a shock mount for the unit. Test conditions included:

- Hard mounting of the module to the vibrator. The thermal insulators were not used.
- Isolated mounting of the module to the vibrator with thermal insulators installed.
- Tests at 5 and 20 g inputs from 50 to 5800 Hz.
- Module mounted with a test ring replacing the inner and outer covers to allow observation of the hybrid package cover.

The test data shown in the attached figure is for vibration in plane #1 defined as vibration along the axis of the electrical connector centerline.

This plane is perpendicular to the PC board and hybrid substrate and represents the most severe condition for the electronics. Planes #2 and #3 were scanned with no significant resonant points (as compared to plane #1) and no traces are included in this report.

No problems were encountered with the electronics during any of the vibration testing.

The thermal isolators were made from a fluorosilicone elastomer and consisted of a sleeve bushing between two flat washers as shown in Figure 10. The isolator also can be seen in Figure 20.

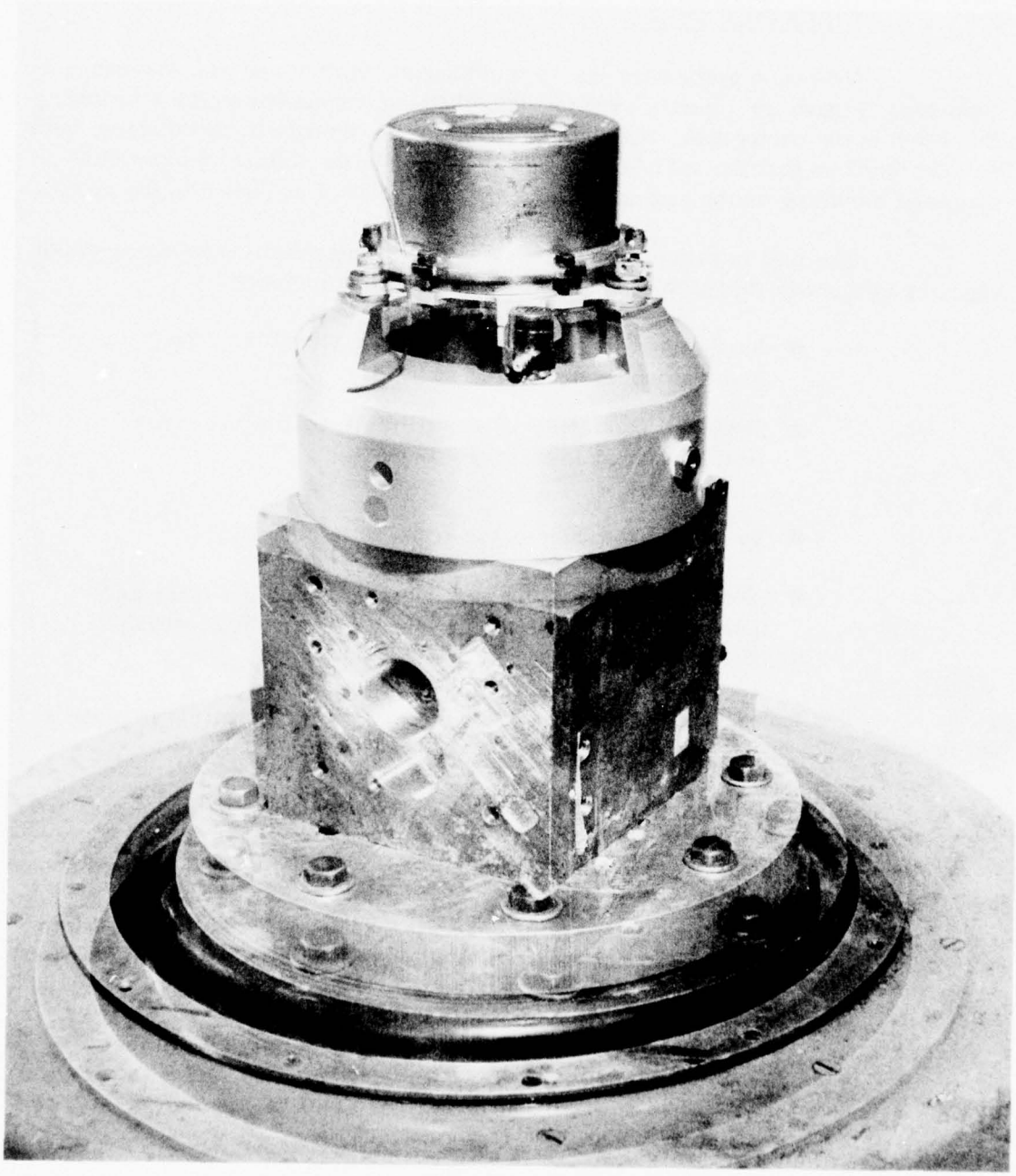

Figure 20 -- Thermally Conditioned Module
Vibration Test Set Up

3.6.1. Hard Mounted Vibration Tests

The initial test was run with a ring replacing the inner and outer covers to hold the assembly together and allow an accelerometer to be placed on the hybrid cover (position 13 Figure 9) and the PC board (position 14 Figure 9).

It was assumed and later demonstrated that this mounting would give the greatest vibration load on the hybrid package. The test results are shown on Figure 21.

The note "connector down" indicates the module was mounted as shown in the photograph of Figure 20. (But covers are removed.)

The output G forces are shown on the curve. The amplification factor at resonance is 25. The curves are displaced with both traces starting at zero. "G's" at less than 50 Hz. The lower resonance of the hybrid cover is caused by the weight of the accelerometer being significant with respect to the cover thickness.

The important point in these tests was that the hybrid circuit was not damaged by the exposure to better than 125 G's for the short period of the test.

It was believed that the high Q (amplification factor) was the result of a spring rate of the mounting plate between the three equal spaced mounting bosses To determine if this was the case, the covers were assembled on the unit and accelerometers placed at position 24 (reference Figure 9) on the mounting plate of the assembly and on the outer cover at position 23 (reference Figure 9).

The module was mounted with the "connector up." Referring to photograph of Figure 20, this places the cover down inside the test adapter or upside down (normal mounting position) with respect to the photograph.

Test results are shown in Figure 22 again with the zero G for the two curves displaced to allow multiple results to be displaced on the same Figure.

The resonant points are very close to the peaks of Figure 21. This demonstrates that the amplification results from the spring rate (and module mass) of the mounting plate and is being transmitted through a rigid structure to the hybrid package.

Note that the frequency scale has been shifted in Figure 22 to cover a greater frequency range.

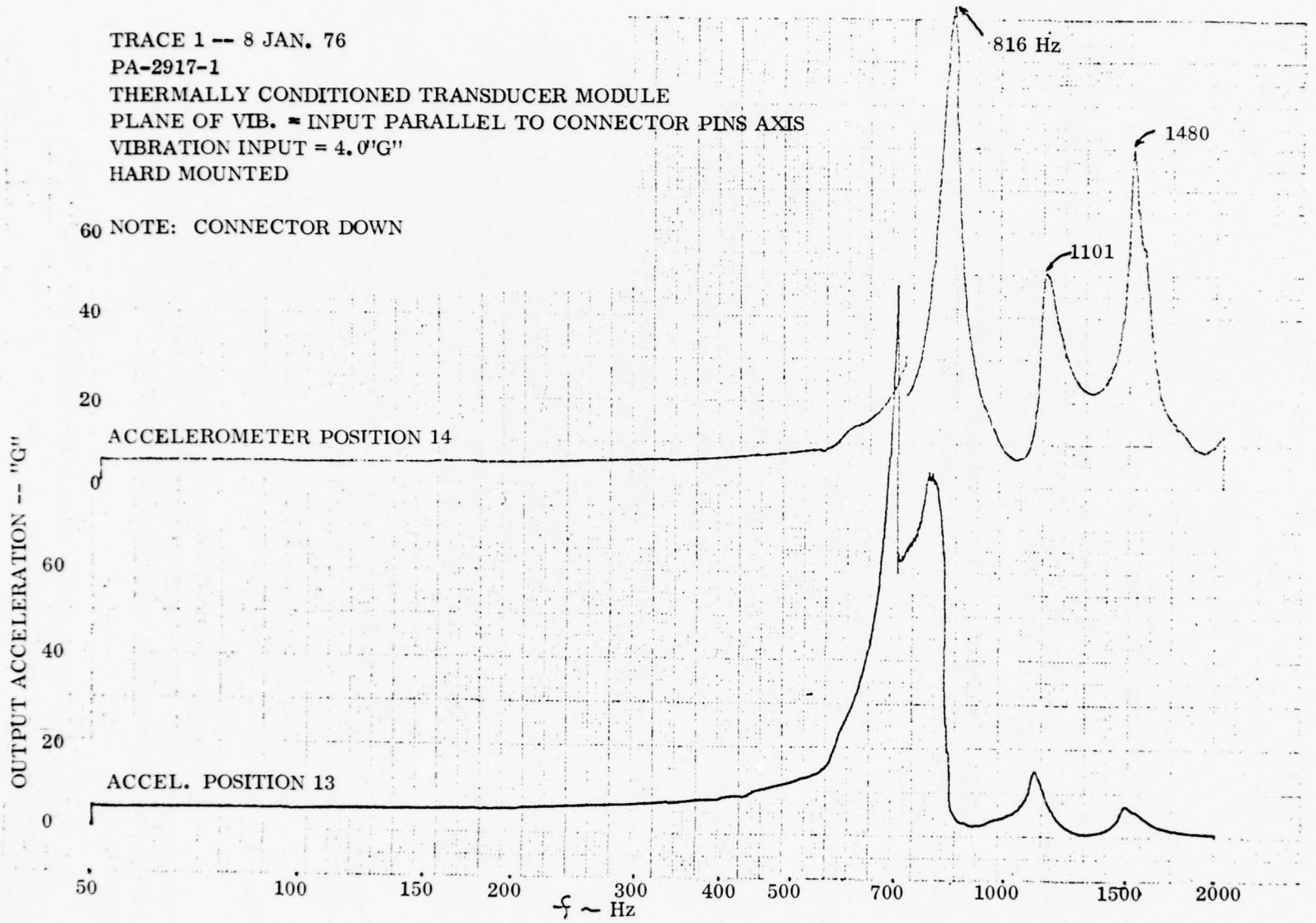

Figure 21 -- Vibration Data - Position 13 and 14

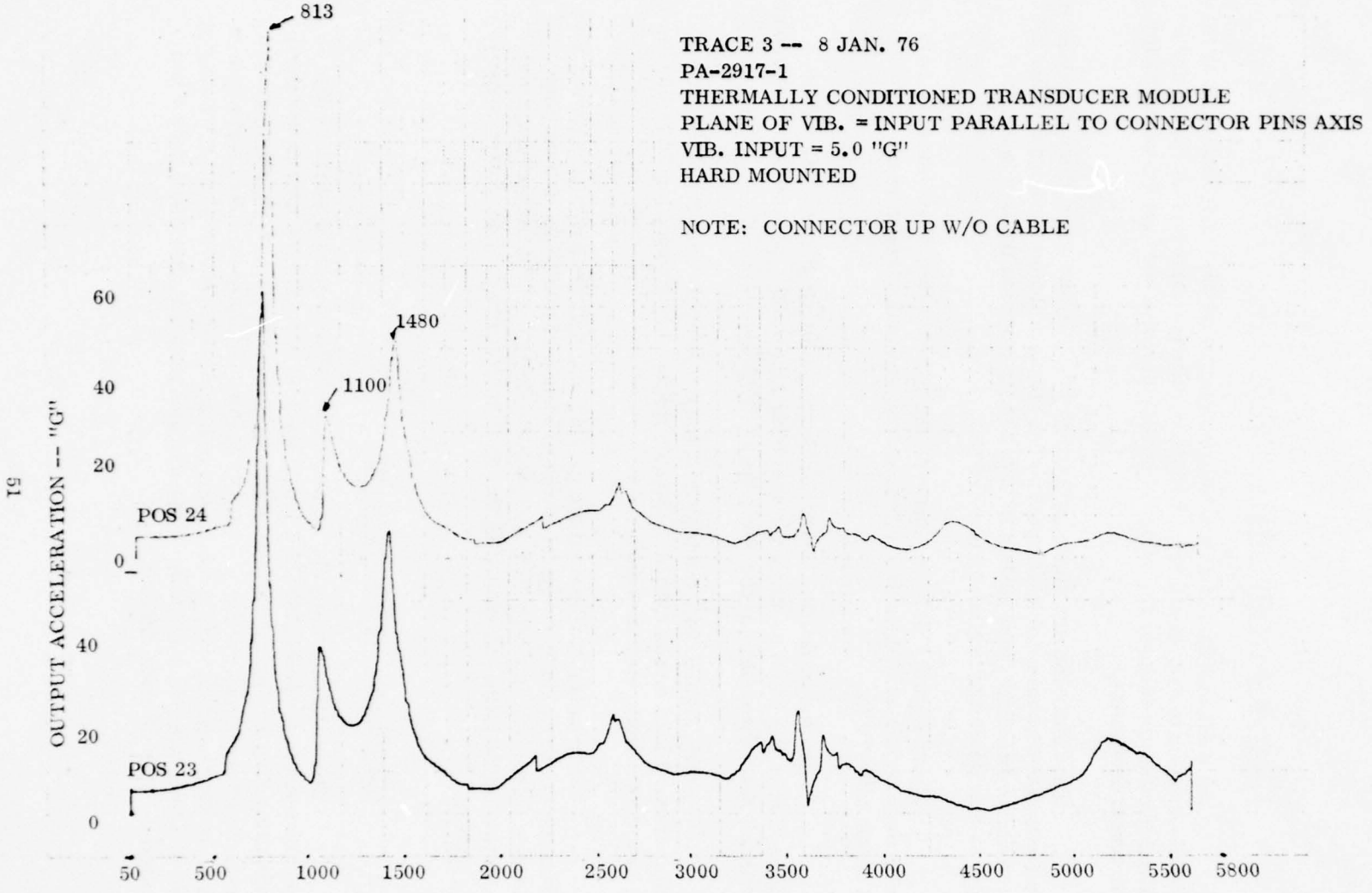

Figure 22 -- Vibration Data Position 23 and 24

3.6.2. Vibration Tests With Thermal Isolators

As positions 23 and 24 are representative of the conditions seen at the hybrid electronics, testing could now procede with accelerometers at the 23 and 24 locations used to investigate the effect of the isolators on the amplification factor and resonant frequency.

These results are shown in Figure 23. Tests were run with connector up and with and without a cable attached. The Q was reduced to about 6 (from 25) and maximum resonant point shifted to 330/350 Hz range at the 5 G input. All testing to this point had been done at 5 G input.

From Figure 23, the loads on the hybrid circuit are inferred as being slightly over 30 G's at 330 Hz and with a second resonance showing at 20 G's and 750/770 Hz.

Tests run at the 20 G input level are shown on Figure 24. The configuration is the same as for tests shown on Figure 23 except one accelerometer is mounted near the center of the outer cover (Position 4).

From Figure 24 the major resonant peak is changed to 180 Hz and the maximum G load on the hybrid circuit as inferred from position 24 is 55 G's. This is a Q of a little less than three.

The results of vibration effects on the top cover are also shown. The resonances occur at 1900, 4100, 4500 and 4735 in addition to the mount ring resonance. Items of interest here are possible fatigue of the outer cover and speculation on the effect of removing the rivit at the center of the outer cover to inner cover.

3.6.3. Conclusions - Vibration Tests

The vibration tests should be run with the structure which would mount the module to the engine included in the test rig. As the unit is designed, the mounting ring spring rate, as defined by plate thickness and distance between support mounting points, defines the major system resonances. By minor design changes in the mounting configuration the resonant point can be shifted. Damping ratios at resonance are a function of the thermal isolator characteristics when considered as a vibration damper.

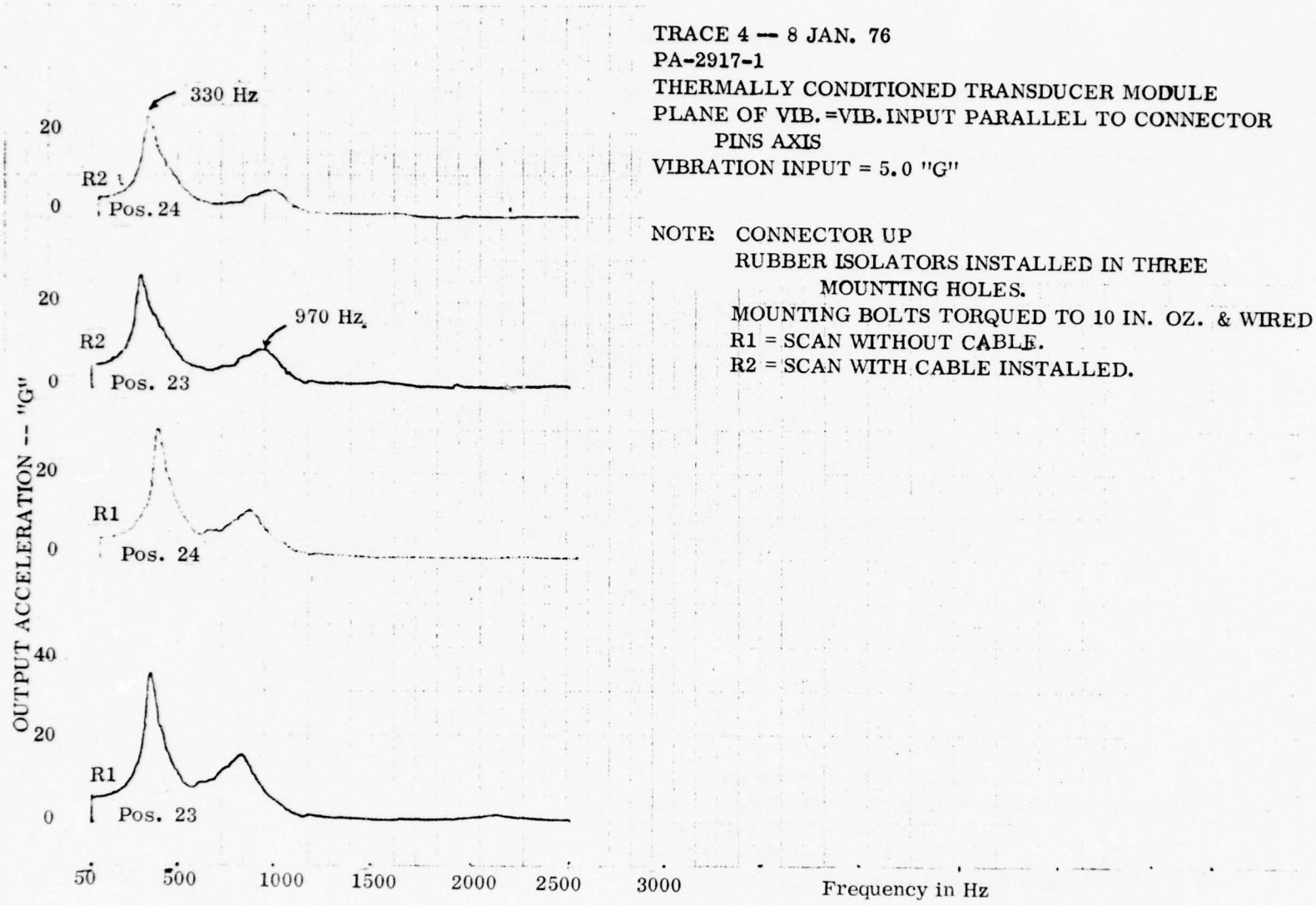

TRACE 4 — 8 JAN. 76
PA-2917-1
THERMALLY CONDITIONED TRANSDUCER MODULE
PLANE OF VIB. =VIB. INPUT PARALLEL TO CONNECTOR PINS AXIS
VIBRATION INPUT = 5.0 "G"

NOTE: CONNECTOR UP
RUBBER ISOLATORS INSTALLED IN THREE MOUNTING HOLES.
MOUNTING BOLTS TORQUED TO 10 IN. OZ. & WIRED
R1 = SCAN WITHOUT CABLE.
R2 = SCAN WITH CABLE INSTALLED.

Figure 23 -- Vibration Data - Effects of Vibration Isolators

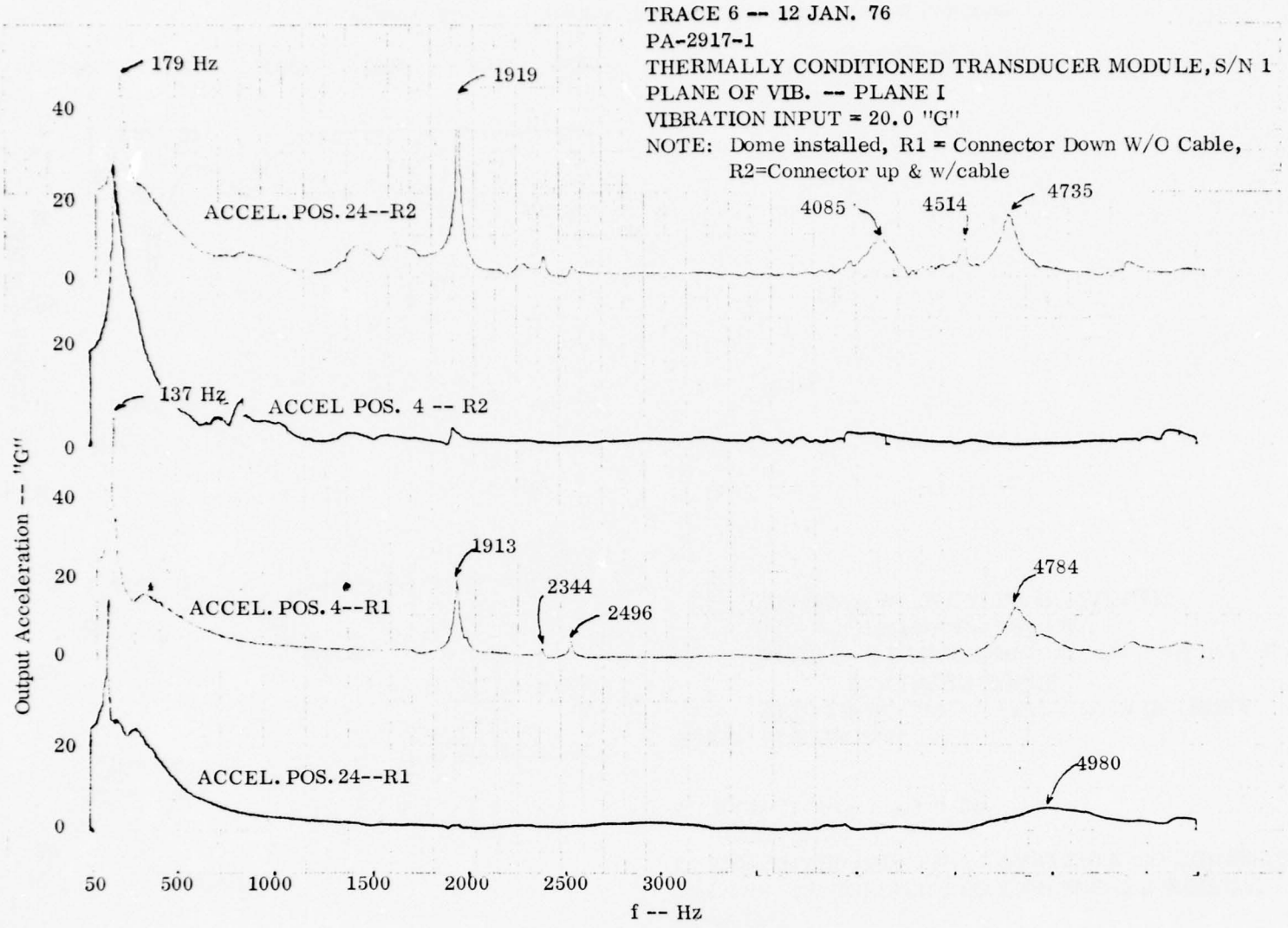

Figure 24 -- Vibration Data Position 4 and 24

The maximum vibratory loads imposed on the electronics with the design are within limits which will allow the electronics to survive at the resonant condition. At frequencies above the first resonant point, the amplification factor is near or less than one.

Test results demonstrate that the unit can withstand the engine environment. Minor design modifications in the mounting ring or thermal isolators can be made to improve performance.

The mount to the engine was not defined during the project. The major problem from a vibration standpoint which should be avoided is a resonant of the same frequency in the mount structure and the transducer module.

3.7. THERMALLY CONDITIONED MODULE ENVIRONMENT

Data on typical mission profiles for advanced engines has been compiled from several sources.

Mission environment data is given in Figures 25 and 26. Figure 25 is the hypotehetical mission profile for an advanced engine control studied by P&WA. Figure 26 is a typical mission environment as specified for control components on a DDA (Detroit Diesel Allison) engine subjected to compressor inlet air temperature. According to this data maximum ambient temperatures are 468°F and maximum fuel temperatures are 210°F. Other advance data from Pratt & Whitney Aircraft indicates that in advanced engines, fuel temperature may reach 285°F in flight and 225°F at taxi conditions. For this project to allow substantial performance margins, a maximum fuel temperature of 330°F and a maximum 750°C ambient temperature were chosen as design goals.

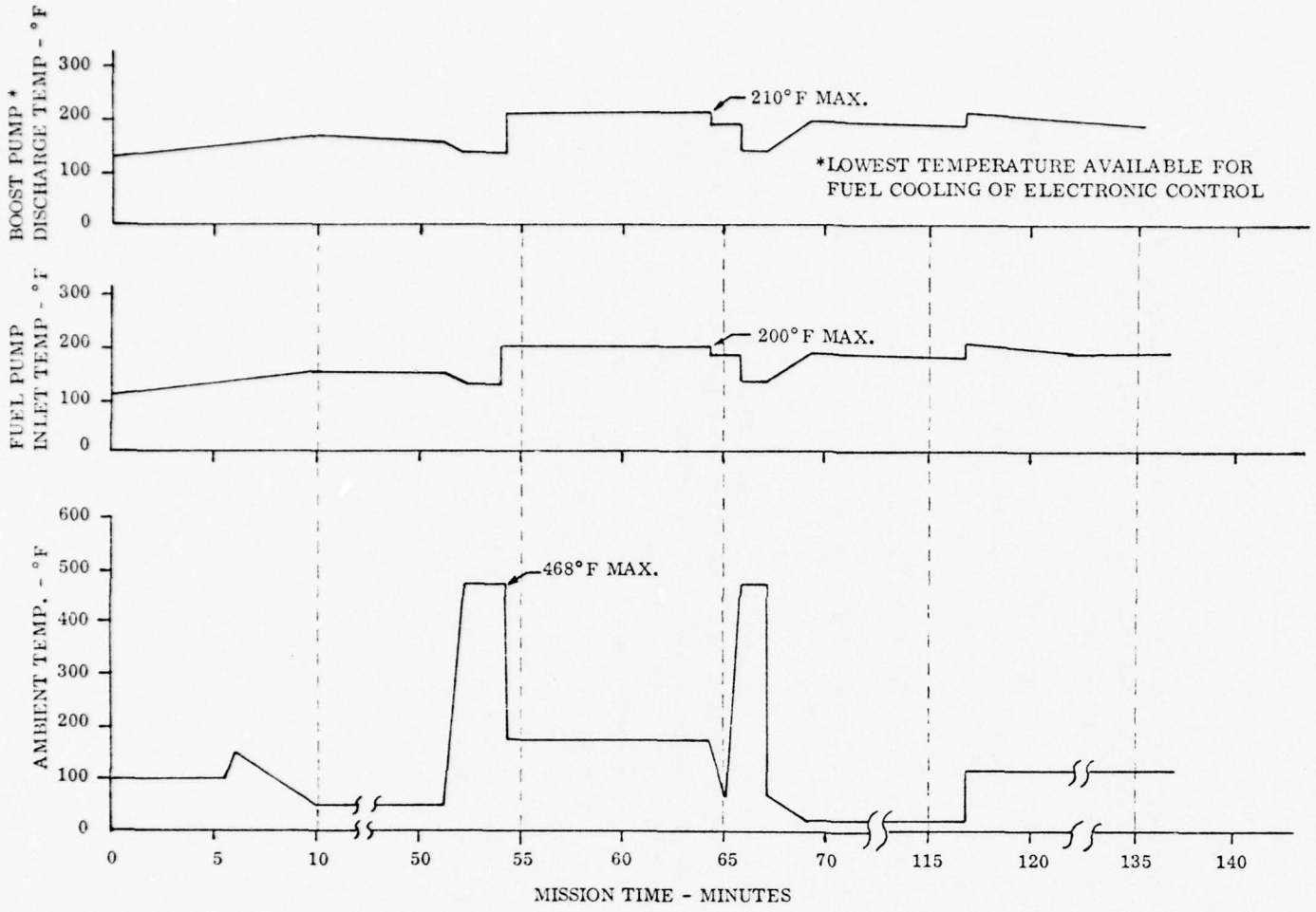

Figure 25 -- Full Authority Electronic Demonstrator Control
Hypothetical Mission Profile Environmental Conditions

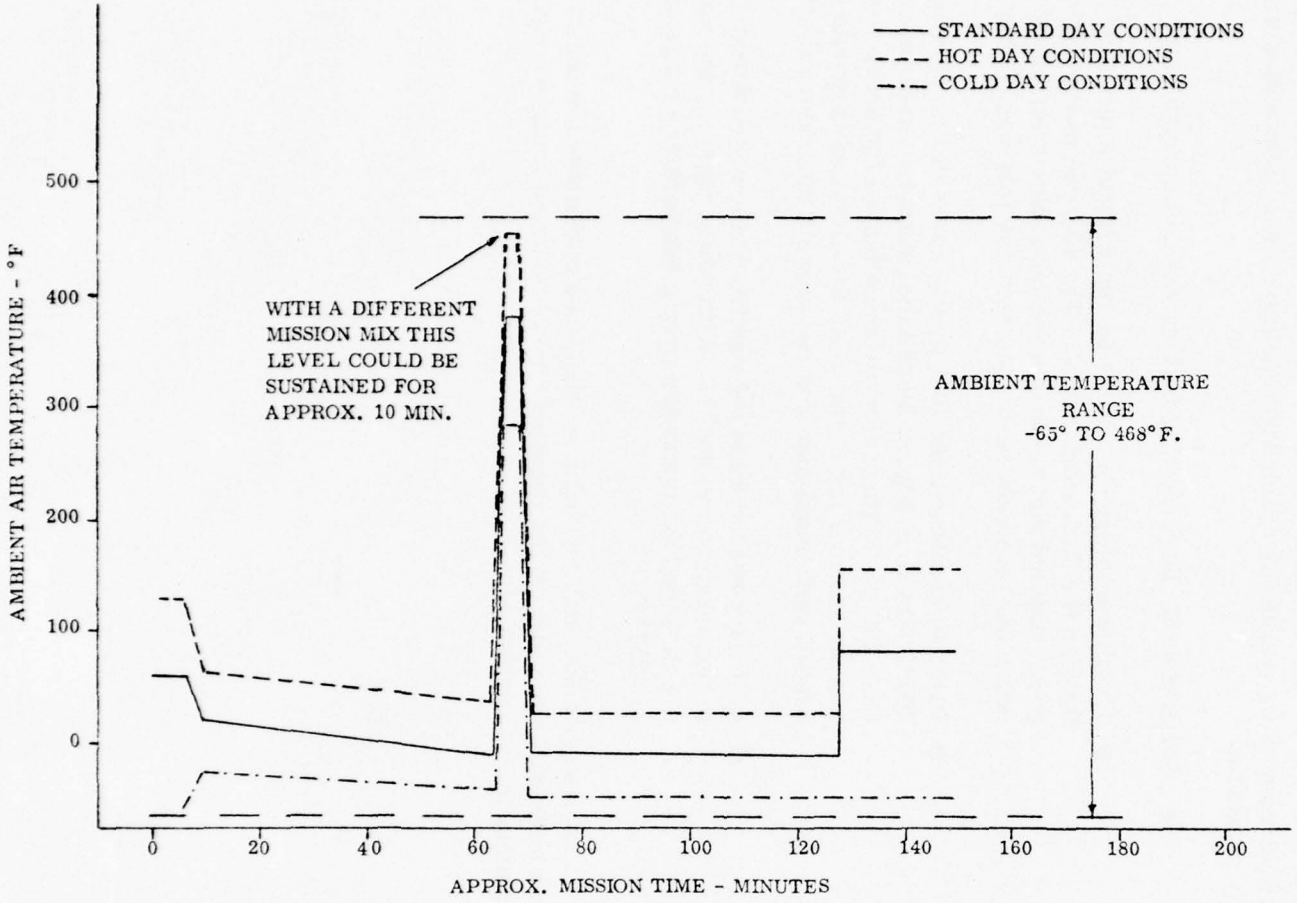

Figure 26 -- Typical Mission Environment

Operating effects must be considered not only during flight conditions but also the effects associated with "heat soak" at shut down. No specific design requirements or conditions which would define a bench simulation are currently available.

On a hot shutdown, the following factors should be considered:

- The thermoelectrics cannot be run without a fuel flow through the heat exchangers. The 40 to 50 watts of electrical power applied and the insulating characteristics of the double cover design would result in extensive internal heating.

- Prior to shutdown, the fuel temperature will be approximately 200° F based on Figure 25 and the protected electronics near 100° F. With the insulating effect of the double cover and the thermal lag of the unit, the electronics should not exceed their maximum non operating temperature limit.

- In the unpowered state the electronics may be stored in temperatures to 302° F. With power applied, the electronics are designed for operation over a temperature range of -65° F to +257° F.

A realistic hot soak or shutdown should be established in terms of maximum ambient temperatures and duration and a simulated shutdown run made on the system for evaluation.

SECTION IV

ELECTRONIC DESIGN

4.1. PRELIMINARY DESIGN

A preliminary design study was performed to determine the optimum overall design features of a thermally conditioned module. To be consistent with aircraft requirements, the module had to be small and light. To meet the weight criteria, a aluminum construction was selected. To meet size requirements, a hybrid integrated circuit became the obvious choice. So that a significant amount of signal processing could be accomplished, a hybrid substrate size of one-square inch was selected. A thermocouple signal was selected as representative of the type of low level signal with the need for conditioning. Multiple sensors were used so as to be representative of aircraft practice. Various forms of signal conditioning were considered. The prime requirement being that the output signal be compatible with the high performance requirements of a digital computer control system.

The simplest method considered consisted of straight power amplification to increase signal power relative to background noise. This was rejected because the output signal did not appear in digital form and could not be readily measured by digital circuits.

A second method considered consisted of changing the voltage of the thermocouple to a frequency. The output frequency would then be proportional to input signal level. The output is immune to amplitude variations due to noise. The frequency type output can easily be measured by digital circuits. The time required for this measurement, however, is rather long. Another problem is the design of precision voltage to frequency converter. Several designs were evaluated; none, however, showed promise of meeting our accuracy requirements. Therefore, this conversion method was rejected.

The third method evaluated and selected for this project results in a pulse width modulated output signal. This method has advantages in accuracy and speed over other methods. Another advantage is the readily available digital circuitry required for pulse width modulation and demodulation. In this demonstration digital pulses were sent over a pair of wires; the signal type, however, is directly applicable

to transmission using fiber optics. A simple circuit modification could accommodate this transmission mode.

To convert the analog thermocouple signal to a pulse width, a rather novel approach was developed. The heart of the conversion circuit used a Motorola monolithic integrated circuit analog to digital (A/D) converter. Normally the A/D converter is thought of as a single unit. The modulator portion uses a dual slope A/D conversion technique to produce a pulse width output. The demodulator is used as the readout device converts the pulse width to a binary number which is displayed. Each input data signal requires only a single conversion to produce a pulse width and a digital display. Multiplexing can, therefore, be used to send different bits of data in succession over the data link between modulator and demodulator.

4.2. BREADBOARD DESIGN

The electronic circuit for the thermally conditioned transducer was initially designed and built in breadboard form for test purposes. The end product, however, was built as a thick-film hybrid integrated circuit. Figure 27 is a block diagram showing the functional interrelationship of the thermally conditioned module and the readout module. Schematic diagrams of the Thermally Conditioned Sensor Module and the Readout Module are shown in Figures 28 and 29 respectively.

In this sensor system, the analog to pulse-width converter is the heart of the system. The unit employed for this application is the Motorola MC1505. It is the analog system of a dual ramp analog-to-digital conversion system. This unit establishes a pulse width proportional to the input voltage. This signal is transmitted through cables where it is subsequently converted to a digital signal in the pulse-to-digital block. The pulse-to-digital block consists basically of a counter into which clock pulses are gated during signal pulse period.

The A/D converter system is shown in detail in Figure 30. The analog subsystem the Motorola MC1505 monolithic integrated circuit shown in the blocked area of the circuitry, consists of an integrator, a comparator, a reference converter amplifier, an input signal converter amplifier, a regulated reference voltage source and a high speed current switch.

Figure 31 illustrates the timing sequence of the integrator charge (signal current i_x), discharge (reference current i_R), comparator level, ramp control level and the mathematical derivation of signal input to output reading.

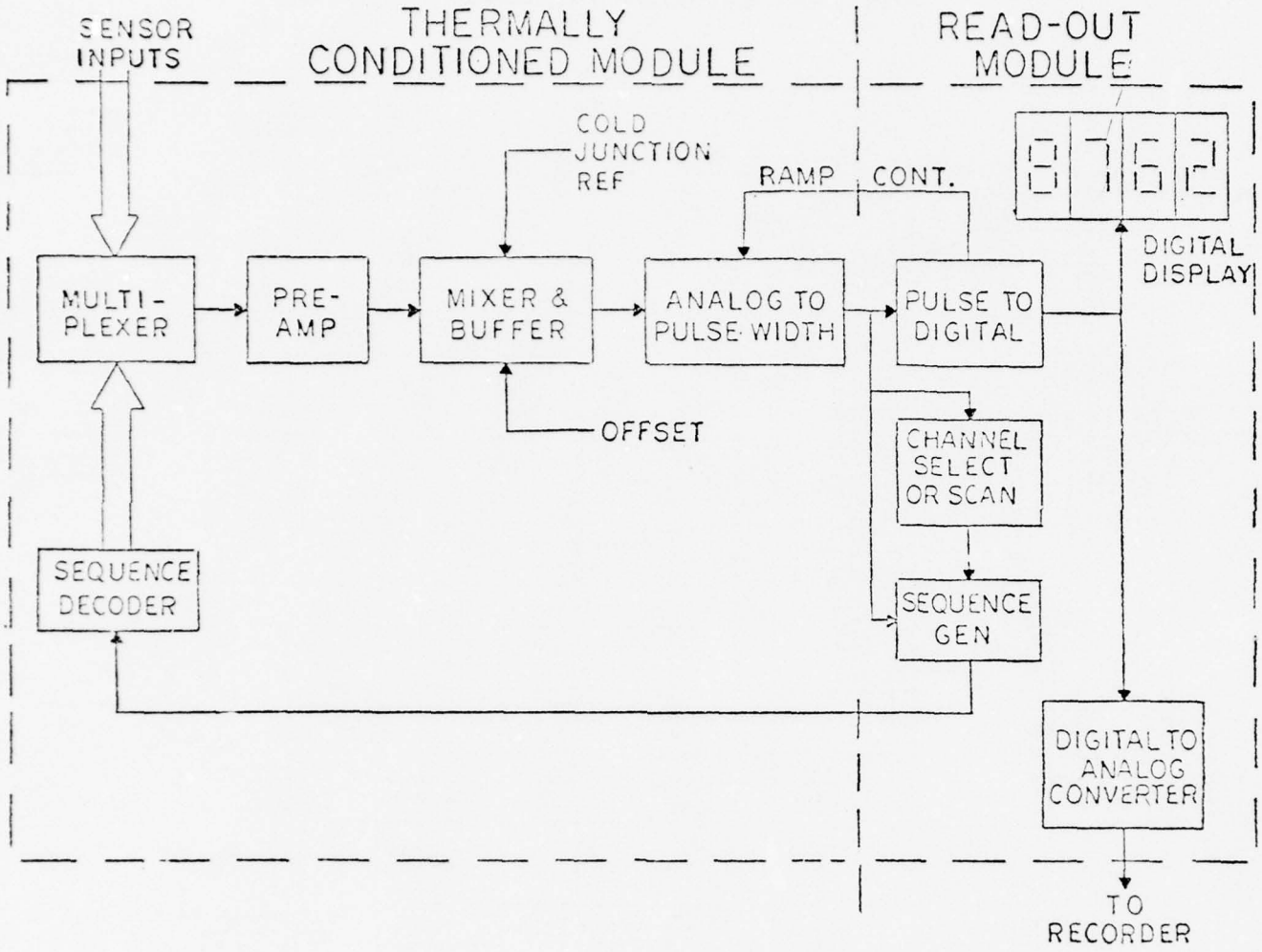

Figure 27 -- Sensor System Electronic Block Diagram

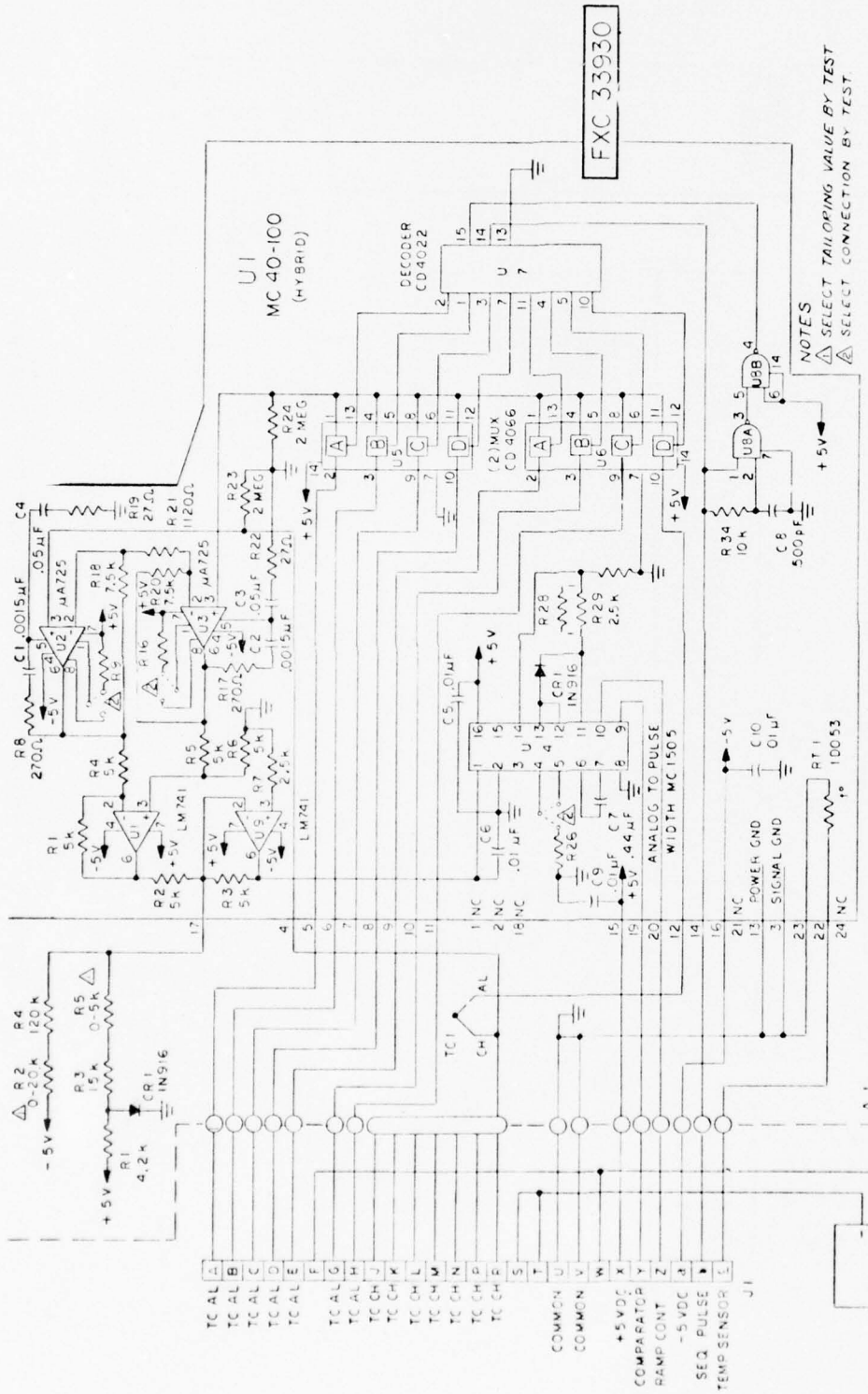

Figure 28 -- Thermally Conditioned Sensor Module
Schematic Diagram

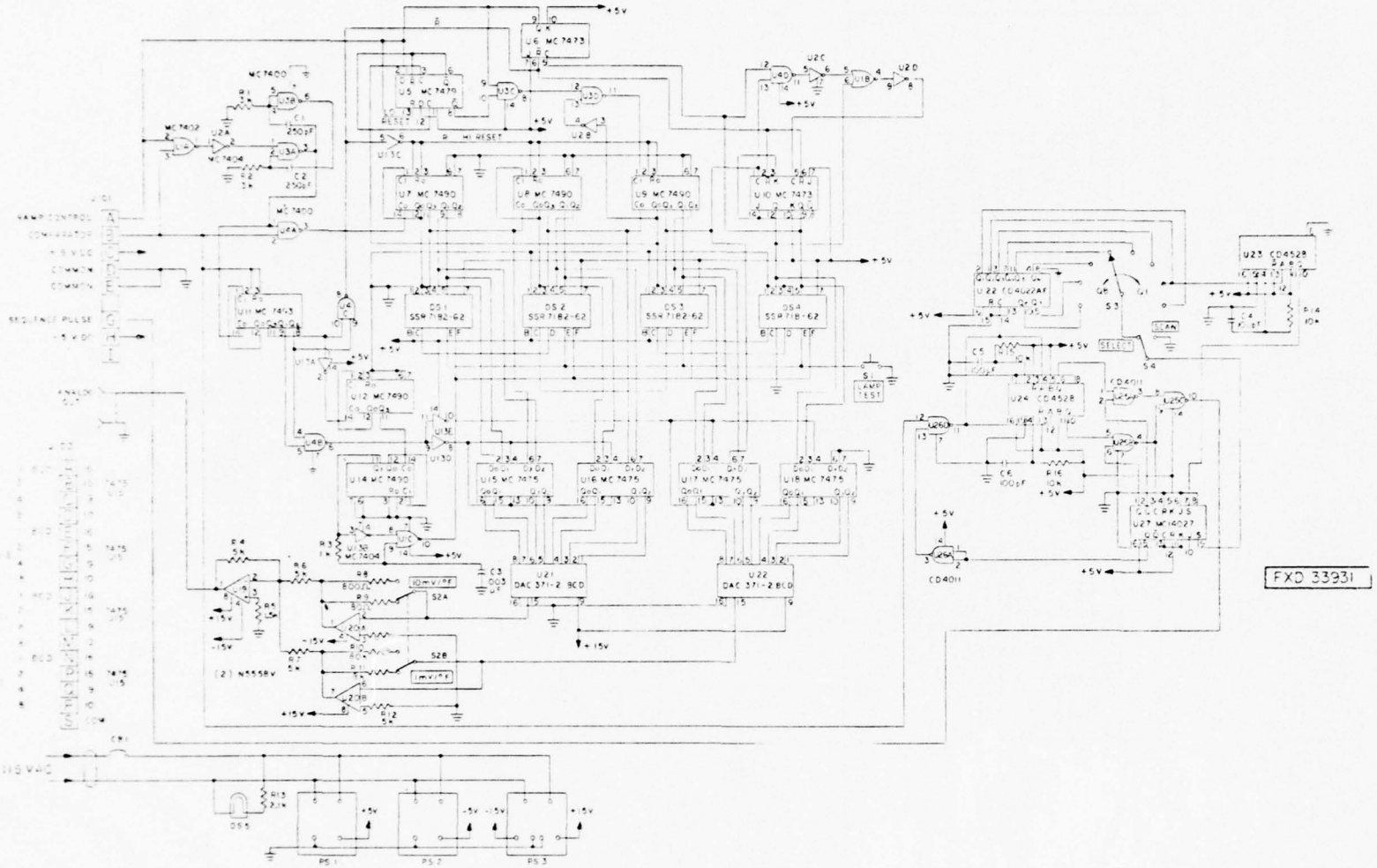

Figure 29 -- Thermally Conditioned Sensor Module Readout Console Schematic Diagram

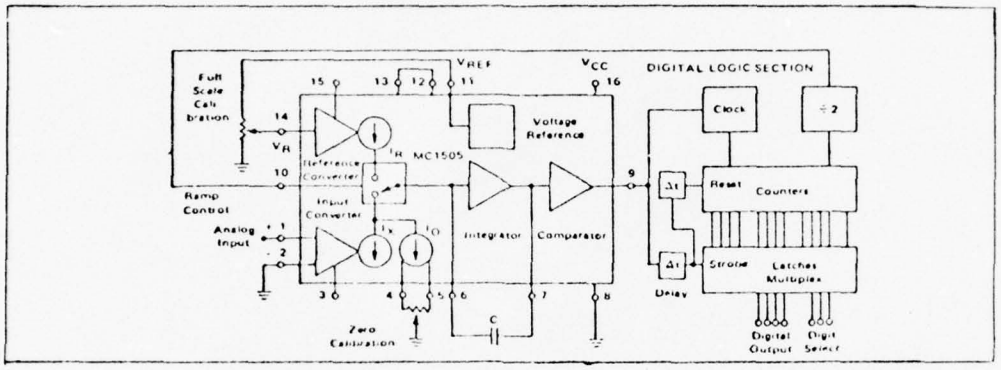

Figure 30 -- A/D Converter Functional Diagram

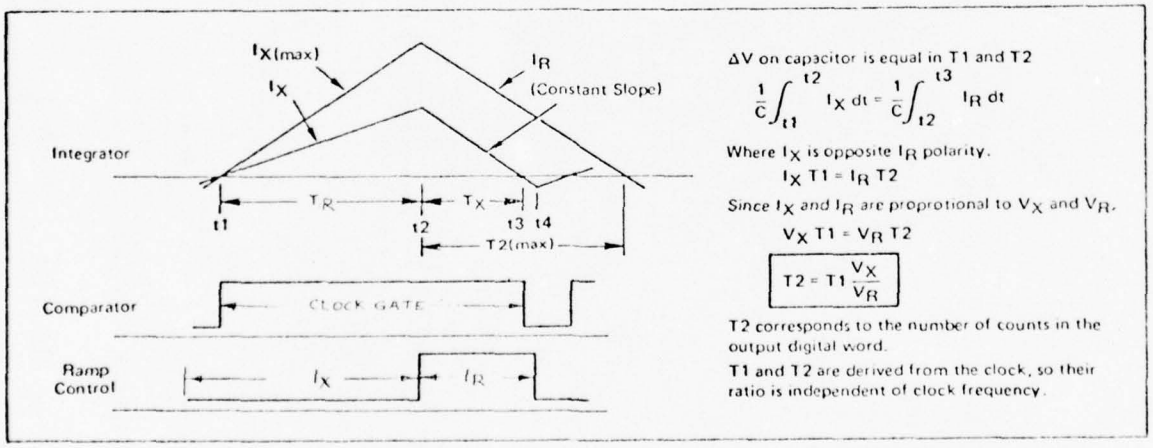

Figure 31 -- Dual Ramp A/D Conversion Waveforms

Initially, the input signal that is converted to current is integrated to linearly increase the charge value and voltage output of the integrator. This process is continued for a fixed period determined by the time required to fill the counter in the logic section of the Readout Module. The clock is gated into the counter when the integrator output crosses zero. When the counter is full, a high signal from the counter is placed on the ramp control line which activates the switch in the analog subsystem (MC1505, Figure 30) to direct the reference current into the integrator with a reversed polarity to linearly reduce the integrator charge and output voltage. When the output crosses zero as sensed by the comparator, the clock is stopped and the count is a measure of the time required to reset the integration back to zero. This time is proportional to the input signal level.

The use of one clock to set the integration time duration and to also establish the count measure of the reference reset interval eliminates any clock frequency variable from the measurement. Also, any integration rate change due to integrating capacitor variation applies to both signal current integration and reference current integration, and is, therefore, cancelled out in the reading.

The clock in the readout was set to run at approximately 800 k Hz. to yield a minimum sample rate of 133 readings per second or 17 complete 8-channel cycles per second. The digital value of each measurement is present on the counter outputs of U7, U8, U9 and U10 of Figure 29 in BCD code form at the end of each measurement. This information is then placed on the two sets of latch registers DS1 through DS4 and U15 through U18. The first of these (DS1-DS4) is for readout and the second (U15-U18) is for BCD code output and for input to the D/A converters U21 and U22. The strobing of the latch registers for readout is reduced 100 to 1 by counters U12 and U14 to give a readout update of 1.7 per second to allow readings with some superimposed ripple.

The thermally conditioned module as shown in Figure 28 has a total of eight thermocouple inputs with multiplexing to permit use of only one pre-amp, one mixer and one A/D converter. Multiplexing was therefore required along with some form of automatic and manual sequencing control. A minimum number of input lines were desired, and accordingly, a pulsed octal counter decoder (U7) was chosen to activate the multiplexers U5 and U6. To step from one input to the next, only a pulse is required. But for proper known channel selection, some means was required for starting each sequence on a definite channel. The "O" select output on the counter decoder U7 which is keyed in with a pulse to the reset input is used for channel selection. A decision was made to use a series of seven pulses and an eighth pulse wider by a factor of five. An R-C filter was placed ahead of the reset input to eliminate

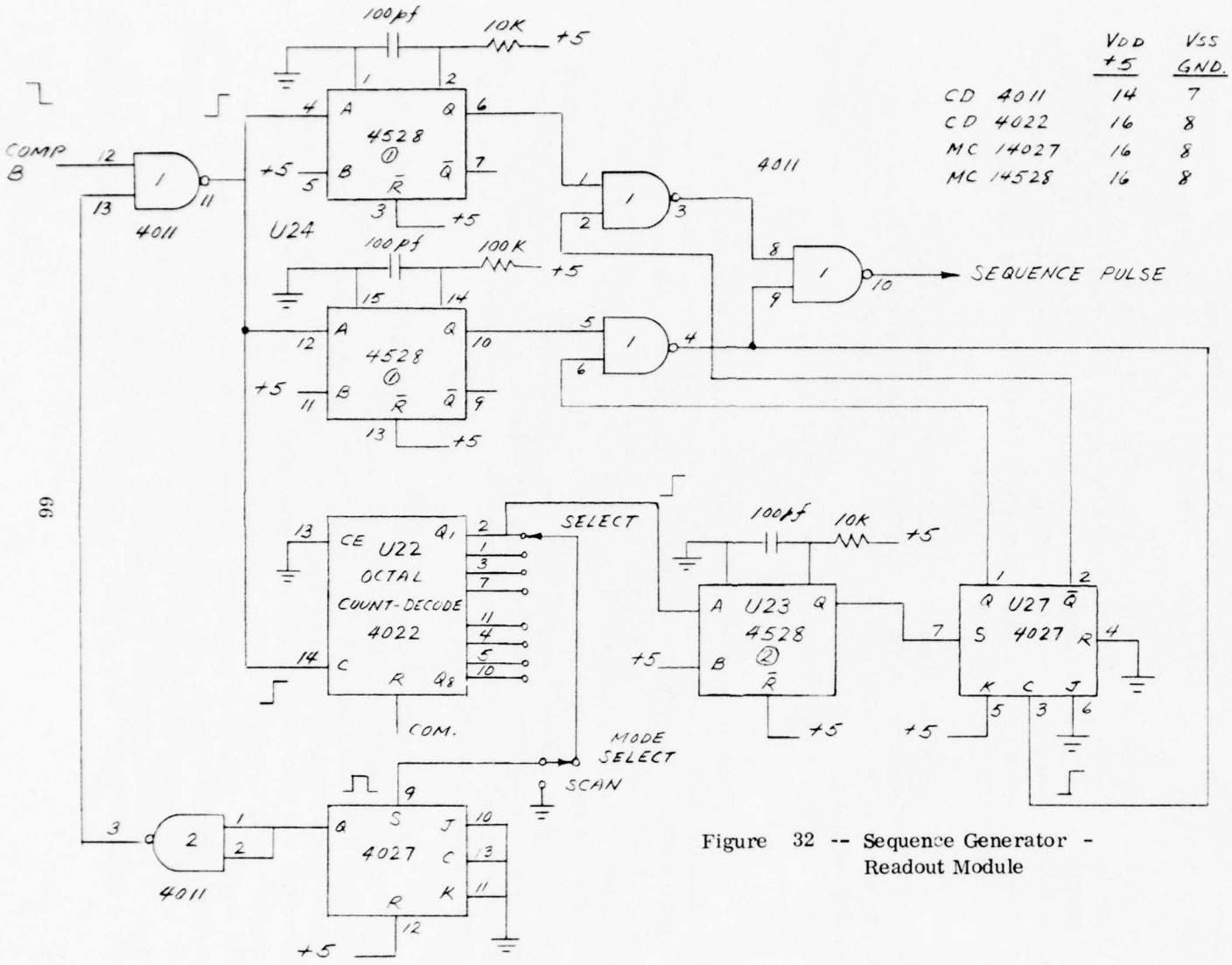

Figure 32 -- Sequence Generator - Readout Module

the narrow pulses. The narrow pulses into pin 14 step the decoder through the eight outputs and the wide channel "O" pulse resets the decoder to "0" by passing through the filter R34 and C8 to activate the reset input. It was then necessary to provide a circuit in the Readout Module that can generate such a series. A design was implemented to generate two concurrent series of pulses of one microsecond and 10 microseconds wide triggered by the completion of each measurement by transition of the comparator line from the A/D converter. The generators were a pair of monostable multivibrators U24 as shown in the Readout Module schematic in Figure 4-3 and the Sequence Generator in Figure 32. The selection of one wide pulse for each seven narrow pulses was generated again with an octal counter decoder clocked by the comparator line. The decoder output triggers an alternate gating reset circuit to insert the wide eighth pulse into the output sequence.

Conditioning of the input signals was needed for differential input, for amplification and mixing of signals, cold junction compensation and offset voltage. The circuit designed for this application employed 3 amplifiers, one for each line of input and a third for mixing. The mixer was designed for use as an instrument type input amplifier with inherent capacity for placing ground line voltage in a common mode for cancellation. This instrument amplifier also presents a high input impedance for both differential and common mode permitting application of the commonly used multiplexer CD 4066.

Cold junction compensation is provided by a silicon diode IN916, the voltage drop of which, with a current source, is inversely proportional to temperature. This voltage drop is applied through a proportioning resistor to the input of the final amplifier in the pre-amp signal conditioning. Also, a fixed reference voltage is applied to this current mixing and proportioning to get a zero output with a signal input of zero degree Farenheit from a chromel-alumel thermocouple. The mixing resistors for signal, cold junction compensation and offset were selected and proportioned to get a zero output for a 0° F thermocouple signal and one volt output for 3000° F signal input.

The sensor system, shown in block diagram in Figure 27 was designed with a minimum number of interconnecting lines between the Conditioned Module and the Readout Module as well as a minimum number of functions and circuits in the sensor module. The interface point in the A/D conversion places the circuit components such as the control, counter, clock and registers in the Readout Module, thus minimizing the number of interconnecting lines. The interface at the output of the analog to pulse-width conversion point provided for a desired pulse signal in place of amplitude, thus eliminating the necessity of many digital lines at such an interface point.

4.3. BREADBOARD TEST

The electronic circuit was designed to operate at an ambient temperature range of -40° F to +180°F with a maximum reading error of 0.5% or 15°F for an equivalent sensed temperature range of 0 to 3000°F. The circuit was designed and components were selected to provide for the minimization of errors and drifts from three sources - input null drift, gain change, and cold junction compensation.

The prime source of null drift is the input offset voltage of the input differential amplifier. A type uA 725 was selected because of its low offset drift of 2uV/°C. This would result in a 5°F or 0.2% for the 3000°F span. The gains were proportioned in the three amplifier stages so that the drifts in the second and third stages are effectively of secondary value.

Another source of drift was due to the amplifier gain change. Therefore, the design criteria was to employ an adequate number of stages and gain values to result in a feedback degeneration of sufficient magnitude to make the gain a function of stable feedback resistor networks. With 25 ppm resistors, the maximum drift contribution is 0.15%.

A third source of drift is the cold junction compensation signal. This is caused by the temperature sensitivity of the forward drop across a silicon diode. This yields a 5°F to 8°F or 0.2% to 0.3% error attributed to the difference in the non-linearity and temperature drift.

The root square summation of these error sources is 0.3 to 0.4% which is within the 0.5% limit. Measurements made over the temperature range of -40°F to +180°F were found to be within the required tolerance of 0.5% error for the bread-board model.

4.4. HYBRID CIRCUIT PERFORMANCE

The final version of the breadboard model, after having completed the temperature performance tests and modification, was used as the circuit for the construction of the thick-film hybrid circuit. Three units of the hybrid circuit was built by the Aerospace Systems Division of The Bendix Corporation in Mishawaka, Indiana.

A multichip approach was selected for this project. This approach limits the substrate circuitry to a conductor pattern. The circuit elements, resistors, capacitors, and semiconductors were purchased items meeting the requirement of

MIL-STD-883A. The package selected for this circuit was the TEKFORM 20139 1.25" x 1.25" platform and a TEKFORM 20270 cover. The unit was backfilled with dry nitrogen and sealed with SN 60 solder. The substrates used are alumina, precoated with sputtered chromium and gold, then gold plated up to a thickness of 150 micro inches. Substrate size was 1" x 1" x 0.025". The substrates were subtractively etched to provide circuit interconnects. Since power dissipation in the circuitry was only 0.07 watts layout and hot spots were not a problem.

Conductive epoxy was used to bond the integrated circuit chips, resistors, and capacitors. The epoxies are microcircuit grade materials which have been proven in military programs and used by Bendix for several years. MIL-STD-883 recognizes the widespread acceptance of organic polymers in military hybrids by providing comprehensive visual inspection criteria for organic polymer attachments and connections.

Connections in the hybrid were made with 1 mil diameter 1% silicon aluminum wire which is ultrasonically bonded by a wedge-wedge tailless bonder. This process is used because of its superior reliability and because no assembly heating is required. A photograph of the unit has been included in Figure 5.

The hybrid units were tested and calibrated at the Aerospace Systems Division. The span calibration data for hybrid S/N 02 was within 3°F or 0.1% of the required values which was well within the overall specification of 0.5%. The null offset was 10°F. Although this appeared to be of some consequence, the overall result includes a final offset balancing value which serves to eliminate the fixed offset of the cold junction compensation.

The hybrid SN 01 was assembled in the Thermally Conditioned Transducer SN 01. Resistors and diodes were selected for proper cold junction compensation signal for the temperature range of -40°F to +180°F. The most common ambient range of 75°F and 180°F were selected as the calibration points.

Tests based on the temperature parameters were conducted on the Thermally Conditioned Transducer SN 01 for gain and cold junction compensation measurements. The maximum error for gain (span) readings was 1.4% which exceeded the 0.5% limit. The amplifier chips for the 2nd and 3rd stages of SN 01 were inadequate for this temperature range and were therefore changed in the subsequent units SN 02 and SN 03.

The second unit, SN 02 was installed in a Thermally Conditioned Transducer Assembly. Thermal tests were conducted on the assembly. The results obtained showed an error of 0.4% and a cold junction compensation of 5°F or 0.2%. A third hybrid module that was produced, SN 03, was built primarily to be used as a spare unit.

The transfer and error curves are shown in Figure 33 and 34 respectively. The cold junction compensation temperature values and the corresponding error curves are shown in Figure 35 . The error curves are indicative of the non-linearity of the silicon diode voltages. The error for the SN 02 module is less than ±5°F. which is within specification limits. The error for the SN 01 module, however was over the limit. This attributed to the excessive drift in the last amplifier stage plus the non-linearity of the diode. Thus, the use of a higher performance op-amp in the SN 02 module has resulted in satisfactory compensation.

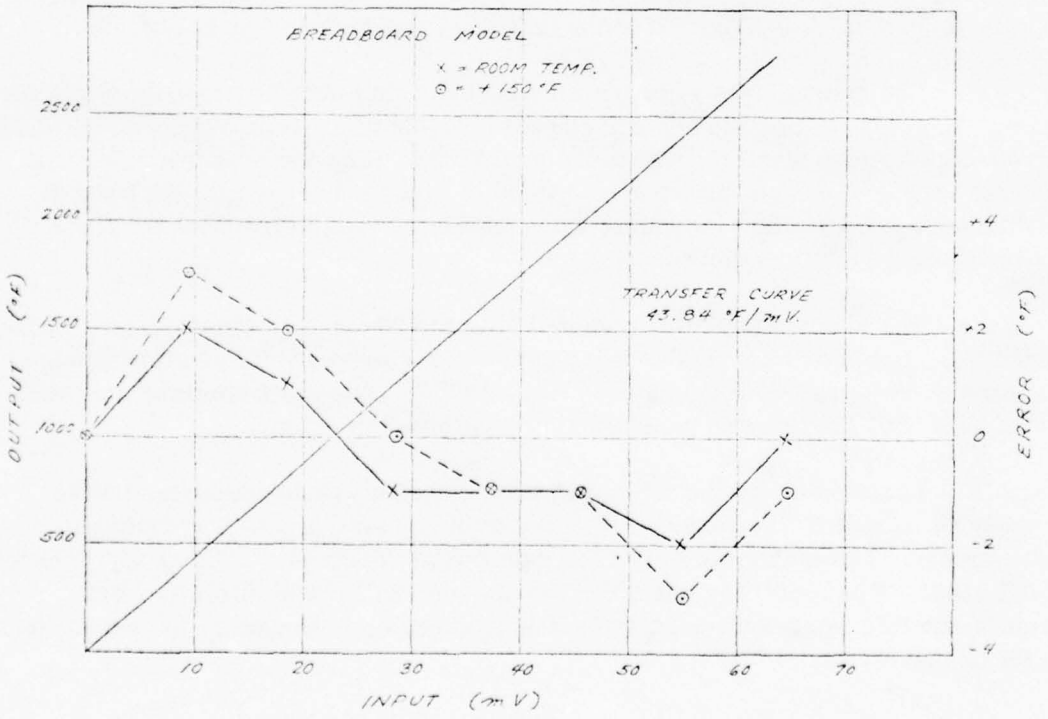

Figure 33 -- Transfer and Error Curves - Breadboard

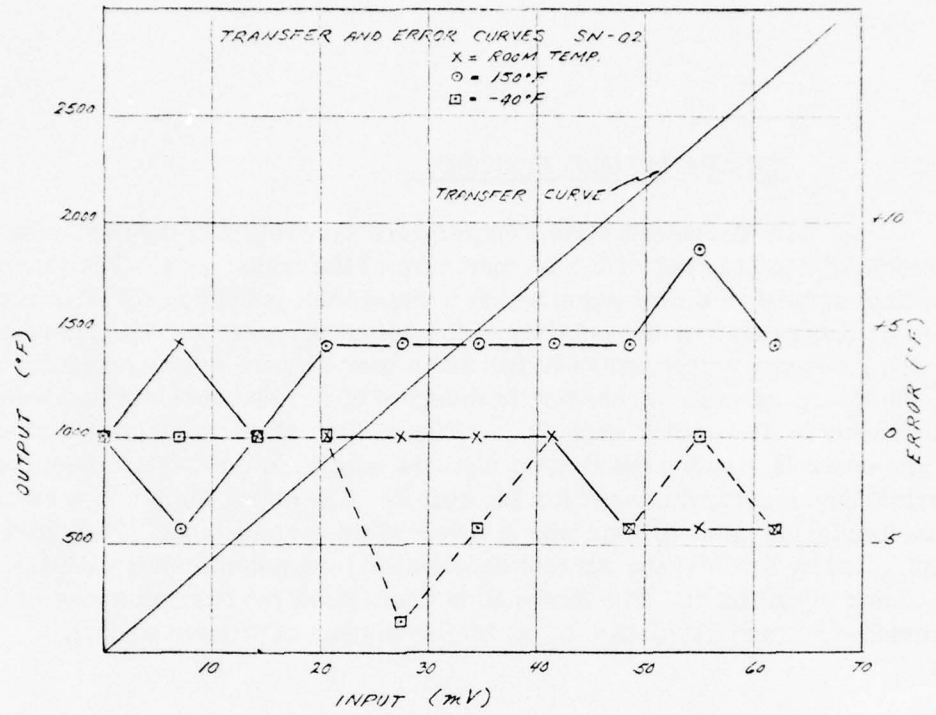

Figure 34 -- Transfer and Error Curves - SN 02

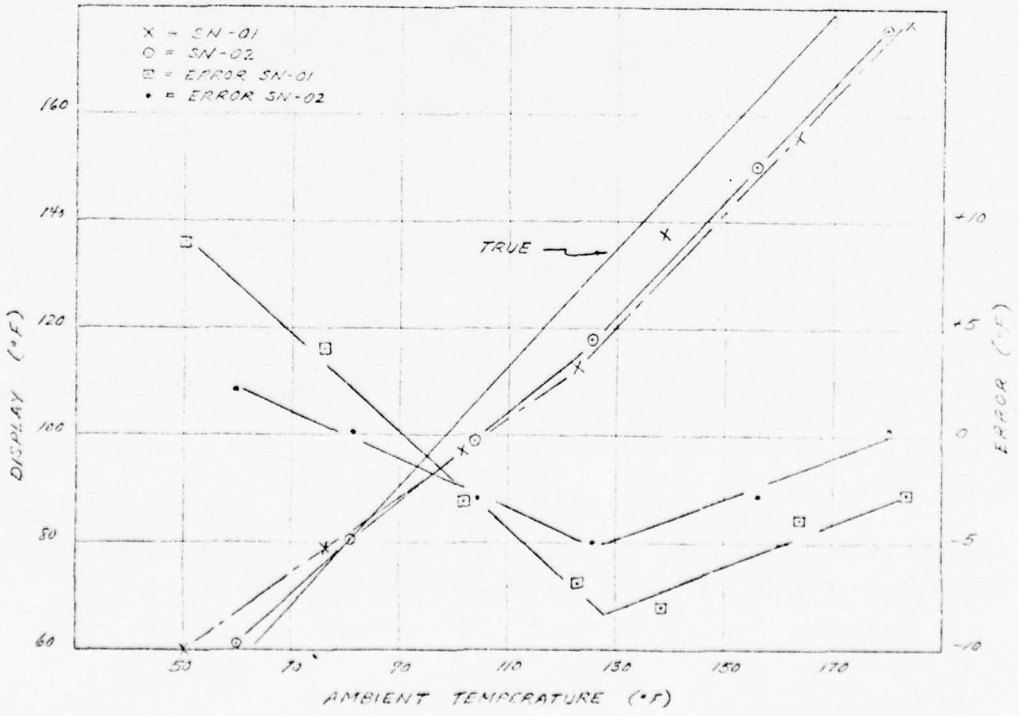

Figure 35 -- Cold Junction Compensation

4.5. TEMPERATURE CONTROL

A Thermoelectric Temperature Controller along with a thermoelectric element is used to control the temperature of the transducer. The thermoelectric element serves as a heat pump which is capable of providing for bi-directional heat flow as determined by the polarity of the actuating current. The current is controlled by the reference temperature limits and a temperature sensing element (a thermistor) on the hybrid circuit. A schematic diagram of the Thermoelectric Temperature Controller is shown in Figure 37. Figure 36 shows a functional block diagram of the controller which consists of a power supply, a three-state semiconductor power switch, and a control circuit for the switch. The power supply is a switching regulator type employing an oscillator with a pulse-width control input. The pulse width is controlled by a reference current established by a potentiometer setting and the control feedback signal input. The feedback is taken from the current sense of the output to provide a current regulation to match the current reference setting.

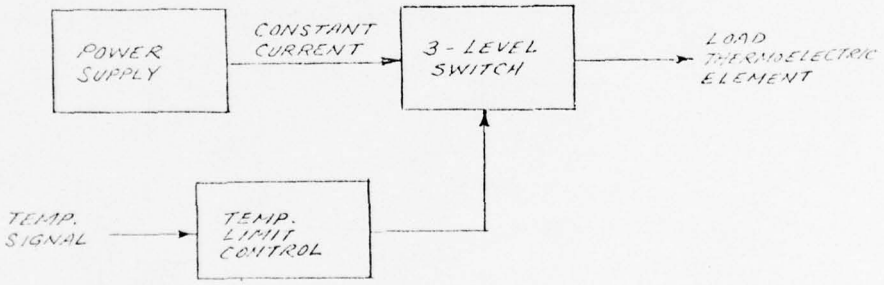

Figure 36 -- Controlled Power Source for Thermoelectric Elements

The output to the thermoelectric load is controlled by the three-stage transistorized power switch. The switch is a four-transistor bridge type which provides for a plus, a minus or a zero current to the load.

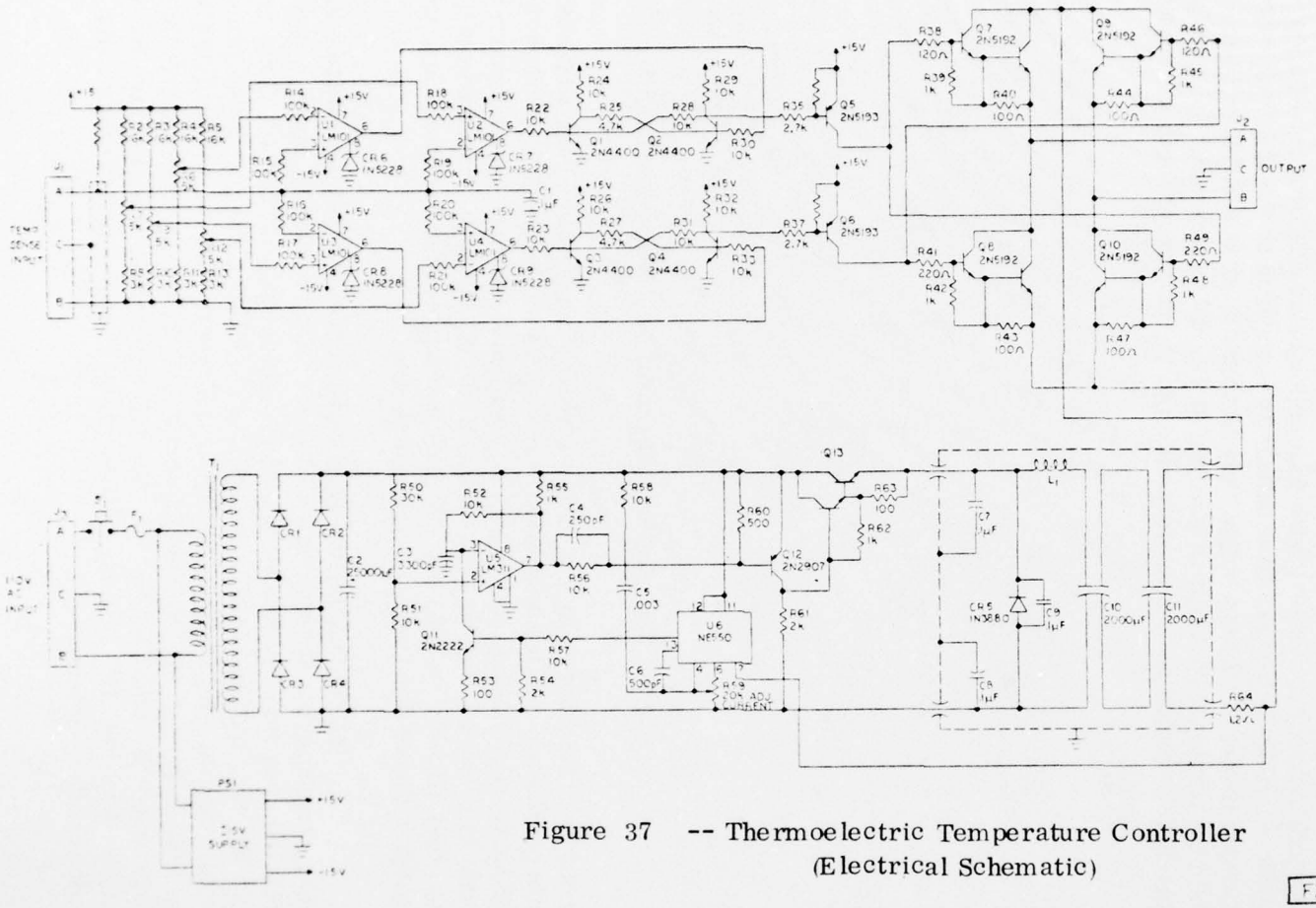

Figure 37 -- Thermoelectric Temperature Controller
(Electrical Schematic)

FXD-33947

The control circuit for the power switch consists of two flip-flops and four comparator amplifiers with four temperature reference voltages. The output of the thermistor temperature sensor is compared to the four references. Figure 38 shows a graph of current output versus thermistor temperature in the hybrid. When the high temperature limit is reached at T4, the comparator triggers the high level flip-flop to switch the output current on to the cooling direction. As the temperature

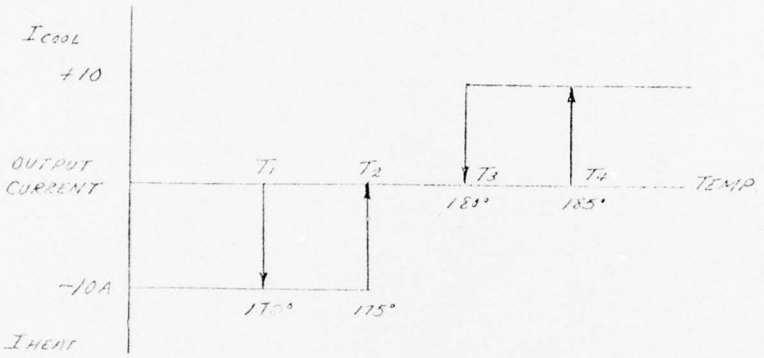

Figure 38 -- Current Output vs Thermistor Temperature

drops below the lower limit T3, the flip-flop is triggered back to the other state which cuts off the two cooling switches. The unit therefore cycles between these limits when the thermal conditions in the hybrid requires a cooling control mode. When a heating mode is required, the control cycles similarly between temperatures T1 and T2 with the other flip-flop and T1 and T2 limit comparators operating to activate the other two bridge switches for heating current direction.

The reference voltages were set for a cooling cycle between 180° to 185°F and a heating cycle between 170°to 175°F. This operating temperature range was selected to provide minimum drift due to temperature changes in the hybrid, consistant with the capabilities of the thermoelectric cooling element. Some penalty in reliability results at this temperature. If the hybrid has a base failure rate of 1 at 70°F then the failure rate at 170°F is multiplied by 4 ; this multiplying factor increases to 10 at 210°F and 18 at 257°F. The 170°F operating temperature increases the failure rate by 4 but the decreased operating temperature range decreases the electronic drift errors by a factor of 31.

SECTION V

THERMOELECTRIC COOLING ELEMENT

The thermoelectric cooling elements were developed under subcontract to Bendix by Ohio Semitronics Inc. of Columbus, Ohio. Standard cooling units available from several manufacturers are generally limited to operation at temperatures below 300° F. Units developed under this contract provided 3 watts of cooling with a hot plate temperature of 345° F and a differential temperature of 130° F. (For references purposes Appendix 1 provides a description of the thermoelectric effect).

Six thermoelectric devices were provided to Bendix. The first three units were used for development tests. The final three were used in the three thermally conditioned modules built under this project.

The thermoelectric elements were built in modules 1-7/16 x 1-7/16 x 5/16 inches. The major differences between the thermoelectric elements was in the number of couples within an element. Unit 1 contained 16 couples, unit 2 contained 31 couples, and the remaining four units contained 44 couples. The last three of these units were designed for operation at temperatures to 345° F. At these temperatures the solder used within the elements becomes a problem. To prevent performance degredation due to solder migration flame sprayed nickel was used for contact formation.

The thermoelectric elements (couples) are formulated from a Bismouth Telluride polycrystaline alloy. The formulation of the alloy and the manufacturing process control the characteristics of the elements. The basic material used in the thermoelectric couples is Bismouth Telluride. The alloying and doping materials include Tellurium, Antimony, Arsenic, Selinium and Antimony Tri-Iodide. Doping determines whether the polycrystals will be P, (excess positive charges) or N (excess negative charges).

Design parameters for the couples within the thermoelectric elements are given in the below for a T_H of 285° F:

$L/A = 4\ cm^{-1}$ = couple leg length to area ratio

$\alpha_p - \alpha_n$ = Seebeck coefficient = 430×10^{-6} volts/°K

$\rho_p + \rho_n$ = Resistivity of couples = 4.0×10^{-3} ohm/cm

$K_p + K_n$ = Thermal conductivity of legs = 2.8×10^{-2} watt/$cm^{-°K}$

R_c = Resistance of a couple 0.8×10^{-3} ohms/junction

K_c = Thermal conductivity of couple 0.7×10^{-2} watts/°K

Performance characteristics for the Ohio Semitronics model TM-1 -10H is given in Figure 39 . The optimum current for this device is in the range of 8 to 10 amps. To obtain the best coefficient of performance 8 amps was selected. In application of this cooling device the cold plate connected to the hybrid package and the hot plate sinks heat to the fuel heat exchanger. From the graph it can be seen that at a cold plate temperature T_c of 180° F and a hot plate temperature(T_H) of 285° F this unit can pump 4.5 watts. From test data the coefficient of performance at this point is 0.18. The dashed line on Figure 39 shows performance data for the thermoelectric cooling elements with a T_H of 345° F. At this point the unit can pump a two watt thermal load and maintain the cold plate temperature at 195° F.

The thermoelectric couples are formulated from a Bismouth Tellurid polycrystaline alloy. Extensive testing of these materials by the manufacturer has revealed two possible failure modes for the elements. Tests at temperatures of 390° F indicate that a decrease of about 5% in the coefficient of performance is probable after 100 hours. At 320° F no change in efficiency has been noted after testing. The high temperatures cause migration of the elements within the alloy resulting in a loss in efficiency. The operating temperature limit can be increased by a reformulation of the alloy. The formulation used in units tested was a compromise to obtain a high coefficient of performance and meet the 330° F hot plate temperature goal.

Since the thermoelectric couples are polycrystaline materials, shock and stress can cause failures due to fractures or a decrease in performance due to microscopic cracks in the material. Therefore any package designed to use thermoelectric elements must be designed so as not to exceed the manufacturers stress limits for the elements. The thermoelectric elements as used in the TCM were mounted between two flate plates to form a rigid structure held with four bolts torqued to 8 inch-pounds.

PERFORMANCE DATA OHIO SEMITRONICS THERMOELECTRIC MODULE MODEL TM-16-10H HOT PLATE TEMP. $T_H = 285°$ F

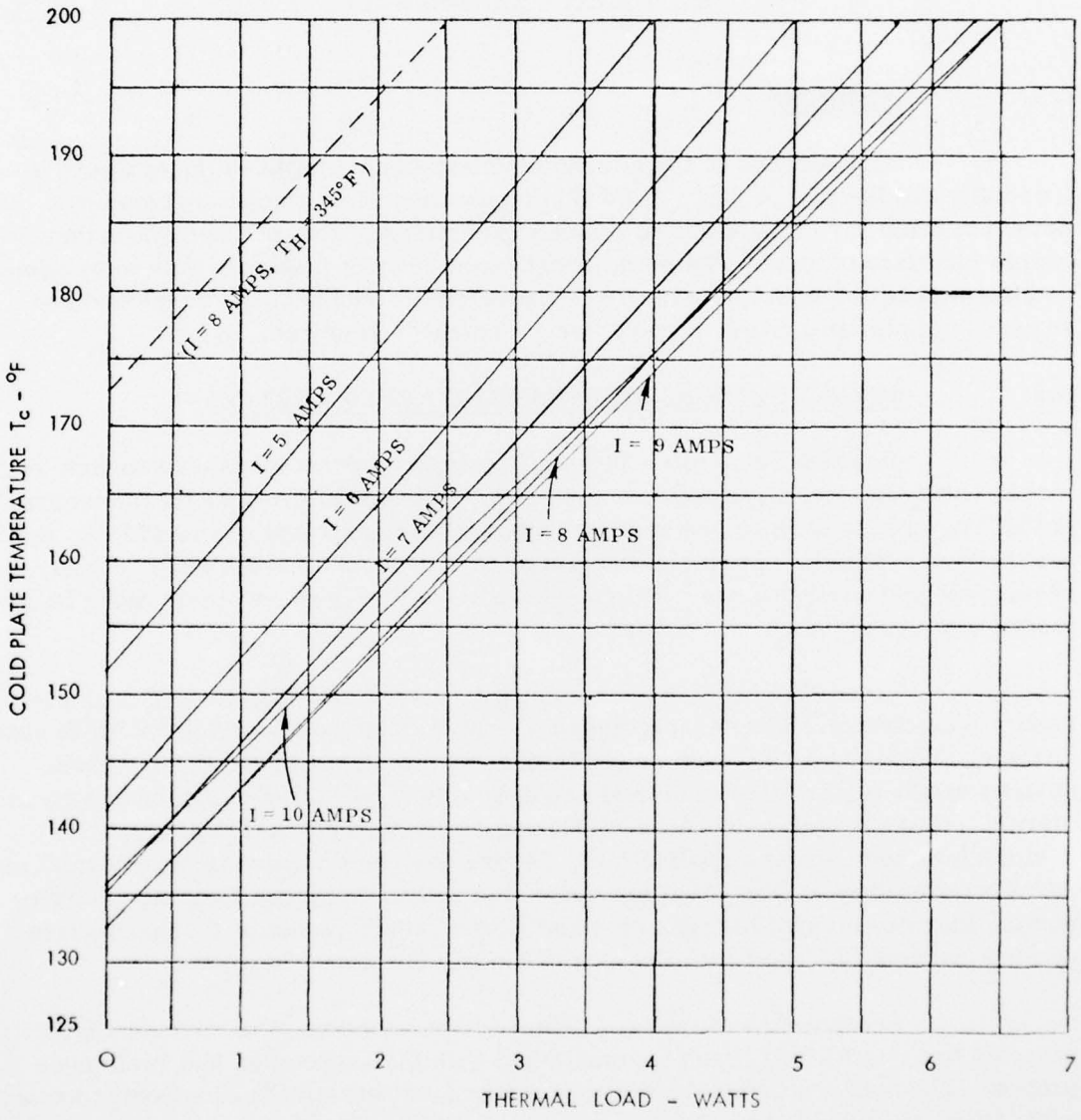

Figure 39 -- Performance Data

SECTION VI

ALTERNATE SENSOR STUDY

6.1 PURPOSE

The purpose of the alternate sensor study was to evaluate where a thermally conditioned package could find application in an engine environment. The selection made for the test and development portions of this project was a thermocouple interface circuit. The main thrust of the project however, was to develop a cooling method for high temperature environments. The package developed can serve any application where a cooled environment is required.

6.2 ENGINE SENSORS AND POSSIBLE APPLICATIONS

Position Sensors -- Types of position sensors found on a turbine engine include; potentiometers, resolvers and linear variable differential transformers (LVDT's). These devices are generally operable in environments to 475° F. Special designs are available that extend that range to 750° F. These devices are best handled by fuel cooling alone. Thermoelectric cooling in these applications is not judged to be practical.

Speed Sensing -- Speed sensing is accomplished by use of variable reluctance sensors. These sensors are operable in environments to 750° F in special designs. These again are best suited to fuel cooling if any is required. These devices would require thermoelectric cooling only if solid state devices are contained therein. Commercial sensors currently employ Hall effect and light sensitive devices for speed sensing applications. These devices are used in commercial products because they exhibit excellent noise immunity. In aircraft engine environments, they are compatible with size and power requirements of thermoelectric cooling and could be used with the type of module developed here.

Temperature Sensing -- Temperature sensing in electronic engine controls has traditionally been accomplished with thermocouples and resistance probes. The sensors themselves do not require cooling but the electronics associated with these sensors can benefit from signal conditioning on the engine as demonstrated in this project. If the engine controller is mounted some distance from the sensor the

capability to buffer and amplify the signal can be advantageous. In this system eight thermocouples were multiplexed and the signals were changed to pulse width modulated form. The multiplexed signals were transmitted over a pair of wires. In applications where weight or extreme noise immunity is required the signal can be transmitted over an optical fiber link.

The optical pyrometer is a new device being developed for turbine engine use. The device uses a silicon diode to measure the radiated energy emitted from the hot turbine blades. The silicon diode suffers from the same temperature limitations as other silicon solid state devices. The operating temperature is limited to 257° F. The device as currently designed use a long optical relay link to remove the sensor from the hot ambient and then uses air cooling to reduce ambient temperatures. The thermally conditioned sensor approach is a natural application for this device.

Pressure -- Extreme accuracy pressure sensors (0.01% of full scale) are required by modern turbine engines. Sensors that meet such accuracy requirements all have electronics packaged with the sensor. Therefore, the sensor must be located in an environment consistent with the electronics. If the sensor is located with an off-engine mounted computer the signal lags and transport delays can become so long as to make the pressure control parameter ineffective for control purposes. The thermally conditioned module could be used to contain several pressure sensors, process the signals and transmit them to a control computer.

Implementation of pressure sensors in the thermally conditioned module was evaluated. The concept for the design of the pressure sensing module is shown in Figure 40. In this design, the thermoelectric component, the primary heat exchanger and isolator are identical to the previous design. Other parts of the module require some modification and the incorporation of additional parts. The modification include a slight enlargement in the electronic package and a reduction in the number of connectors. The size of the printed circuit board remains the same as that of the thermocouple circuit. The cold plate is modified to accommodate the new electronic package. These elements, along with the thermoelectrics, heat exchangers and isolator are attached to the mounting plate. The pressure sensitive elements are located on the opposite side of the mounting plate.

Mechanically, the mounting plate is ridged to prevent resonant vibration in the range of frequencies associated with jet engines. To accommodate for the proper ducting of the fuel for cooling and pressure to the proper locations, ports are drilled in the plate near the mounting lugs and fluid channels.

The heat conduction covers and convection shields used are similar to the one used for the thermoelectric module. The assembly is void of any direct metal heat conducting path between the ambient heated surface and the heat exchanger except at the mounting lugs and the electrical connector. The areas should be lagged after installation. The lagging should cover the exposed parts of the mounting plates and some length of the attaching lines.

Structurally, the inner cover of the electronic package is in direct contact with the secondary heat exchanger. The inner cover of the pressure sensing elements is in direct contact with the secondary heat exchanger. Using this construction and some lagging over the mounting lugs and lines, the pressure sensing elements will have a temperature environment of about 10° F to 15° F above the fuel temperature. The electronics will have a thermoelectric cooler to bring the mounting plate for the electronics about 80° F below the temperature of the fuel.

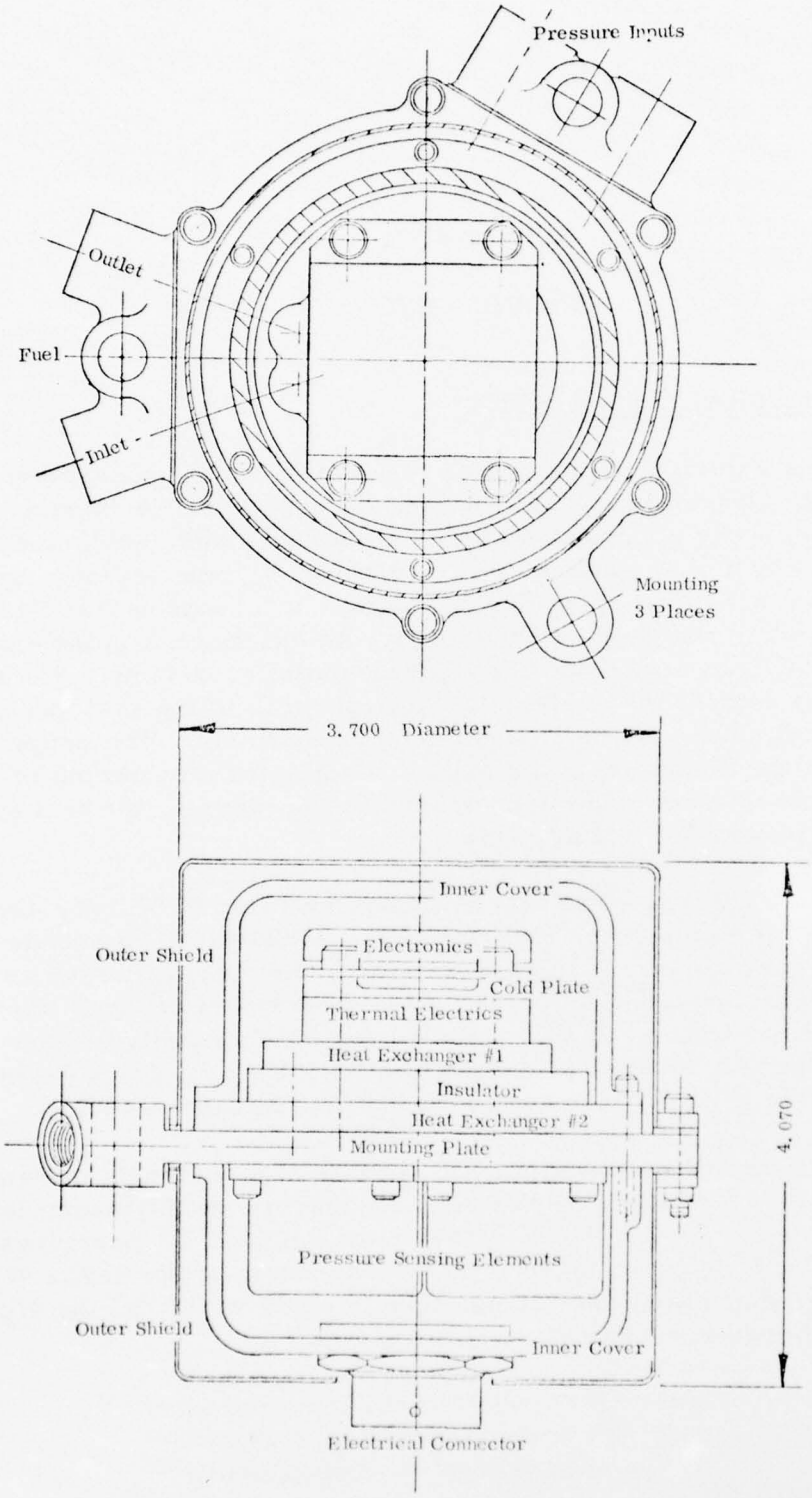

Figure 40 -- Thermally Conditioned Pressure Sensor Module

SECTION VII

ENGINE TESTS

7.1. GENERAL DESCRIPTION

The objective of the engine test phase of the program was to demonstrate the operational capability and endurance of the Bendix FXD-33900 thermally conditioned electronic module when subjected to the acoustic and vibration environment of an aircraft turbine engine. The module was installed on a JT9D turbine engine in a sea level test cell at Pratt & Whitney Aircraft in Hartford, Connecticut. An existing on-going engine test program was utilized to provide the environmental conditions. The module was not used to control the engine since the purpose of the test was only to evaluate the unit under engine environmental conditions. The program goal was to operate the module with the engine running for a minimum of 100 hours. Since no failures were encountered in the module, the test exposure was arbitrarily extended to 200 hours.

The JT9D engine is manufactured by Pratt & Whitney Aircraft and is a two spool high-bypass turbofan in the 43500 to 52000 pounds of static thrust power class. It is used on wide bodied aircraft such as the Boeing 747 and McDonnell Douglas DC-10 and is typical of large high performance turbine engines. It was selected for the thermally conditioned module test program because of the availability of the on-going engine test program and also because it is a modern high performance engine.

The module was designed to operate at ambient temperatures to 750°F with fuel coolant flows to 330°F. The thermal performance levels of the test unit were proven in laboratory tests because temperatures in the test cell would not approach these levels. The intent of the engine tests was to show that the thermally conditioned module could withstand the vibration environment of engine mounting.

7.2. TEST EQUIPMENT

The electronic equipment used for the test program was supplied by Bendix. The equipment included a readout module, a thermoelectric power supply and connecting cables. Power to the thermoelectric power supply is provided through an interlock module so that power and cooling flow to the thermally conditioned module are all present at the same time.

7.3. TEST CONDITIONS

The unit was mounted on a JT-9D turbine engine and connected to the test equipment as shown in the block diagram of Figure 41. During testing, the engine was running. Also, the cooling fluid flow, thermoelectric power and readout module power were all turned on. The readout module was used to read the eight channels of thermocouple data. The cooling fluid used for the test was ordinary tap water at its normal temperature. The water supplied to the interlock assembly was maintained at a minimum pressure of 25 psia. The flow rate through the module was to be approximately 20 lbs/hr. or 2.5 gal/hr. This provides about the same cooling capacity as JP-4 fuel at 100 lb/hr. After passing through the test module, the water, whose temperature rise was negligible, was routed to a drainage for disposal.

The original intent of the program had been to use fuel as the heat sink in the engine test program. The use of fuel, however, conflicted with P&WA safety requirement and had to be abandoned. The use of other fluids which could be temperature controlled over a range of -65°F to 300°F was considered but rejected on the basis of cost. The thermal performance of the thermally conditioned module had been adequately documented in laboratory tests, and the engine tests were intended to document mechanical integrity and endurance. The type of fluid used as a heat sink was of secondary importance for the test conditions.

7.4. ENGINE TEST RESULTS

Engine-mounted testing of the thermally conditioned electronic module was performed at Pratt & Whitney Aircraft. The test vehicle was a JT-9D engine (X-493). The module was mounted in place of a station 3.5 bleed on the engine. The eight available thermocouple channels were allocated to the following temperature measurements:

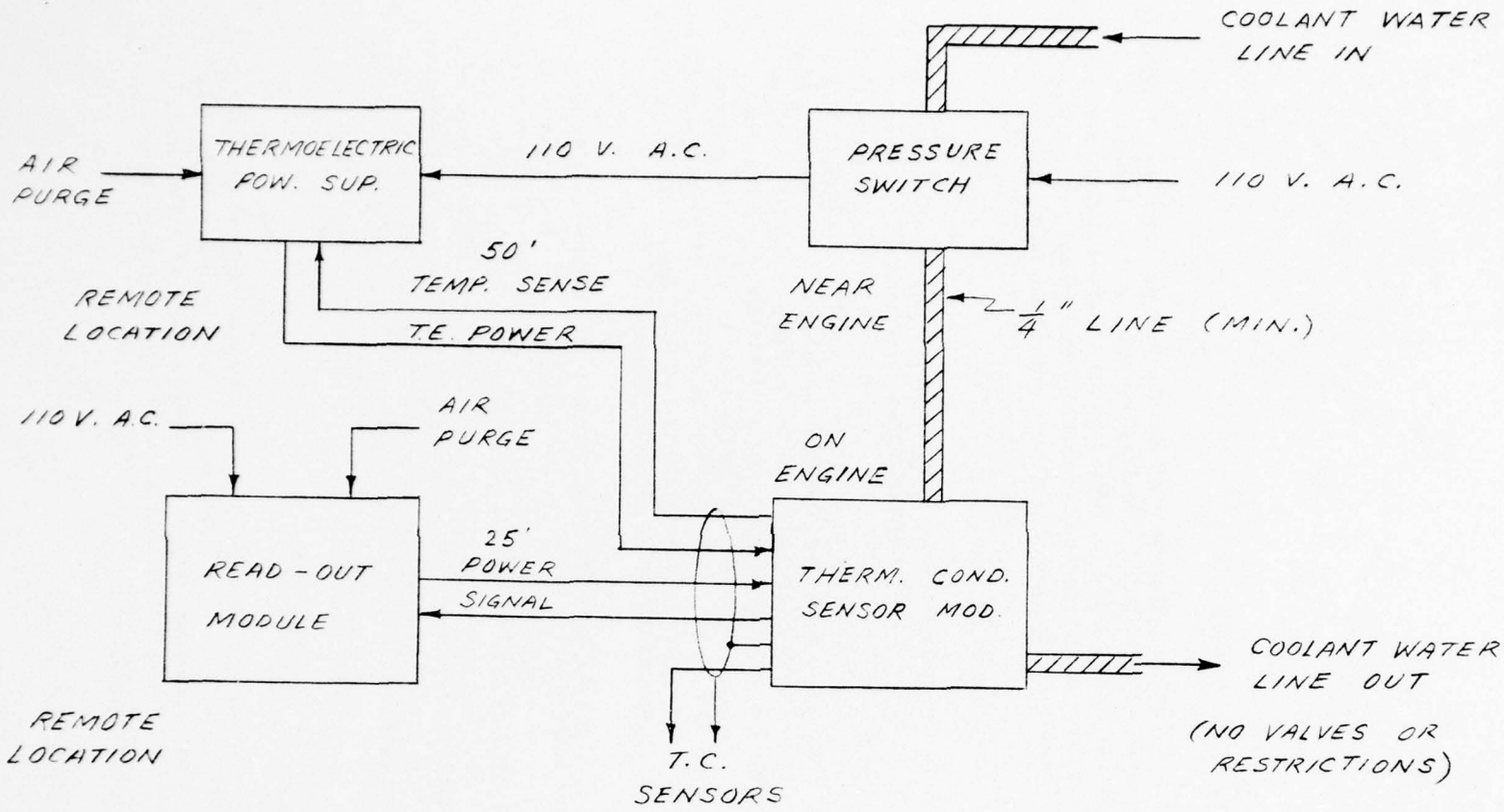

Figure 41 -- Engine Mounted Test System

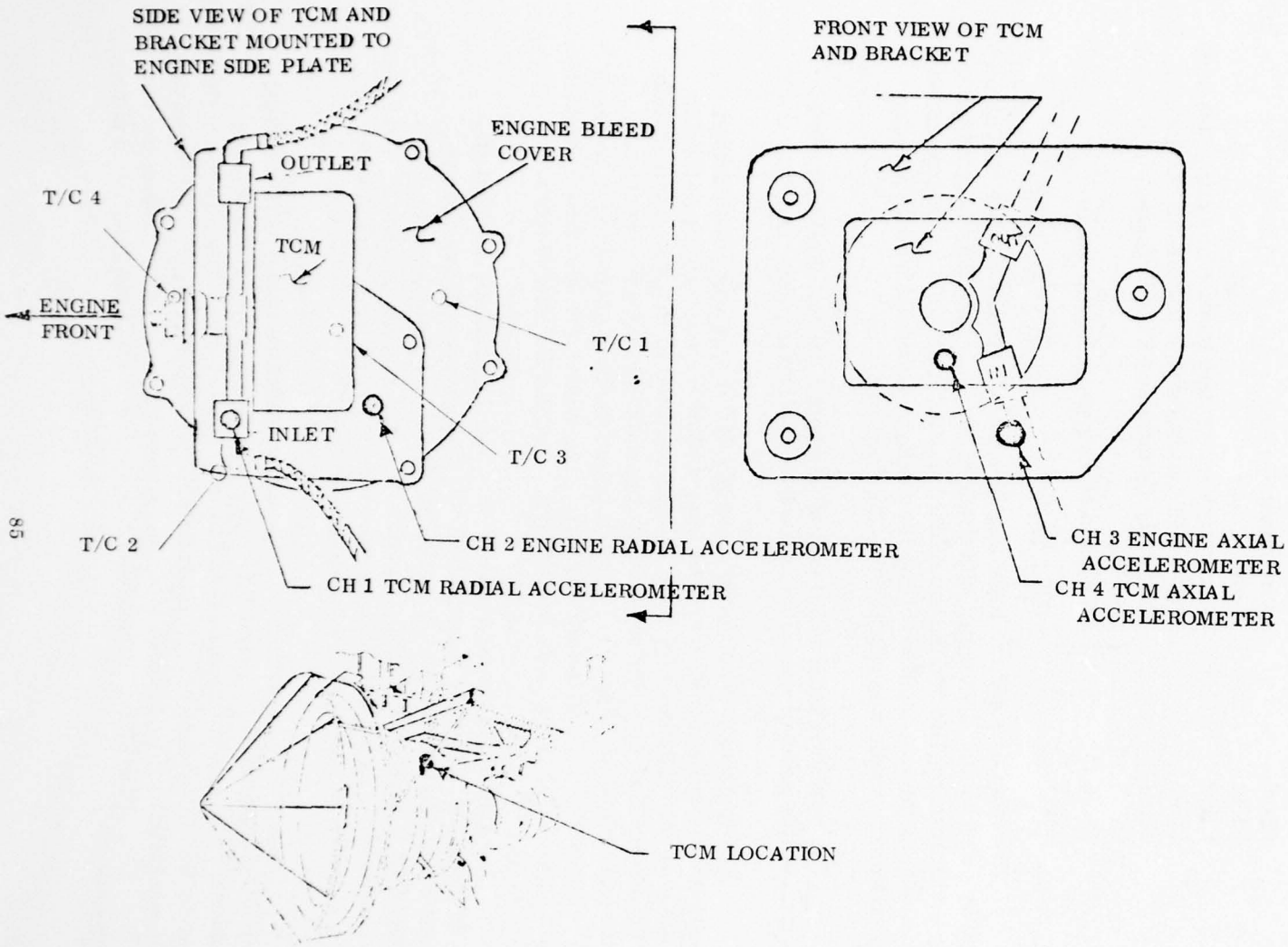

Figure 42 -- TCM , Vibration Pick-up and T/C Locations.

Channel	T/C Location
CH#0	Hybrid temperature
CH#1	Engine Cover
CH#2	Thermally Conditioned Module Mounting Bracket
CH#3	Thermally Conditioned Module Elec. Connector
CH#4	Thermally Conditioned Module Cover
CH#5	Ambient 6 inches above engine case
CH#6	
CH#7	

Vibration data for the mounting location of the test module was also obtained by using an accelerometer and readout device. This data is intended to provide a vibration profile for the mounting location at the various engine speeds. Figure 42 shows the test location of the thermally conditioned module and the associated thermocouple and vibration pickup location.

The total test time accumulated was 200.5 hours. Failures were encountered on the readout console and the thermoelectric power supply.

The thermally conditioned module S/N 101 was shipped to P&WA for engine tests. In the initial checkout stages after engine mounting, the unit was found to leak. The unit was removed and returned to Bendix. Disassembly of the unit showed that the transfer tubes between the primary and secondary heat exchanges were too long. This had damaged the heat exchanges in the area of the O-ring seals and resulted in the leak. The tubes were shortened, unit S/N 102 was assembled, leak tested, and shipped to P&WA for engine tests.

A summary of the test data is shown in Figures 43, 44, and 45. Figure 43 gives a history of the hybrid circuit temperature during the test. The cross hatched area represents the limits of the temperature data points. Data was taken before each engine run and after each engine shutdown. Time between successive data points varied from less than one hour for the early data to every 24 hours for the last 100 hours of test data.

During the first twenty hours, the temperature of the hybrid circuit was maintained between 165°F and 175°F and was independent of the ambient temperature. The readout module then failed to display data. Twenty hours of test time on the TCM were accumulated before the engine test schedule permitted removal and repair of the readout module. These wires in no way effect the operation of the TCM. Therefore, it has been assumed that the TCM functioned normally during that period.

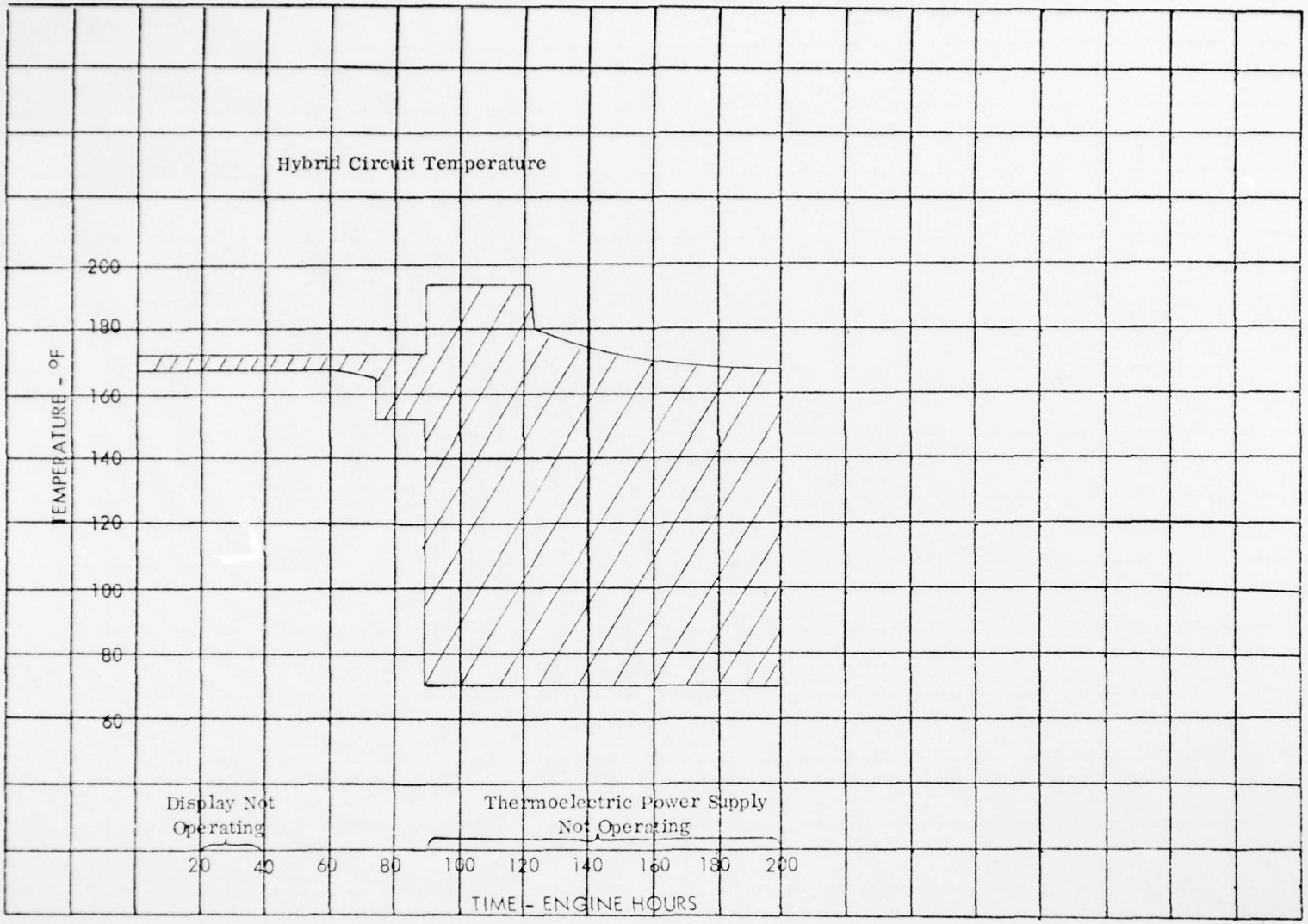

Figure 43 Hybrid Circuit Temperature

AD-A042 378 BENDIX CORP SOUTH BEND IND ENERGY CONTROLS DIV F/G 21/5
AN EVALUATION OF THERMOELECTRIC COOLING AS APPLIED TO ENGINE CO--ETC(U)
MAY 77 C S LONGSTREET, W LORENZ, W J MCPHEE F33615-74-C-2068
UNCLASSIFIED AFAPL-TR-77-24 NL

2 OF 2
ADA042378

END
DATE FILMED
8-77
DDC

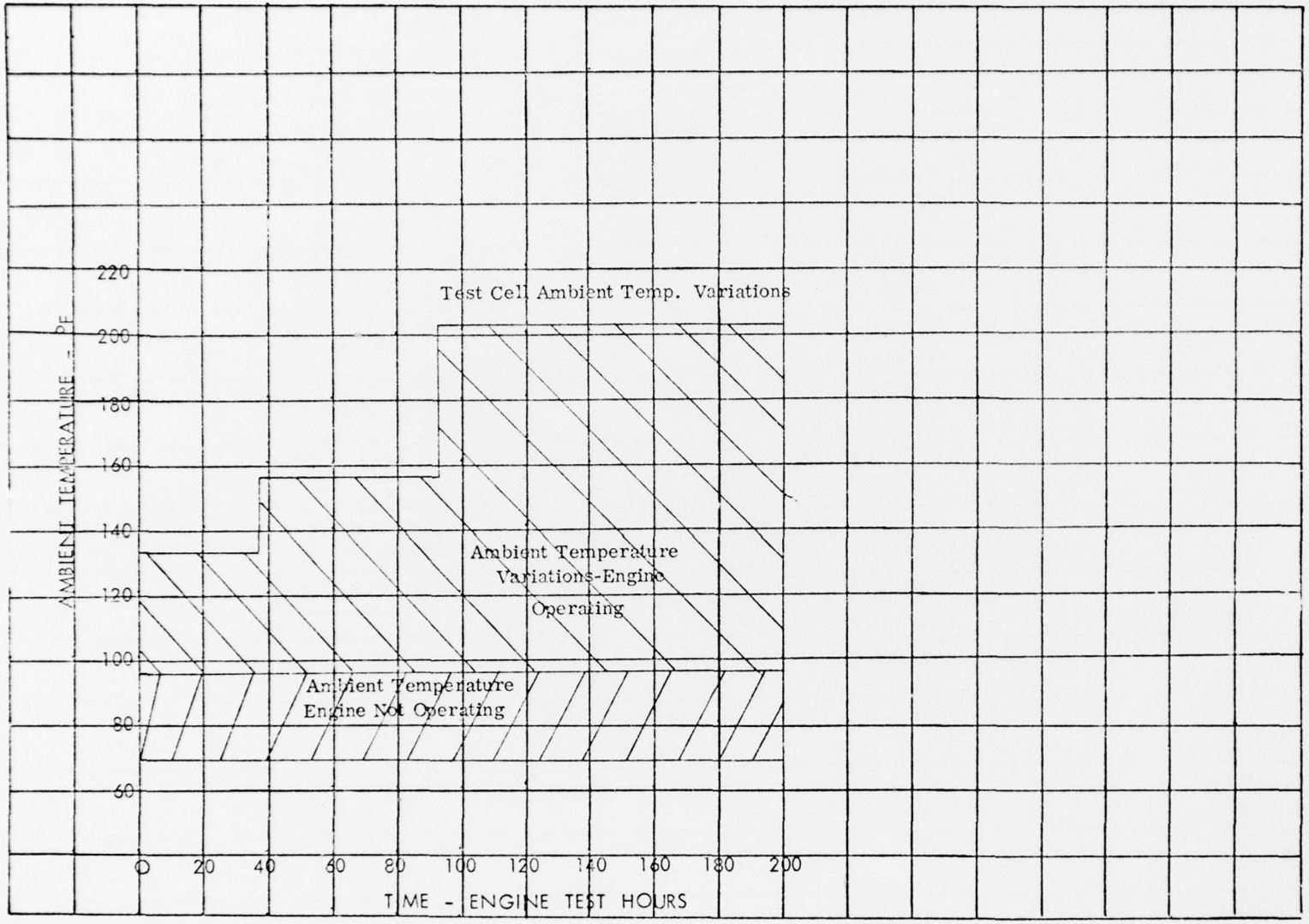

Figure 44 -- Test Cell Ambient Temperature Variations

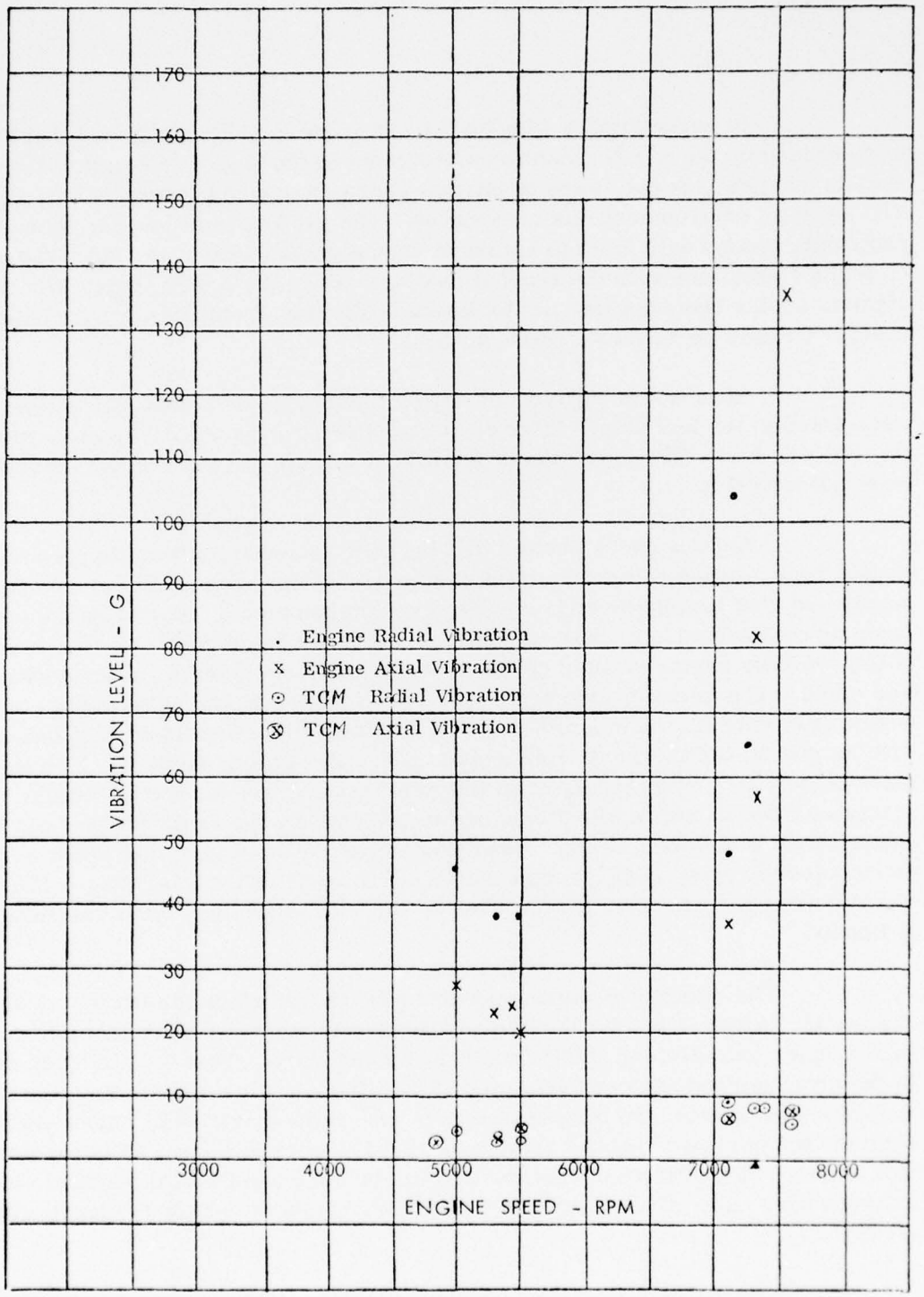

Figure 45 -- Engine and TCM Vibration Comparisons

In consultations with P&WA test engineers it was agreed that the failures were caused by the harsh acoustic environment in the engine test cell. The readout module and power supply were constructed for a standard laboratory environment. The acoustic environment was unexpected. The readout module was, therefore, externally padded with foam to act as an acoustic absorbing material. There were no further problems with the readout module. Since the power supply for the thermoelectric cooler requires free air to dissipate the heat from the unit, acoustic insulation could not easily be added to power supply.

After about 70 hours of engine testing, some below normal temperatures were noted in the test data. After 88 hours of testing the ability to temperature control the unit was lost. The operation of the hybrid circuit and the readout module, however, were not affected.

A quick check showed that the thermoelectric power supply had failed. At this time a crucial decision in the test program was made. Either repair the power supply and risk having the engine endurance run completed before repairs could be made or continue running without power to the thermoelectrics. Since a majority of the 100 hour engine running goal had been met, a decision to continue without repairs was made. The intent of the engine test was to show that the TCM would survive the engine environment. It was felt that this intent could be met under test cell conditions with or without the thermoelectrics operating. The failure mode to which the thermoelectrics would be subject in this test was due to mechanical stress. This stress was due to engine vibration and was essentially the same whether the thermoelectrics were powered or not. After completion of the engine test program, the thermoelectric power supply was examined. A broken wire was found. The unit was repaired and was used for checkout of the TCM after the engine test program at Bendix.

The effect of removing power to the thermoelectrics is clearly shown in Figure 43. After 88 hours, the hybrid circuit temperatures were now controlled by the water temperature and the ambient temperature. Test data is again scattered in the crosshatched area and generally determined by when the reading was taken. Before engine starts, the temperature was generally about 70°F. After engine runs, the temperature reached as high as 178°F. Data in Figure 44 is presented so that ambient temperature during the test can be compared with the hybrid circuit temperature. The effect of operating the thermoelectric cooler is clearly demonstrated.

To evaluate the effectiveness of the shock mounts used on the thermally conditioned module (TCM) vibration data was compared for the radial and axial directions of the engine and module. Typical data points are shown in Figure 45 . At the engine speeds where data was available, the shock mounting reduces vibration levels by a factor of 10 to 20 in all planes. Even though engine vibration levels reached 186 G's, the module vibration did not exceed 10 G's.

7.5. POST TEST EVALUATION

Upon completion of the engine test, the thermally conditioned module was returned to Bendix where the unit was retested. The unit was first checked out at room temperature without fuel cooling flow. The hybrid signal conditioning circuit performed normally. The thermoelectrics were powered and were also found to be functioning. Based on the above bench test, it was concluded that the unit had survived the engine test without detrimental effects.

Following bench check, tests were performed to determine if the thermal characteristics of the unit had changed. Test data, as in Figure 15, was to be taken at 750°F ambient air with JP-4 fuel at several temperatures. Several problems were encountered in this attempt. The heat exchangers were found to be partially clogged with lime due to the hard tap water used in engine tests. A meaningful comparison of data could not be made with an obstructed heat exchanger. The lime was removed by flushing with phosphoric acid. This acid is non-reacting with the aluminum heat exchanger and, therefore, would not damage the unit.

Retest of the heat exchanger showed the pressure drop across the unit and flow rates were back to normal. Thermal tests on the unit were reinitiated. The unit operated, but the thermoelectrics were only able to maintain a 50°F differential from hot plate to cold plate. The SN101 unit had been able to maintain a 90°F differential.

A teardown inspection of the unit revealed that fuel had leaked into the module cavity. This had acted as a thermal path for heat from the covers to reach the thermoelectrics. This resulted in a sufficient heat load to limit the cooling capacity of the thermoelectrics.

Pressure testing revealed a leak in the primary heat exchanger upper surface. The aluminum at this surface in 0.010" to 0.015" thick. The

wall had been weakened due to corrosive action of the tap water. The test unit is presumed to have survived engine test because of the reduced pressure and flow rates. In the laboratory, JP-4 fuel at 130 psi was used. Engine tests used water at about 25 psi. The combination of test pressure and corrosion of the aluminum are presumed to have caused the failure. As a result of these failures in the heat exchanger, no further performance tests were attempted on the thermally conditioned module.

Since one of the objectives of this program had been the test and development of a thermoelectric cooling module, the thermally conditioned module was disassembled, the thermoelectrics were removed and sent to the manufacturer for retest.

The manufacturer reported two related problems with the thermoelectric element. The first was that the cold plate of the thermoelectric element was no longer flat and had to be ground flat before testing. Heat pumping capacity had decreased about 20%. Further checking in this area showed that several of the thermoelectric couples at the perimiter of the thermoelectric module had increased resistance from a normal 5 milliohms to 38 to 75 milliohms. This change in resistance was also found to be pressure sensitive. The manufacturer concluded that several of the solder joints between couples had broken.

It is evident that the .010" to .015" wall of the heat exchanger did not provide adquate support for the thermoelectric module and allowed movement sufficient to break the solder joints.

Future applications will require redesign such that stress levels for the thermoelectric elements will not be exceeded.

Further examination of the components and consultation with the manufacturer pinpointed the probable cause of the solder joint failure. The heat exchanger showed a depressed area in the center section where the leak had developed. This depressed area corresponded with the surface on the thermoelectric module that had to be ground flat. The depressed area showed evidence of overpressure from the outside. It is therefore believed that fuel or water leaked into the area between the thermoelectric couples. When power was applied, the fuel or water vaporized since the temperature in this area reaches 300°F. The vapor expanded resulting in deformation of the heat exchanger and overstress in the boundary area between the heat exchanger cooling surface and the heat exchanger perimeter support area. The cause of the solder joint failure

is therefore deduced to be due to overstress due to vaporization of the fuel or water leakage due to the heat exchanger leak. The heat exchanger leaked as a result of corrosive action of water used in the engine test program. No such problem is expected when jet engine fuels are used as a coolant.

SECTION VIII

CONCLUSIONS AND RECOMMENDATIONS

The significant result of the program is that it both demonstrated the feasibility of the concept and provides correlation between the analytical approach and tests results that will allow design of future applications with a high degree of confidence that actual performance will conform to predicted performance.

8.1. CONCLUSIONS

1. Correlation between analyis and tests was good.

2. The design is sufficiently rugged to withstand the engine operating environment currently projected for Mach 3.5 aircraft.

3. In applying results of this study to specific applications, improvements in performance can be achieved in several areas:

   - The thermoelectric performance can be improved.
   - By correlating the module design with engine mounting, the module could be shielded from the 50 ft/sec. velocity and performance would be improved.
   - Improvement in shielding in the base area and sides of the secondary heat exchanger are possible and will improve performance.
   - Additional development of the heat exchanger would result in equal performance with a lower pressure drop through the heat exchanger channels. Redesign is also repaired to provide better structural support for the thermoelectrics.

4. In implementing any specific applications, special attention should be given to the considerations associated with "hot soak" after landing and engine shut down.

5. The heat load imposed on the fuel by module operation is less than one (1) percent of that projected for the fuel to oil cooler on high Mach number aircraft. Reference report AFAPL-TR-73-51, "Aircraft Fuel Heat Sink Utilization."

6. A design approach such as that studied here is necessary in those applications where for survivability or reliability reasons the electronics must be maintained below the temperature of fuel available as a sink. The penalty paid is the power consumption of the thermoelectrics.

7. While the emphasis of the program was on "small" individual circuits or sensors, there is no inherent limitation on the approach because of size. Subject to the thermoelectric power consumption penalty the approach is applicable to an engine mounted digital controller.

8.2. RECOMMENDATIONS

1. At such a time as specific requirements are defined for thermally conditioned components, the design concepts demonstrated in this program should be utilized.

2. The areas where additional development would improve overall operation are considered to be:

   - Thermoelectrics -- Any improvements that effect the heat load pumping capability, power consumption (efficiency) and/or will increase the temperature differential from cold to hot plate would enhance the value of the concepted approach.

   - Heat Exchangers -- Equivalent effectiveness with a decreased pressure drop through the channels is attainable with some development effort.

REFERENCES

1. Altman, Manfred; Elements of Solid State Energy Conversion; Van Norstrond Reinhold 1969.

2. Codeff, Irving B.; Thermoelectric Materials and Devices; Reinhold Pub. Corp. 1960.

3. Goldsmith, H.; Applications of Thermoelectricity, J. Weley & Sons, 1960.

4. Goldsmith, H.; Thermoelectric Refrigeration; Plenum Press 1964.

5. Gray, Paul E.; The Dynamic Behavior of Thermoelectric Devices; Technology Press of MIT 1960.

6. Heikes, Robert; Thermoelectricity, Interscience Publishers 1961.

7. Ioffe, Fedorovich; Semiconductor Thermoelectrics, Infosearch Ltd., 1957.

APPENDIX

THERMOELECTRIC CHARACTERISTICS

1.0 THE THERMOELECTRIC PHENOMENA

Four basic physical phenomena can be associated with the operation of thermoelectric devices: The Seebeck effect, the Peltier effect, the Thomson effect, and the Joule effect. The Seebeck effect is the emf generated when two sides of a thermoelectric module are maintained at different temperatures. The Peltier effect is the heating or cooling effect observed when an electrical current is passed through two dissimilar junctions. The Thomson effect is a heating or effect in a homogeneous conductor observed when an electrical current is passed in the direction of a temperature gradient. The Joule effect is the heating effect observed in a conductor as an electrical current is passed through the conductor.

1.1 SEEBECK EFFECT

In 1821 Thomas J. Seebeck discovered that when two dissimilar conductors are connected and if the junctions are maintained at different temperatures, an emf can be observed in the circuit. This emf is called the Seebeck emf and the effect is known as the Seebeck effect. The effect is illustrated in Figure A-1.

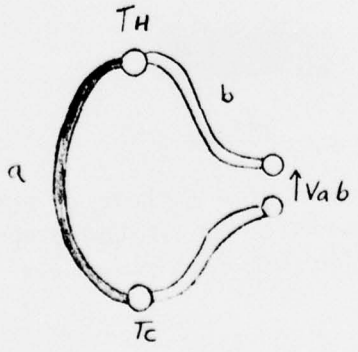

Figure A-1

This open-circuit voltage is a function of the materials making up the couple and the temperature of two junctions.

$$V_{ab} = C_1 (Th - Tc) + \frac{C_2}{2} (Th - Tc)^2 + \text{----} \qquad (1\text{-}2\text{-}1)$$

And the Seebeck coefficient is defined as

$$\alpha_{ab} = \frac{\partial V_{ab}}{\partial Th} = C_1 + C_2 (Th - Tc) + C_3 (Th - Tc)^2 + \text{---} \qquad (1\text{-}2\text{-}2)$$

1.2 PELTIER EFFECT

It is well known that the passage of an electrical current through the junction of two dissimilar conductors in a certain direction produces a cooling effect, and when in the opposite direction, a heating effect. This was found by Jean C. A. Peltier in 1834 and is now called the Peltier effect. The rates of both heat generation and absorption are proportional to the current and dependent on the temperature of the junction and the Peltier effect is expressed as:

$$Q_p = \pi I \qquad (1\text{-}2\text{-}3)$$

The process is illustrated in Figure A-2.

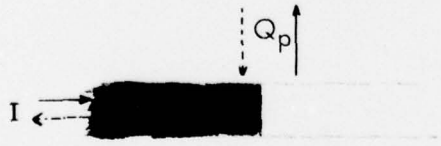

Figure A-2

By Kelvin's relation we have $\pi = \alpha T$ where α is the Seebeck coefficient of two dissimilar conductors and T is the absolute temperature at the junction, then the Peltier term equation (1-2-3) is written as:

$$Q_p = \alpha TI \qquad (1\text{-}2\text{-}4)$$

1.3 THOMSON EFFECT

William Thomson (later Lord Kelvin) examined the effects of Seebeck and Peltier and derived a relation between the respective coefficients.

In this process, he predicted the existence of a new effect called the Thomson effect. There is a heating or cooling effect in a homogeneous conductor when an electrical current passes in the direction of temperature gradient.

The Thomson effect per unit volume is written as:

$$q_t = \tau J \frac{dT}{dx} \qquad (1\text{-}2\text{-}5)$$

where τ = The Thomson coefficient

J = Current density.

$\frac{dT}{dx}$ = Temperature gradient

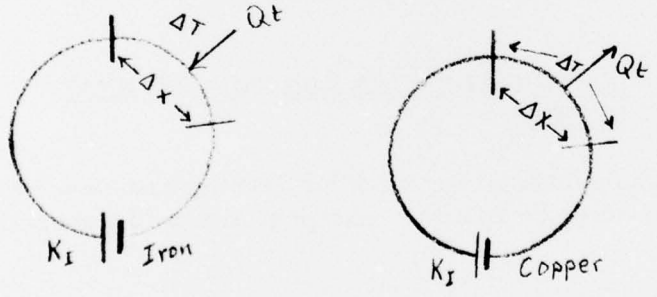

Figure A-3

Iron has a positive Thomson coefficient and copper has a negative Thomson coefficient.

If Q_t is the heat absorbed when the direction of J and $\frac{dT}{dx}$ coincide with each other, then τ is positive. τ is negative if Q_t is the heat generated when the current flows in the same direction as the temperature gradient. The Thomson effect per length is written as:

$$Q_t = \tau I \frac{dT}{dx} \qquad (1\text{-}2\text{-}6)$$

These three effects: Seebeck, Peltier and Thomson are reversible phenomena.

1.4 JOULE EFFECT

When an electrical current is passed through a conductor, which is isothermal, there is a heat generation called Joule heat. Joule heat per unit volume is written as:

$$q_j = \rho J^2 \qquad (1\text{-}2\text{-}7)$$

where ρ : Electrical resistivity
J : Current density

This is an irreversible process and for the actual operating condition of thermoelectric devices there is another irreversible process, thermal conduction.

1.5 THERMOELECTRIC FORMULA FOR PELTIER HEAT PUMPING DEVICES

In this section a useful approach for defining heat flow for thermoelectric modules is developed utilizing a concept of averaged transport properties.

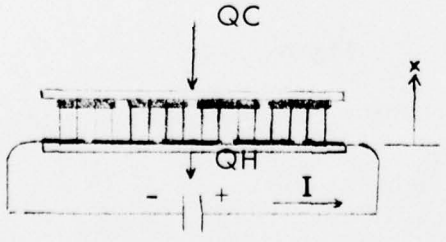

Figure A-4

In the operation of thermoelectric modules it is reasonable to assume that heat flows only in the direction of X, this means there is no heat flow except through the junctions, as shown in Figure A-4.

Moreover, all the heat may be considered to flow through the plates which sandwich the thermoelectric couples. To find a formula for QC or QH it is necessary to look at one of these thermoelectric couples.

A couple consists of two dissimilar conductors and therefore, as mentioned before, it has all the thermoelectric effects, and for thermoelectric devices the proper materials are coupled to produce extensive thermoelectric effects or to have higher performance.

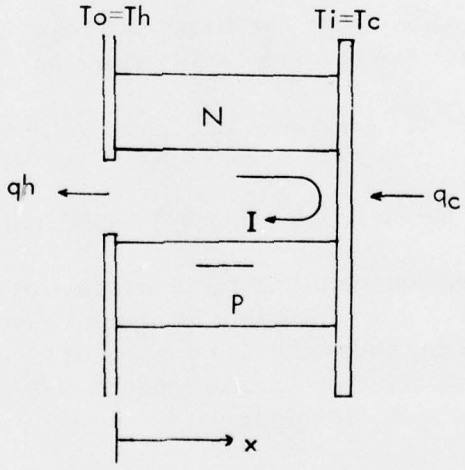

Figure A-5

As shown in Figure A-5 the direction of the current is opposite for N versus P material. Most of the properties of these two materials differ from each other, in fact. If one makes use of these differences one can derive the equation of the heat flow for a couple having the equation of heat flow along a bar.

Now consider a bar having a different temperature at each end through which the current is flowing in Figure A-6.

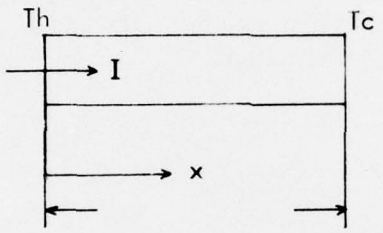

Figure A-6

Under steady state conditions as Figure 1-6, the differential equation for energy flow through a unit volume is written as:

$$TJ\frac{\partial \alpha}{\partial x} + \tau J \frac{dT}{dx} - \rho J^2 - \frac{d}{dx}\left(k \frac{dT}{dx}\right) = 0 \qquad (1\text{-}3\text{-}1)$$

where k is the thermal conductivity of the material.

To solve equation (1-3-1), the numerical method would be applied knowing the transport properties as a function of location and temperature. Therefore, it is rather necessary and convenient to assume averaged transport properties. With averaged properties equation (1-3-1) will be applied for the N arm of the couple and written as:

$$k_n \frac{d^2T}{dx^2} - \tau_n J \frac{dT}{dx} + \rho_n J^2 = 0 \qquad (1\text{-}3\text{-}2)$$

where kn, τ_n, ρ n are averaged properties of the N arm. From equation (1-3-2), one can derive the equation of heat flow at X = 0 and X = ℓ .

The same equation will be applied for the P arm, but with different properties and an opposite direction of current. Thus, adding Peltier terms, one can have the equation of heat flow at the junction of two dissimilar conductors.

Heat flow at Tc is

$$q_c = \alpha TcI + \frac{1}{2}\bar{\tau} I\Delta T - \frac{1}{2} I^2\bar{R} - \bar{K}\Delta T \qquad (1\text{-}3\text{-}3)$$

Heat flow at Th is

$$q_h = \alpha ThI - \frac{1}{2}\bar{\tau} I\Delta T + \frac{1}{2} I^2\bar{R} - \bar{K}\Delta T \qquad (1\text{-}3\text{-}4)$$

where: $\Delta T = Th - Tc$,

α is the net Seebeck coefficient of a couple at the temperature of the junction.

$\bar{R}$, $\bar{K}$ and $\bar{\tau}$ are average properties of a couple in the temperature range of Tc< T < Th.

One should notice that these transport properties are all temperature dependent; extensive experiments are needed to find out their relationship to temperature.

1.6 THERMOELECTRIC PROPERTIES AS A FUNCTION OF TEMPERATURE

The following section describes the experimental method utilized to obtain the module Seebeck coefficient α_m, module resistance R_m and module thermal conductivity K_m as a function of temperature.

The properties found in the experimental method are actually averaged properties of a module at certain temperature and therefore those assumptions made in the preceding section can be applied, that is, those equations in the section (1-3) can be calculated with the results of this section.

1.7 CALCULATION OF THE THERMOELECTRIC EFFECTS

A thermoelectric module contains a number of couples connected electrically in series and thermally in parallel. Therefore, if a module is made of a number of couples, the refrigerating effect of a module may be written from equation (1.3.3).

$$QC = n\left(\alpha T_c I + \frac{1}{2}\bar{\tau} I\Delta T - \frac{1}{2} I^2\bar{R} - \bar{K}\Delta T\right) \qquad (1\text{-}7\text{-}1)$$

let $\alpha_c = n\alpha$; α_c is a module Seebeck coefficient at temperature of Tc

$\tau_m = n\tau$; τ_m is an averaged Thomson coefficient of a module with temperature of $Tc \leq T \leq Th$

$R_m = nR$; R_m is an averaged electrical resistance of a module in the temperature of $Tc \leq T \leq Th$

$K_m = nK$; K_m is an averaged thermal conductance of a module of $Tc \leq T \leq Th$

Equation (1-6-1) will be rewritten as

$$QC = \alpha_c T_c I + \frac{1}{2}\tau_m I\Delta T - \frac{1}{2} I^2 R_m - K_m \Delta T \qquad (1\text{-}7\text{-}2)$$

Similarly, the heat pump effect of a module can be written with equation (1-7-4)

$$QH = \alpha_h T_h I - \frac{1}{2}\tau_m I\Delta T + \frac{1}{2} I^2 R_m - K_m \Delta T \qquad (1\text{-}7\text{-}3)$$

Where α_h is the module Seebeck coefficient at Th.

A refrigerator and a heat pump are essentially the same device; they bring heat from a cold body to a hot body with a certain input power. This device is called a refrigerator when an object is cooled and called a heat pump when an object is heated.

To bring heat from a cold body to a hot body certain power is always necessary. This power is called input power to the module. The input power required is determined by temperature conditions of a module and the current passing through a module.

The input voltage to have a current of I may be written as:

$$V = \int_{T_c}^{T_h} \alpha \, dT + IR_m \qquad (1-7-4)$$

$$= \alpha_m \Delta T + IR_m$$

The input power to a module will be expressed as:

$$P = V \cdot I$$

$$= \alpha_m \Delta T I + I^2 R_m \qquad (1-7-5)$$

Where α_m is a mean value of the Seebeck coefficient in the temperature range of Tc < ΔT < Th, and $\alpha_m \Delta T$ is a Seebeck voltage which tends to draw a current I from N to P material at the hot junction. The operation of a thermoelectric module is shown in Figure A-7.

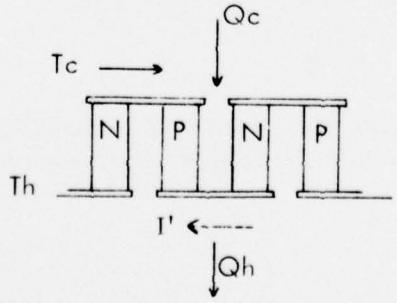

Figure A-7

The coefficient of performance of a refrigerator and a heat pump are defined in equations (1-6-12) and (1-6-13), respectively.

$$CORP = QC/P \qquad (1\text{-}7\text{-}12)$$

$$COPH = QH/P \qquad (1\text{-}7\text{-}13)$$

To calculate QC, QH, P, CORP and COPH, , , , R, and K have to be calculated at each temperature level.

1.8 OTHER PROPERTIES OF A THERMOELECTRIC MODULE

There are many variables in a thermoelectric module, expecially the properties of the material which are all temperature dependent; these changes with temperature have to be considered in the calculations. There are other properties in a module which are not temperature dependent but still allow significant changes in the performance of a module, namely, the number of couples in the module and the shape ratio of the element used for a couple.

An increase in the number of couples increases the heat pumping capacity and input power to a module, since the couples are connected electrically in series and thermally in parallel.

It will be noted from these equations that a unique module design for a given application may be derived. It must be cautioned, however, that not all module designs are necessarily manufacturable.

$$QC = n\, q_c \text{ and } QH = n\, q_h \qquad (1\text{-}8\text{-}1)$$

where QC and QH are the refrigerating and the heat pumping effects of a module, q_c and q_h are that for a couple, n is the number of couples in a module.

The input voltage can be written as

$$V = \alpha_m \Delta T + I R_m = n \ (\alpha \Delta T + I R) \qquad (1\text{-}8\text{-}2)$$

The input power is

$$P = VI = nI \ (\alpha \Delta T + I R)$$

COPR and COPH are:

$$COPR = QC/P = \frac{q_c}{I (\alpha \Delta T + I R)} \qquad (1\text{-}8\text{-}4)$$

$$COPH = QH/P = \frac{q_h}{I (\alpha \Delta T + I R)} \qquad (1\text{-}8\text{-}5)$$

The preceding equations state that the coefficient of performance is independent of the number of couples and that the input power and the heat pumping effect is proportional to the number of couples for fixed condition.

These relations hold also true for a different number of modules if they are connected electrically in series and thermally in parallel

☆ U. S. GOVERNMENT PRINTING OFFICE: 1977 — 757-001/515